

Distributed Opportunistic Spectrum Access via Adaptive Carrier Sensing in Cognitive Radio Networks

Mahsa Derakhshani



Department of Electrical & Computer Engineering
McGill University
Montreal, Canada

August 2013

A thesis submitted to McGill University in partial fulfillment of the requirements for the degree
of Doctor of Philosophy.

© 2013 Mahsa Derakhshani

*To my parents and to my husband, Mohammad Moeini Aghkariz,
with all my love.*

Abstract

The limitations of current static spectrum management policy drive the idea of a more dynamic access policy to improve the efficiency of radio spectrum usage and accommodate the increasing demand for wireless communication applications. Known as the opportunistic spectrum access (OSA), the new paradigm allows cognitive secondary users (SUs) to access the licensed spectrum, provided that the interference to the licensed primary users (PUs) is limited. In a cognitive radio network, since SUs are intended to track and take advantage of instantaneous spectrum opportunities, adaptive learning-based spectrum access schemes are desired to optimize spectrum utilization and ensure a peaceful coexistence of licensed and unlicensed systems. This thesis deals with the modeling, development and analysis of OSA schemes in a cognitive radio network from both SU and PU perspectives. The research objective is to maximize the overall throughput of SUs, while sufficiently protecting the ongoing operation of PUs.

From the SU perspective, to avoid the high-risk data loss due to the random return of PUs, we present a dynamic hopping transmission strategy for SUs to access the temporarily idle frequency slots of a licensed frequency band, with adaptive activity factors. Upon applying the dual decomposition, the optimal activity factor allocation algorithm is developed. To facilitate spectrum sharing in a decentralized manner, we propose an adaptive carrier sense multiple access (CSMA) scheme. Based on the proposed CSMA scheme, learning-based distributed access algorithms for SUs are devised, including non-game-theoretic and game-theoretic approaches. The proposed algorithms can be independently performed by each SU to learn its optimal activity factors from the locally available information. To evaluate the effects of inevitable collisions among SUs in the proposed adaptive CSMA scheme, the collision probability and saturation throughput are studied by both analysis and simulation. Simulation results show significant performance improvements in terms of the achievable throughput compared to the conventional CSMA scheme.

From the PU perspective, by applying the proposed access scheme to SUs, we study the interference caused by SUs to the PU due to miss-detection, and also its effects on the capacity-outage performance of the PU in a cognitive radio network. Based on the developed statistical models for the interference distribution, closed-form expressions for the capacity-outage probability of the PU are derived to examine the effects of various system parameters on the performance of the PU in the presence of interference from SUs. The model is extended to investigate the effects of cooperative sensing on the aggregate interference and the capacity-outage performance, considering OR (logical OR operation) and maximum likelihood cooperative detection techniques.

Sommaire

Les limites de la politique d'utilisation statique du spectre ont conduit à l'idée d'une politique d'accès plus dynamique pour améliorer l'efficacité du spectre radio utilisé et accommoder l'augmentation de la demande des applications de communication sans fils. Connue sous le nom d'accès opportuniste au spectre (AOS), ce nouveau modèle permet à un utilisateur secondaire (US) cognitif d'accéder à un spectre licencié, tout en limitant l'interférence de l'utilisateur primaire (UP) licencié. Dans un réseau radio cognitif, puisque les USs sont sensés traquer et profiter des instants d'opportunité spectrale, des schémas d'accès spectral basés sur l'apprentissage adaptatif sont désirés pour optimiser l'utilisation spectrale et assurer une parfaite coexistence entre les systèmes licenciés et non licenciés. Cette thèse se consacre à la modélisation, au développement et à l'analyse des schémas d'AOS dans les réseaux radio cognitif du point de vue des UP et US. L'objectif de cette recherche est de maximiser le flux total des USs, tout en protégeant suffisamment le fonctionnement de l'UP.

Du point de vue de l'US, afin d'éviter un risque élevé de perte de données causée par le retour aléatoire de l'UP, nous présentons une stratégie de transmission basée sur le saut dynamique pour les USs afin d'accéder aux blocs de fréquences temporairement libres dans une bande licenciée, avec un facteur d'activité adaptatif. Lors de l'application de la double décomposition, un algorithme d'allocation optimale des facteurs d'activité est développé. Afin de faciliter le partage du spectre de manière décentralisée, nous proposons un schéma adaptatif basé sur la technique CSMA (accès multiple avec détection de porteuses). En se basant sur le schéma proposé, des algorithmes d'accès distribués pour les USs basés sur l'apprentissage sont conçus, incluant des approches basées sur la théorie des jeux et d'autres non. Les algorithmes proposés peuvent être utilisés indépendamment par chaque US pour apprendre son facteur d'activité optimal à partir de l'information localement disponible. Pour évaluer les effets de collisions inévitables entre les USs dans le schéma CSMA proposé, la probabilité de collision et le flux de saturation sont étudiés analytiquement et à travers simulations. Les résultats des simulations démontrent une amélioration considérable de performance, particulièrement de point de vue de débit réalisé par rapport à celui réalisé selon le CSMA conventionnel.

Du point de vue de l'UP, nous employons le schéma d'accès proposé pour les USs, et étudions l'interférence causée par les USs aux UPs à la suite d'une erreur de détection, ainsi que ses effets sur la capacité de coupure de l'UP dans un réseau radio cognitif. En se basant sur les modèles statistiques de la distribution de l'interférence, des expressions exactes de la probabilité de la

capacité de coupure pour l'UP sont dérivées afin d'examiner les effets des différents paramètres du système sur la performance de l'UP en présence des USs interférant. Le modèle est étendu pour investiguer les effets de la détection coopérative sur l'interférence totale et la capacité de coupure, en considérant l'opérateur logique OR et une détection coopérative de maximum de vraisemblance.

Acknowledgments

I would like to express the deepest appreciation to my supervisor, Professor Tho Le-Ngoc, for giving me the opportunity to pursue my doctoral studies at McGill university and guiding me through this journey. Without his patience, guidance, and support, this thesis would have not been possible. The excitement he constantly conveyed regarding research will always be with me in my academic career. Thank you for teaching me how to do research.

I also wish to express my appreciation to the other members of my Ph.D. supervisory committee, Professor Benoît Champagne and Professor Bruce Shepherd, whose insightful comments significantly contributed to improving this thesis. My doctoral study has been supported by the McGill Engineering Doctoral Award (MEDA) program and the John Bonsall Porter Prize. I would also like to acknowledge the financial support received from the Natural Sciences and Engineering Research Council of Canada (NSERC) Strategic Projects Grant and Black-Berry (formerly Research In Motion). Without such generosity, I would have been unable to pursue my doctoral studies.

I am also thankful to my colleagues and friends at McGill university, especially the Broadband Communications Research Laboratory members: Robert, Leila, Leonardo, Sanjeewa, Danny, Ahmed, Berri, Sean, Kevin, Chris, Jamshid, Suman, and Amir. In particular, thank you to Leonardo Jiménez Rodríguez, Sanjeewa Priyad Herath and Duy Trong Ngo for proofreading my dissertation. Also thanks to Ahmed Masmoudi for helping me with the French translation of the thesis abstract. I will never forget you.

My heartfelt love and gratitude go to my family members: mom, dad, my sister Mahshad, and my brother Keyvan. Your unconditional support enabled me to overcome the difficulties I faced in different steps of my life and in particular, made my higher education endeavor possible. And most of all, thank you to my husband, Mohammad, for the love that made it all worthwhile. I am forever grateful to all of you and I hope that this accomplishment makes all of you proud.

Contents

1	Introduction	1
1.1	Cognitive Radio and Opportunistic Spectrum Access	1
1.2	Emerging Cognitive Radio Standards	3
1.3	Technical Challenges of Opportunistic Spectrum Access	4
1.4	Thesis Contributions and Organization	6
2	Literature Review	9
2.1	Opportunistic Spectrum Access Design	9
2.1.1	Time Slotted versus Un-Slotted Transmission Structure for Primary Users	10
2.1.2	Centralized versus Distributed Design	13
2.2	Aggregate Interference Analysis	15
2.3	Concluding Remarks	17
3	Opportunistic Spectrum Access with Hopping Transmission Strategy	18
3.1	Introduction	18
3.2	System Model and Problem Formulation	20
3.3	Optimal Hopping-Based Opportunistic Spectrum Access	23
3.3.1	Single-User Opportunistic Spectrum Access	23
3.3.2	Multi-User Opportunistic Spectrum Access	25
3.4	Learning-Based Distributed Opportunistic Spectrum Access	28
3.5	Convergence Analysis	32
3.6	Numerical Results	34
3.6.1	Performance of the Optimal Opportunistic Spectrum Access	34
3.6.2	Convergence of the Learning-Based Opportunistic Spectrum Access Algorithm	35

3.6.3	Robustness to the Perturbations of Primary User Return Probability . . .	38
3.7	Concluding Remarks	38
4	Distributed Opportunistic Spectrum Access: Game-Theoretic Approaches	40
4.1	Introduction	40
4.2	System Model	42
4.3	Game-Theoretic Design of Hopping-Based Opportunistic Spectrum Access . . .	42
4.3.1	Existence of the Nash Equilibrium	44
4.3.2	Feasibility of the Nash Equilibrium	44
4.3.3	Efficiency of the Nash Equilibrium	45
4.4	Iterative Learning-Based Access Algorithms with Perfect and Noisy Observations	45
4.4.1	Best-Response Dynamics with Perfect Observations	46
4.4.2	Log-Linear Dynamics with Perfect Observations	48
4.4.3	Best-Response Dynamics with Noisy Observations	50
4.5	Competition and Cooperation in Opportunistic Spectrum Access	54
4.5.1	Problem Formulation	54
4.5.2	Game-Theoretic Design	55
4.5.3	Cooperative Design with Dynamic Pricing	57
4.5.4	Learning Equilibrium	58
4.6	Concluding Remarks	62
5	Throughput Analysis for Adaptive Carrier Sense Multiple Access	63
5.1	Introduction	63
5.2	IEEE 802.11 Distributed Coordination Function Review	65
5.3	System Model and Problem Formulation	67
5.4	Throughput Analysis	69
5.5	Numerical Results	72
5.6	Concluding Remarks	78
6	Aggregate Interference and Capacity-Outage Analysis	79
6.1	Introduction	79
6.2	System Configuration and Modeling	81
6.3	Beacon Transmitter at the Primary User Receiver	84
6.3.1	Interference Model	84

6.3.2	Capacity-Outage Probability	86
6.4	Beacon Transmitter at the Primary User Transmitter	90
6.4.1	Interference Model	90
6.4.2	Capacity-Outage Probability	92
6.4.3	Beacon Transmitter Placement Comparison	93
6.5	Cooperative Sensing	96
6.5.1	OR Detector	96
6.5.2	Maximum Likelihood Detector	100
6.6	Concluding Remarks	105
7	Conclusions	107
7.1	Summary	107
7.2	Potential Future Studies	108
A	Appendix to Chapter 3	110
A.1	Proof of Proposition 1	110
A.2	Proof of Proposition 2	111
A.2.1	Step 1 ($0.5 < c < 1$)	113
A.2.2	Step 2 ($c = 1$)	114
B	Appendix to Chapter 4	116
B.1	Proof of Theorem 3	116
B.2	Proof of Theorem 4	118
	References	120

List of Figures

1.1	Example of spectrum holes in time and frequency domains in a licensed frequency band.	2
1.2	Interference situations between a SU and a PU.	5
2.1	Example of a general 2-phase time-slot structure for SUs.	10
2.2	Example of transmission strategies for a single SU proposed in [27, 28].	12
3.1	An example of a SU activity in three idle channels with different activity factors during a transmission slot.	22
3.2	Performance comparison of the proposed OSA and conventional OSA versus the number of idle channels N_a for fixed $\alpha_i = 0.3$ and $\text{SNR} = 10\text{dB}$	35
3.3	Performance comparison of the proposed OSA and conventional OSA versus the PU return probability α_i for fixed $N_a = 10$ and $\text{SNR} = 10\text{dB}$	36
3.4	Performance comparison of the proposed OSA and conventional OSA versus SNR for fixed $N_a = 10$ and $\alpha_i = 0.3$	36
3.5	Convergence of the proposed distributed learning-based OSA.	37
3.6	Convergence of the proposed distributed learning-based OSA.	37
3.7	Effect of the PU return probability change on the SU throughput.	38
4.1	Convergence of the SU activity factors with best-response dynamics.	47
4.2	Convergence of the potential function with best-response dynamics.	48
4.3	Convergence of the SU activity factors with log-linear dynamics.	51
4.4	Convergence of the potential function with log-linear dynamics.	51
4.5	Convergence of the SU activity factors with noisy best-response dynamics.	53
4.6	Convergence of the potential function with noisy best-response dynamics.	53

4.7	Performance comparison of the NE of game \mathcal{G}' (with non-binary β_k^i) and the globally optimal solution (with non-binary and binary β_k^i) versus the PU return probability α_i for fixed $N_s = 2$, $N_a = 2$ and SNR = 10dB.	57
4.8	Performance comparison of the NE of game \mathcal{G}'' and the globally optimal solution versus the PU return probability α_i for fixed $N_s = 2$, $N_a = 2$ and SNR = 10dB.	59
4.9	Convergence of the SU activity factors in the proposed iterative algorithm considering the game \mathcal{G}'	61
4.10	Convergence of the SU activity factors in the proposed iterative algorithm considering the game \mathcal{G}''	61
5.1	Example of the channel-access procedure of two users using CSMA with the RTS/CTS access mechanism in time domain.	66
5.2	Saturation throughput versus number of users using the basic access mechanism.	73
5.3	Saturation throughput versus number of users using the RTS/CTS access mechanism.	74
5.4	Collision probability versus number of users using the RTS/CTS access mechanism.	75
5.5	Probability of successful transmission versus number of users using the RTS/CTS access mechanism.	75
5.6	Saturation throughput versus packet length with $N_s = 20$	76
5.7	Saturation throughput versus minimum contention window size using the basic access mechanism.	77
5.8	Saturation throughput versus minimum contention window using the RTS/CTS access mechanism.	77
6.1	Network model.	81
6.2	CDF of the aggregate interference in a Rayleigh fading channel for the beacon transmitter at the PU receiver.	85
6.3	CDF of the aggregate interference in Nakagami fading channels with non-cooperative sensing and the beacon transmitter at the PU receiver.	87
6.4	PU capacity-outage probability versus required threshold rate for various SINRs in a Rayleigh fading channel with the beacon transmitter at the PU receiver.	89
6.5	Histogram and PDF of interference I_0 in a Rayleigh fading channel with path-loss exponent $\alpha = 2.1$	91

6.6	CDF of aggregate interference in a Rayleigh fading channel for the beacon transmitter at the PU transmitter.	92
6.7	PU capacity-outage probability versus required threshold rate for various SINRs in a Rayleigh fading channel with the beacon transmitter at the PU transmitter. . .	93
6.8	Interference mean $E[I_0]$ versus PU transmitter-receiver distance R_0	94
6.9	PU capacity-outage probability versus required threshold rate.	95
6.10	CDF of aggregate interference in Nakagami fading channels with OR sensing ($R_c = 10$).	98
6.11	PU capacity-outage probability versus required threshold rate for various SINRs with OR sensing in a Rayleigh fading channel.	100
6.12	CDF of aggregate interference in Nakagami fading channels with ML sensing ($R_c = 10$).	103
6.13	Interference mean $E[I_0]$ versus cooperation range R_c in Nakagami fading channels.	104
6.14	PU capacity-outage probability versus required threshold rate for various SINRs with ML sensing in a Rayleigh fading channel.	104
6.15	PU capacity-outage probability versus required threshold rate for ML and OR sensing in a Rayleigh fading channel.	105

List of Tables

5.1	IEEE 802.11 MAC parameters used in the numerical results.	72
5.2	Percentage of successfully transmitted packets for different users with different SNR _s , assuming $\beta = 0.8$	78

List of Acronyms

ACK	Acknowledgement
AP	Access point
AWGN	Additive white Gaussian noise
BS	Base station
CDF	Cumulative distribution function
CPE	Customer premises equipment
CSMA	Carrier sense multiple access
CSMA/CA	Carrier sense multiple access with collision avoidance
CTS	Clear-to-send
DCF	Distributed coordination function
DIFS	Distributed inter-frame space
DSC	Diagonally strict concavity
FCC	Federal Communications Commission
IEEE	Institute of Electrical and Electronics Engineers
i.i.d.	Independent and identically distributed
ISM	Industrial, scientific and medical
KKT	Karush-Kuhn-Tucker
LIFS	Long inter-frame space
MAC	Medium access control
ML	Maximum likelihood
NE	Nash equilibrium
OFDM	Orthogonal frequency-division multiplexing
OFDMA	Orthogonal frequency-division multiple access
OSA	Opportunistic spectrum access

OR	Logical OR operation
PCF	Point coordination function
PDF	Probability density function
PHY	Physical layer
POMDP	Partially observable Markov decision process
PU	Primary user
QoS	Quality-of-service
RTS	Request-to-send
SIFS	Short inter-frame space
SINR	Signal-to-interference-plus-noise ratio
SNR	Signal-to-noise ratio
SU	Secondary user
TDM	Time division multiplexing
TDMA	Time division multiple access
TVWS	TV white space
UHF	Ultra-high-frequency
VHF	Very-high-frequency
WRAN	Wireless regional area network
WLAN	Wireless local area network
WiMAX	Wireless Interoperability for Microwave Access

Chapter 1

Introduction

1.1 Cognitive Radio and Opportunistic Spectrum Access

Over the last two decades, there has been a growing interest in wireless communication devices and applications, and hence, an ever-increasing demand for radio spectrum. Since radio spectrum is an open and shared broadcast medium, all radios operating over the same frequency band and within the same geographical location interfere with each other. Conventionally, to avoid co-channel interference, static spectrum allocation strategy is deployed in which different frequency bands are licensed to different types of wireless users who will have an exclusive right to use that portion of the spectrum. As the number of wireless users has been exponentially increasing, the spectrum allocation chart has become severely crowded and the availability of frequency bands for emerging wireless applications has become limited.

However, recent studies [1–4] have indicated that the conventional static spectrum allocation strategy leads to significant spectrum underutilization. It has been revealed that while almost all frequency bands have been assigned to licensed users, at any given time and any given location, many frequency slots are unoccupied in a licensed frequency band. In other words, despite the activity of licensed users, measurements show that there still exists plenty of instantaneous spectrum availabilities (also referred to as “spectrum opportunities”, “spectrum holes” and “white spaces”) in the licensed spectrum. Figure 1.1 illustrates an example of the spectrum holes in both frequency and time domains in a licensed frequency band.

The limitations of static resource allocation on one hand and the success of wireless technologies in unlicensed bands on the other hand demonstrate the need for a more flexible spectrum allocation strategy that could enable further growth for wireless communications. This moti-

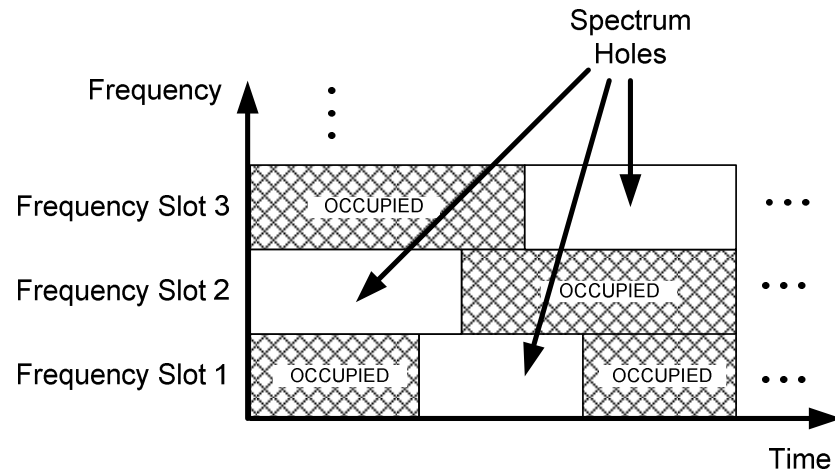


Fig. 1.1 Example of spectrum holes in time and frequency domains in a licensed frequency band.

vates the idea of opportunistic spectrum access (OSA) to exploit such spectrum availabilities, aiming to improve spectrum utilization [5–9]. OSA allows the unlicensed users (also referred to as secondary users) to identify and utilize instantaneous spectrum opportunities, while limiting the level of interference to the high-priority licensed users (also referred to as primary users). Therefore, the two fundamental elements of OSA are opportunity identification and opportunity exploitation. In the opportunity identification (also known as spectrum sensing), secondary users (SUs) need to identify and track dynamically changing idle frequency slots (or channels) in an intelligent way. Based on the observations obtained from the opportunity identification, the opportunity exploitation is responsible to determine the optimal transmission strategy for the secondary access in an idle channel [7].

The key enabling technology for OSA is cognitive radio. More specifically, a cognitive radio is an intelligent and reconfigurable wireless communication system that enables monitoring the radio environment, learning, and accordingly, adapting transmission parameters in order to achieve the optimal spectrum utilization [10–12]. Cognitive radios, together with opportunistic spectrum access, attempt to overcome the dilemma between the increasing spectrum requirements and the scarce spectral resources.

1.2 Emerging Cognitive Radio Standards

In the past few years, there have been worldwide efforts on developing new spectrum policies to accelerate opportunistic usage of spectrum. In particular, the Federal Communications Commission (FCC) in the USA allowed unlicensed operations in the unused TV broadcast bands [13], and later released the rules and the technical conditions for such transmission in rural and urban areas using fixed and portable devices [14, 15]. The white space in the TV band (TVWS) is viewed as one of the first opportunities to adopt and realize the OSA model. This is because of its relatively high robustness to interference (due to the high power transmission) and convenience in opportunity identification (due to the fixed location of TV broadcast sites). Furthermore, the analogue to digital TV switchover results in a reduction of the required spectrum and generates a considerable amount of vacant spectrum in the TV bands [3, 4].

In order to take advantage of these spectrum availabilities, new wireless standards are being developed. Some developing standards for using TVWS are namely IEEE 802.22 for wireless regional area networks (WRAN) [16, 17], and IEEE 802.11af for wireless local area networks (WLAN) [18, 19]. These developing standards are actually extensions of two existing standards, namely IEEE 802.16 Wireless Interoperability for Microwave Access (WiMAX) and IEEE 802.11 WLAN (Wi-Fi). They provide incremental improvements on the existing standards towards comprising and realizing full cognitive features [20].

IEEE 802.22 WRAN is designed to provide broadband access in rural areas for fixed cognitive radio devices that operate in unused channels in the very-high-frequency/ultra-high-frequency (VHF/UHF) TV bands between 54 and 862 MHz. It is an infrastructured cellular network which includes the base station (BS) and the end-user devices called customer premises equipment (CPE). In the IEEE 802.22 standard, each BS is responsible for the resource allocation among the CPEs within its cell. This standard adopts a centralized medium access control (MAC) and the orthogonal frequency-division multiple access (OFDMA) for its physical layer (PHY). To protect PUs (i.e., analogue TV, digital TV and licensed low-power devices such as wireless microphones), spectrum sensing techniques and a geolocation database are considered to be used in order to enable a PU-SU coexistence. Although IEEE 802.22 is the first international cognitive radio standard, considering the deployment cost of WRAN infrastructure, it still remains unclear whether the WRAN could create a profitable service in rural areas [16, 17, 19, 21].

Furthermore, as another potential application for OSA, IEEE 802.11af (also known as “White-Fi” or “Wi-Fi 2.0”) is being developed to enhance the capacity and quality-of-service (QoS) of

current Wi-Fi systems with the use of the TVWS. IEEE 802.11af is a wireless network comprising a cognitive access point (AP) and associated cognitive end users. Due to the better propagation characteristics of the VHF/UHF bands compared to the industrial, scientific and medical (ISM) band, it is expected that IEEE 802.11af offers higher speed and wider coverage than the current Wi-Fi, and also supports better QoS guarantees [19]. According to [20], modern WLANs could already be considered as cognitive radios because of their coexistence capabilities and dynamically changing frequencies and transmission power. The basic coexistence capability of IEEE 802.11 is its listen-before-talk MAC based on the carrier sense multiple access with collision avoidance (CSMA/CA). The simplicity and success of the listen-before-talk contention-based MAC has the potential to be applied for the early cognitive systems [20].

1.3 Technical Challenges of Opportunistic Spectrum Access

Opportunistic spectrum access causes a revolutionary change in the radio spectrum regulations and also plays an important role in enhancing the spectrum usage efficiency. That is because it enables time-varying and flexible usage of radio spectrum, while taking into account technical and regulatory considerations. The spectrum opportunities are time-varying depending on the activities of primary users (PUs) in the licensed channels (e.g., TVWS are dynamic due to digital TV multicasting and activity of low-power devices such as wireless microphones). This fact makes a cognitive radio network a highly dynamic and challenging wireless environment. To get the most out of such dynamic spectrum opportunities while protecting the spectrum licensees from interference, it is critical to design an OSA scheme that is capable of filling the spectral gaps of PUs in an intelligent way. Thus, the need for intelligent coexistence capabilities and autonomous coordination in OSA raises a new set of technical challenges which are not present in the existing radio systems.

First, modeling the dynamic behavior of the PUs and the interactive behavior of SUs in response to PUs' dynamics is a major design issue in a cognitive radio network. To provide sufficient benefit to SUs, an accurate model is needed to simultaneously capture the dynamics of spectrum opportunities and describe the decision process of SUs. Furthermore, since cognitive radio can be viewed as an enabler for distributed radio resource management, it is important that such a model can support distributed operations of SUs, in which each SU autonomously coordinates its usage and independently achieves the optimal transmission strategy.

Second, to design an OSA scheme for SUs, there is a tradeoff between two conflicting objec-

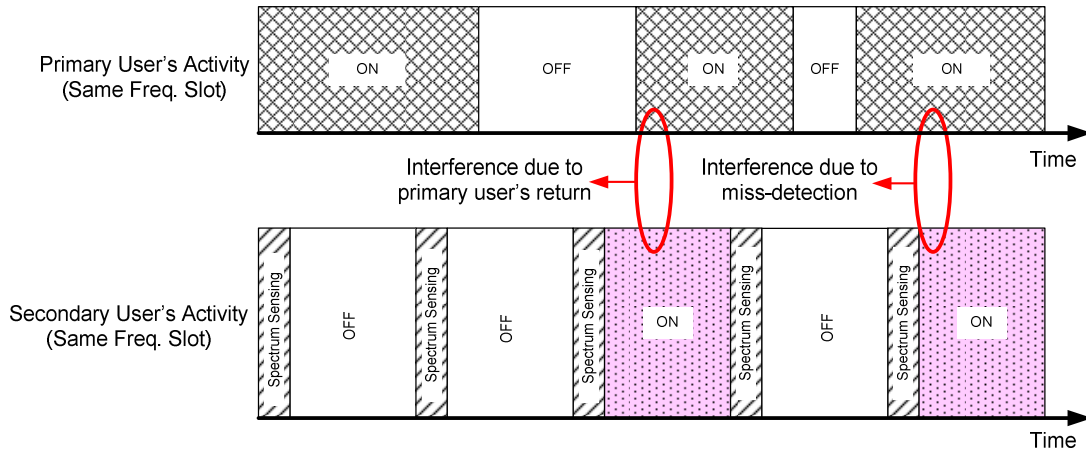


Fig. 1.2 Interference situations between a SU and a PU.

tives, i.e., maximizing the opportunistic spectrum utilization for SUs and minimizing the possible collisions between SUs and PUs. To identify the time-varying spectrum holes for transmission, SUs need to periodically monitor the channels to determine whether or not PUs are active. Although SUs are intended to only exploit the spectrum holes for communications, two types of collision between SUs and PUs could happen. First, a SU may miss-detect the PU's activity and start transmitting while the PU is present. Such a miss-detection is due to inevitable errors in spectrum sensing which are caused by noise and fading. Second, even if an idle channel is perfectly detected and used by a SU, a collision may still occur since the PU may return and reoccupy that idle channel at any time during the SU transmission. Figure 1.2 illustrates these interference situations between a SU and a PU in a given frequency slot. In the presence of miss-detection errors and non-zero PU return probabilities, to reduce the effects of collisions between PUs and SUs, an adaptive transmission strategy needs to be adopted for SUs. As such, SUs need to optimally configure their transmission parameters in order to simultaneously minimize collisions and make the best use of the available opportunities.

Third, to guarantee the compatibility with legacy systems, it is important to define and impose an appropriate interference constraint to sufficiently protect PUs' communications. This is because different definitions of the interference constraint may result in different levels of protection for PUs. Generally, an interference constraint must reflect two parameters: first, the maximum

tolerable interference level at an active primary receiver and second, the maximum tolerable probability that the interference level exceeds its maximum level [7]. However, to precisely define an interference constraint, there are other aspects that need to be addressed. For example, in a cognitive radio network with multiple SUs, the locations of SUs with respect to the primary receiver and the channel propagation characteristics must be considered to set a constraint on the aggregate interference caused by SUs to a PU.

1.4 Thesis Contributions and Organization

Opportunistic spectrum access is a promising approach to overcome the spectrum scarcity and increase the spectral efficiency by taking advantage of unused spectrum that belongs to the incumbent radio systems. Nevertheless, the development of OSA schemes has to deal with many technical and practical issues, so that its full potential can be realized. Addressing the aforementioned technical challenges in a cognitive radio network, the objective of this Ph.D. research is to develop optimal OSA schemes by properly modeling PUs' dynamics and SUs' interactions in a cognitive radio network. In particular, we aim to propose adaptive access schemes for SUs that could effectively handle the tradeoff between the SUs' demand for spectrum access and the PUs' requirement for protection.

Furthermore, our goal is to present solutions that help to achieve a fair and efficient spectrum sharing among the SUs. Given the restrictions on the exchange of overhead information in either infrastructureless or infrastructure-based networks, we aim at developing learning-based distributed algorithms in which system parameters are adapted to their optimal values over time based on the locally available information. In addition, this research attempts to devise a network-level interference constraint imposed on the aggregate transmission activities of all SUs.

The remainder of this thesis is organized as follows. Chapter 2 reviews relevant studies on the OSA design and the aggregate interference analysis in cognitive radio networks that will be used for the development of OSA schemes in the subsequent chapters.

Chapter 3 studies and develops OSA schemes for SUs, taking into account the time-varying and dynamic behavior of PUs. Aiming to reduce the effects of collision between PUs and SUs due to the PU random return, a transmission strategy is proposed for SUs to dynamically hop over multiple idle frequency slots, each with an adaptive activity factor to be determined. Taking into account the spectrum sharing among SUs, the dynamic PU activity and channel characteristics, the SU activity factor optimization problem for maximizing the overall SU throughput is

formulated. More specifically, two sets of constraints are considered to support a fair access and enable orthogonal spectrum sharing in the time domain among individual SUs. Furthermore, the throughput of each user is defined as the successful transmission rate. Subsequently, the optimal OSA algorithm is developed based on the dual decomposition method. By introducing an adaptive carrier sense multiple access (CSMA) scheme, a learning-based distributed access algorithm for SUs is proposed. Using the stochastic gradient descent optimization framework, an analysis is provided on the convergence properties of the proposed algorithm.

Chapter 4 is concerned with the game-theoretic design of the activity factor optimization problem, while using the proposed adaptive CSMA scheme for spectrum sharing among SUs. Via the game theory framework, it is shown that the formulated game is an exact potential game. The conditions assuring the feasibility and optimality of the Nash equilibrium (NE) in this non-cooperative design are examined. To achieve the globally optimum solution, learning algorithms including best-response dynamics and log-linear dynamics are developed. In addition, to reflect the inherent competition among SUs in the adaptive CSMA scheme and to enable contention control, a different design objective is introduced for the activity factor optimization problem. Since the new problem is non-convex, obtaining its globally optimal solution is highly intractable. Thus, the OSA design is cast into a game-theoretic framework that enables a distributed implementation and fast convergence. In the formulated game, each SU selfishly determines its optimal activity factors, without any coordination with other SUs. In this competitive design, it is shown that the NE may be highly inefficient compared to the globally optimal solution of the fully coordinated design. To improve the efficiency of such an NE, the SUs are forced to act in a more cooperative manner by applying a dynamic pricing mechanism. Finally, to reach the steady state, an iterative algorithm based on best-response dynamics is proposed.

Chapter 5 evaluates the performance of the proposed adaptive CSMA scheme by developing an analytical model to compute the system throughput in a single channel. The system throughput is defined and derived as the fraction of opportunities used to successfully transmit data, taking into account the inevitable collisions among SUs. It is shown that the adaptive CSMA scheme is able to intelligently control the contention among the users, while effectively reducing the collision probability. Thus, it achieves a higher throughput compared to the conventional CSMA. This is because the adaptive CSMA allocates a higher chance of transmission to those users with more favorable conditions through granting higher activity factors. Moreover, the effects of network configuration parameters (e.g., the number of users in the network, the minimum contention window, and the packet length) on the throughput performance are investigated.

Chapter 6 studies the OSA design from the PU perspective and proposes a network-level interference constraint to ensure non-intrusive communications of SUs. Given that errors in spectrum opportunity detection are inevitable, a study is presented to examine the aggregate interference induced by SUs to a PU due to miss-detection errors. Specifically, a statistical model of the aggregate interference is provided considering both the random SU locations and the signal attenuation model in a fading environment. Based on the developed statistical model for the interference distribution, the closed-form expressions for capacity-outage probability of the PU are derived to be used as a measure of maintaining PU's QoS in the design of OSA strategy. The effects of the beacon transmitter placement and cooperative sensing on the aggregate interference distribution and capacity-outage performance are also investigated.

Finally, Chapter 7 concludes this thesis with an overall summary of the key results and a brief discussion of possible future research.

Chapter 2

Literature Review

This chapter presents some current state-of-the-art OSA designs for cognitive radio networks, from both SU and PU perspectives. The first part discusses and categorizes the design approaches for opportunistic access of SUs, considering the transmission model of PUs and the network structure of SUs. Then, the second part presents studies on the aggregate interference analysis for PUs.

2.1 Opportunistic Spectrum Access Design

Consider a frequency band licensed to PUs, which is divided into N_p non-overlapping frequency slots (or channels), each with bandwidth $B^i, i = 1, \dots, N_p$. Also, assume a secondary network with N_s SUs looking for temporal spectrum opportunities in these N_p channels. Each SU is assumed to follow a slotted transmission scheme. Each time-slot with an equal duration T consists of two periods: *sensing* of duration τ and *transmission* of duration $(T - \tau)$. Figure 2.1 depicts an example of the general time-slot structure employed by SUs.

In the OSA design, the main objective is to maximize the spectrum utilization of SUs by properly designing their spectrum access strategies, while limiting the conflicts between SUs and PUs. In the following, we categorize the design approaches under two different criteria, including the transmission model of PUs and the network structure for SUs.

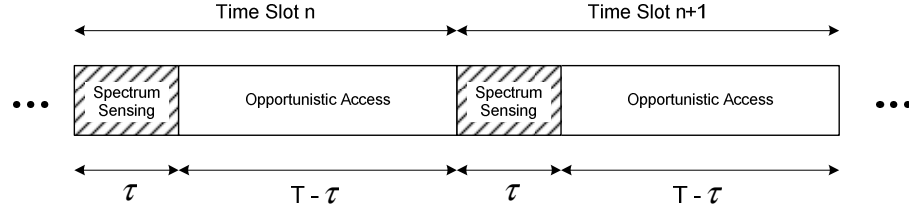


Fig. 2.1 Example of a general 2-phase time-slot structure for SUs.

2.1.1 Time Slotted versus Un-Slotted Transmission Structure for Primary Users

In the OSA design literature, two different transmission structures, i.e., time slotted and un-slotted transmission, are considered for PUs. To develop OSA schemes for SUs, several studies assume that both PUs and SUs have the same transmission time-slot structure [22–26]. In this case, the collision between SUs and PUs occurs only due to the miss-detection errors. With such assumption of synchronous slotted transmission structure, time coordination is required between PU and SU networks. Nevertheless, since time coordination between PU and SU networks cannot be feasible in many scenarios, the transmission of PUs is assumed to be un-slotted in [27–30]. Accordingly, the traffic pattern of PUs is modeled as a continuous-time ON/OFF random process with the ON (1) and OFF (0) states respectively representing the *busy* and *idle* periods of the PU. In this case, even if an idle channel is perfectly detected and used by a SU, a collision can still happen since the PU may return and reoccupy that idle channel at any time during the SU transmission.

Assuming a synchronous slotted transmission structure between PU and SU networks, in [22], an optimal design of OSA is developed. To address hardware limitations and energy costs, it is considered that the SU cannot sense all channels at a certain time. In particular, it is assumed that each SU can sense and access only Q_1 channels in each time-slot, where $Q_1 < N_p$. Prior to start spectrum sensing at the beginning of each time-slot, a SU needs to select a subset \mathcal{A}_s ($|\mathcal{A}_s| \leq Q_1$) of channels to sense. Then, given the sensing observations for channels in \mathcal{A}_s , the SU picks a subset \mathcal{A}_a ($\mathcal{A}_a \subset \mathcal{A}_s$) of the sensed channels to access [22].

In [22], it is assumed that the PU activities in different channels follow a discrete-time Markov process with $M = 2^{N_p}$ states, while each state represents ON/OFF status on all N_p channels. Since the SU is able to sense only parts of the available channels, the overall state of the network is partially observable. Thus, the joint design of sensing and access strategies of a SU is modeled as a partially observable Markov decision process (POMDP) [31]. In the formulated POMDP,

the actions of a SU are sensing and access strategies (i.e., $\{\mathcal{A}_s, \mathcal{A}_a\}$) and the observations of a SU are the results of its sensing. According to the decision and observation history, a SU updates a belief vector which reflects its knowledge about the system state. More specifically, the belief vector of a SU is represented by $\Omega(t) = [\omega_1(t), \dots, \omega_M(t)]$ where $\omega_i(t)$ is the probability that the network is in the state i at the beginning of time-slot t .

In [22], when a SU senses some channels (\mathcal{A}_s) and transmits in a subset of them (\mathcal{A}_a), it then receives a reward which is defined as the number of transmitted bits, i.e.,

$$r(t) = \sum_{i \in \mathcal{A}_a} S_i(t) B^i \quad (2.1)$$

where $S_i(t) \in \{0, 1\}$ is the state of channel i in time-slot t . Subsequently, with a constraint on the maximum collision probability between a SU and a PU, an optimization problem is designed to maximize the expected total number of transmitted bits in N_{ts} time-slots, i.e.,

$$\begin{aligned} \max \quad & \mathbb{E} \left[\sum_{t=1}^{N_{ts}} r(t) | \Omega(1) \right] \\ \text{subject to} \quad & P_{col} \leq \zeta \end{aligned} \quad (2.2)$$

where P_{col} is the probability of collision between the SU and the PU, ζ is the the maximum tolerable probability of collision by the PU, and $\Omega(1)$ is the initial belief vector.

The optimal solution of this POMDP model can be obtained using a linear programming algorithm. However, as the number of channels (i.e., N_p) increases, the computational complexity grows exponentially, due to the state space growth. Thus, by reducing number of states, a suboptimal strategy is also devised with reduced complexity [22]. In addition to the sensing and access strategies, the design of the spectrum sensor operating characteristics is studied in [23], under the assumption of erroneous spectrum sensing.

In [22, 23], it is assumed that the channel occupancy follows a Markovian model for which the state transition probabilities are known to the SUs. However, such information may not be available for the SUs. Assuming that the statistics of the channel availabilities are not available a priori, the studies in [24–26] investigate learning-based OSA approaches for SUs that have partial sensing ability. In [24, 25], the design of optimal sensing and access strategies is formulated as a multi-armed bandit process [32], where there is a tradeoff between using well-explored channels and searching unexplored channels. The study in [26] extends the earlier work in [24]

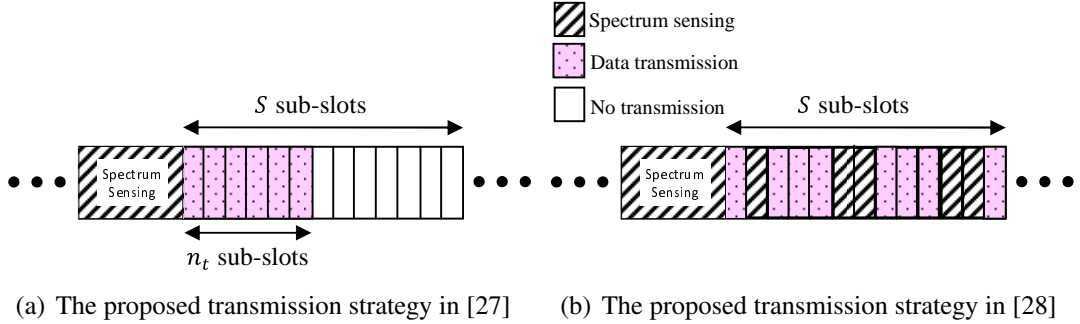


Fig. 2.2 Example of transmission strategies for a single SU proposed in [27, 28].

by considering sensing errors.

Assuming no time coordination between SUs and PUs, in [27], a transmission strategy for a single SU is proposed to prevent a possible collision between the SU and the PU due to the random return of the PU. In the proposed access scheme for the SU, the transmission duration within each time-slot (i.e., $T - \tau$) is divided into S sub-slots. The SU can transmit data in the first n_t consecutive sub-slots. Then, it does not transmit in the remaining $S - n_t$ sub-slots (see Figure 2.2(a)). This transmission strategy helps to reduce the collision probability between the SU and the PU. This is because the PU return probability during the SU transmission is an increasing function of time, given that channel is detected idle in the sensing duration. Subsequently, n_t is optimized based on the PU traffic models, while bounding the collision probability between the SU and the PU below a target level.

In [28], the OSA design is studied for a single SU that shares spectrum with a data-centric PU network (e.g., GSM networks and 802.11-based WLANs). To take advantage of the short-lived opportunities created between the packet bursts in such PU network, a different transmission strategy is proposed for the SU. In the proposed access scheme, the SU can transmit in each separate sub-slot during a transmission duration (see Figure 2.2(b)). Compared to [27], the proposed access strategy in [28] allows more flexibility for the SU to optimize its spectral efficiency. Using a POMDP framework, the SU decides to either access or perform extra spectrum sensing in each sub-slot, by maximizing its probability of successful transmission over S sub-slots.

For a multi-channel scenario, [29] presents an OSA strategy for a single SU. In the proposed method, the SU periodically senses the channels, assuming that the SU can sense only one channel in each sensing phase. Based on the spectrum sensing history, the SU decides either to transmit on one of the channels or not to transmit in each transmission phase. By learning from

the sensing outcomes in different channels, the optimal channel to access is selected by maximizing the SU throughput, while limiting the collision probability caused by a SU to the PU due to sensing errors and PU random return.

When studying OSA design under the effect of PU return, past OSA studies mainly focus on designing optimal channel access schemes, considering a single SU or a simple mechanism for random sharing among SUs without taking into account the competition or coordination among SUs. Thus, further research is needed to develop OSA schemes that apply some sharing incentives among SUs to avoid the channel degradation due to the crowding effects. This coordination can lead to a higher network performance compared to when each SU picks actions independently and competes randomly to capture the channel.

2.1.2 Centralized versus Distributed Design

In the multi-user OSA design, a key challenge is how to coordinate and share opportunities among SUs to achieve a network-level objective. There are two common designs, i.e., centralized and distributed, according to the network architecture. The centralized OSA schemes would be mostly applicable when there exists a central controller, such as a BS, that is responsible for managing the spectrum access of all SUs. When such central controller is not available, for instance in ad-hoc cognitive radio networks, the distributed OSA is required. In the distributed design, each SU separately makes the decision on its own spectrum access strategy [8, 33].

For the centralized design, a central controller synchronizes and coordinates the spectrum allocation and sharing among SUs, aiming to maximize the overall network performance. To obtain the optimal solution, the central controller needs to communicate with SUs in order to know their transmission requirements. Furthermore, it needs to gather and process the information about channel availabilities. The centralized OSA design has been investigated in some recent works (e.g., in [34]). Furthermore, IEEE 802.22 is a centralized standard in which the BS manages the spectrum allocation and sharing among CPEs within its own cell. In IEEE 802.22 MAC, time division multiplexing (TDM) and demand-assigned time division multiple access (TDMA) are respectively used in the down stream and upstream directions [35].

For the distributed design, the spectrum access decisions need to be made independently by each SU. To autonomously access the spectrum, the SU may need to collect and exchange information about the spectrum usage pattern of PUs and other SUs. Based on the available information, the optimal access strategy is obtained by each SU. Corresponding to different design

objectives, the way SUs manage spectrum allocation could be cooperative or non-cooperative. In a cooperative design, each SU optimizes its spectrum access strategy, aiming to enhance the overall performance of the network. However, in a non-cooperative design, each SU maximizes its own benefit, without being concerned about the overall network performance [8, 33]. In the distributed OSA design literature, both ways are explored. On one hand, optimization and cooperative game-theoretic approaches are devised, enabling SUs to achieve a network-level objective (e.g., [36]). On the other hand, non-cooperative game-theoretic designs are applied in which each SU selfishly maximizes its own performance (e.g., [37, 38]).

In distributed OSA schemes, a common way of sharing the spectrum by SUs is to use random access schemes. Accordingly, random access-based MAC protocols are developed in multi-channel and multi-user cognitive radio networks [22, 39–46]. A random access-based MAC protocol should be able to perform the channel contention and reservation to manage the spectrum sharing among SUs. In [22], a simple mechanism is considered for the random sharing among SUs based on the CSMA scheme with an in-band signaling. Nevertheless, the effect of contention among SUs is not reflected in the optimal design of access strategies for SUs. In the proposed method, each SU picks actions independently and competes randomly to capture the channel. In [39, 40], SUs perform contention on an out-of-band control channel prior to the optimization process. In each time-slot, the winner of the contention continues to find its optimal sensing and access strategy. Since the winning SU is able to sense only a subset of channels (i.e., \mathcal{A}_s), there might be spectrum opportunities that are overlooked and wasted in each time-slot [47].

Such random access-based MAC schemes, in comparison with contention-free centralized protocols, degrade the channel utilization because of collision avoidance overheads and inevitable collisions among users. Therefore, to improve the efficiency and throughput, efforts have been exerted on optimizing random access performance. For example regarding IEEE 802.11 MAC operation, there are two different directions in MAC enhancement studies, including collision avoidance overhead reduction (e.g., [48–51]) or/and collision probability decrease (e.g., [52–56]).

On one hand, to decrease the collision avoidance overhead, IEEE 802.11e amendment offers frame bursting in which the user that obtains transmission opportunity (after winning in the backoff competition) can send a burst of back-to-back packets based on its channel quality [48]. Furthermore, MAC frame aggregation is introduced in IEEE 802.11n to decrease the frequency of PHY and MAC overheads during transmission of multiple packets [49]. In the frame aggregation, by concatenating or packing multiple packets together, overheads can be added over a group of packets rather than over separate ones [49].

On the other hand, to reduce the collision probability, there are works that focus on optimizing backoff algorithms, and hence, maximizing the overall throughput. For instance, in [52, 53], the contention window size is optimized depending on the network and load configuration (e.g., number of active users and packet length) to control contention among users. In [54], a collision-minimizing CSMA is proposed in which the probability distribution using which users randomly select their backoff time is not necessarily uniform; rather, it is carefully chosen to minimize the collision among the competing users. Furthermore, in [55], an opportunistic CSMA scheme is proposed in which throughput is improved by exploiting the multi-user diversity gain. The proposed opportunistic CSMA prioritizes the users with high-SNRs by granting earlier access to them.

2.2 Aggregate Interference Analysis

Recently, the characteristics of aggregate interference caused by multiple SUs in a cognitive radio network have been investigated in several works. Past studies mostly study the aggregate interference analysis for a cognitive radio network, considering the underlay spectrum access model [57–62]. The underlay paradigm allows SUs to concurrently transmit with PUs in the licensed spectrum band, while maintaining the aggregate interference induced by SUs to PUs below a certain threshold [12]. In the underlay cognitive radio networks, the aggregate interference analysis does not take into account the sensing errors.

In this thesis, our focus is on cognitive radio networks with OSA in which SUs identify and utilize spectrum holes in the licensed spectrum band. In the context of cognitive radio networks with OSA, interference characteristics have been explored in [63–67]. In [63], the effects of power control and sensing performance on the aggregate interference are discussed in a cognitive radio network where SUs are scattered continuously around the primary transmitter. Nevertheless, the aggregate interference is modeled as a deterministic value since the random locations and sensing errors (due to fading) are not taken into account. Addressing random variations in both SUs' locations and propagation characteristics, efforts have been made to study the statistical model of the aggregate interference in a cognitive radio network with OSA (e.g., [64–67]).

In [64], the probabilistic properties of the aggregate interference are investigated by considering random variations in the number and location of SUs, as well as the signal attenuation model in a fading environment. In that study, it is assumed that SUs spread out according to an homogenous Poisson point process of intensity λ_d around the PU receiver which is placed at the

center. In a Poisson point process of intensity λ_d , the number of SUs in a region \mathcal{R} of area A is a Poisson random variable with parameter $\lambda_d A$. Furthermore, the propagation power loss of SU k at distance r_k from the PU receiver is modeled by $|\tilde{h}_k|^2 r_k^{-\alpha}$, where $r_k^{-\alpha}$ is the distance-dependent path-loss with the path-loss exponent $\alpha \geq 2$, and \tilde{h}_k is a unit-mean random variable representing the small-scale fading effects. It is assumed that $|\tilde{h}_k|^2, k = 1, \dots, N_s$ are independent and identically distributed (i.i.d.) for different SUs, each with probability density function (PDF) of $f_H(\tilde{h})$.

Subsequently, assuming that all SUs transmit at the same constant power level P , the aggregate interference (i.e., I_0) is represented as

$$I_0 = \sum_{k \in \Pi_t} P |\tilde{h}_k|^2 r_k^{-\alpha} \quad (2.3)$$

where Π_t is the set of transmitting SUs due to the erroneous sensing. It is shown that Π_t can be modeled as a different Poisson point process with a different intensity, given by

$$\lambda_t(r, \tilde{h}) = \lambda_d f_H(\tilde{h}) P_m(r, \tilde{h}) \quad (2.4)$$

where $P_m(r, \tilde{h})$ represents the miss-detection probability of each SU, which is a function of its location and fading. By developing the statistical characteristics of I_0 , the distribution of the aggregate interference is approximated by a shifted log-normal distribution with the same mean and variance as I_0 [64].

Assuming a network model with a different distribution for SUs, [65] studies the aggregate interference caused by SUs to a PU. It is assumed that N_s SUs are uniformly located with a density of λ_d SUs per unit area in a ring centered at the PU receiver. Accordingly, the aggregate interference (i.e., I_0) is represented as

$$I_0 = \sum_{k=1}^{N_s} P_{m,k} P |\tilde{h}_k|^2 r_k^{-\alpha} \quad (2.5)$$

where $P_{m,k}$ represents the miss-detection probability of SU k . The upper bounds for mean and variance of aggregate interference in Rayleigh fading channels are derived. Furthermore, the aggregate interference is approximately modeled with a Gaussian random variable (based on the central limit theorem) for a large number of SUs. However, it has been shown that the aggregate interference is in fact a positively-skewed and right-tailed random variable.

Moreover, a statistical model for the aggregate interference caused by SUs is developed in [66], although only the path loss is considered for the propagation channels. In [67], the characteristic function and the cumulants of the aggregate interference are numerically derived considering fading channels. Subsequently, the aggregate interference distribution is approximately characterized with truncated-stable distributions.

2.3 Concluding Remarks

In this chapter, we have provided a survey on the available techniques in the OSA design for SUs and statistical models in the aggregate interference analysis for PUs in cognitive radio networks. For the OSA design, it has been discussed that the assumption about the transmission structure of PUs plays an important role. Only a limited number of works, such as [27–30], have considered the OSA design under the assumption of no time coordination between SUs and PUs. However, these proposed schemes mainly focus on the design for a single SU. Furthermore, in a ad-hoc cognitive radio network, there is a need for a fully distributed OSA design with the cooperative behavior for SUs. These observations motivate us to study the distributed OSA design in a multi-user cognitive radio network, considering the effect of random returns of PUs.

For the aggregate interference analysis, previous research has mainly examined modeling the aggregate interference without measuring the effect of this interference to the PU performance. This motivates us to study the aggregate interference and the PU performance in the presence of interference, aiming to examine the effects of system parameters, such as the sensing capability and the density of SUs.

Chapter 3

Opportunistic Spectrum Access with Hopping Transmission Strategy in Cognitive Radio Networks

3.1 Introduction

As previously discussed in Chapter 1, the development and implementation of OSA schemes in the cognitive radio environment involve challenges that are not present in the existing radio systems. More specifically, in a cognitive radio network, each SU needs to identify spectrum opportunities, coordinate their sharing with other competing SUs, and release them when they are acquired by PUs. Since PUs have higher priority to access the spectrum, two conflicting objectives arise in designing an optimal OSA scheme for SUs. In particular, the opportunistic spectrum utilization of SUs needs to be maximized, while possible collisions between SUs to PUs must be kept limited [22, 29]. Considering such conflicts between SUs and PUs, in this chapter¹, we aim to develop an efficient OSA strategy for the SUs.

Recently, the design of OSA schemes has received considerable attention [6–9, 20, 33]. There are several OSA strategies presented in the literature that allow SUs to choose a frequency slot (or channel) to sense and, if available, access for an entire transmission duration. These strategies assume that both PUs and SUs have the same transmission time-slot structure [22–26]. Such

¹Parts of Chapter 3 have been presented at the 2011 IEEE Global Communications Conference (GLOBECOM) in Houston, TX, USA [68] and the 2012 IEEE Wireless Communications and Networking Conference (WCNC) in Paris, France [69], and published in the IEEE Transactions on Wireless Communications [70].

assumption of synchronous slotted transmission structure between PU and SU networks is not a sensible assumption since it needs good coordination in time between the PU and SU networks. Without assuming synchronization between PUs and SUs, PU activity in a channel with respect to SUs is dynamic and can be represented as a continuous-time ON/OFF random process (e.g., [71]). As a result, even if an idle channel is perfectly detected and used by a SU, a collision can still occur since the PU may return and reoccupy that idle channel at any time during the SU transmission.

To deal with the aforementioned issue, in this chapter, we propose an adaptive hopping transmission strategy for SUs. In particular, this transmission strategy aims to reduce the effects of collision between PUs and SUs due to PU return in consideration of the PU dynamics assuming no time coordination between SUs and PUs. In the proposed scheme, instead of sensing and selecting one idle channel for the entire transmission as in previous studies, the SU accesses multiple idle channels, each with a different sojourn time (called activity factor). In this case, possible PU return in a channel may destroy only a small fraction of the SU transmission that can be recovered by erasure-correction coding to improve the SU transmission performance. Taking into account spectrum sharing among SUs, the dynamic PU activity, and also channel characteristics, the SU activity factor optimization problem is formulated to maximize the overall SU throughput. Subsequently, optimal OSA algorithms are developed for SUs, based on the Lagrange dual decomposition method.

In addition, the proposed dual decomposition method—that provides a global solution to the optimization problem with affordable complexity—gives rise to the realization of distributed implementation. In other words, the optimal OSA algorithm can be potentially performed in a distributed manner by each SU, provided that the knowledge of other SUs' activity factors are available. Such information can be obtained either with the aid of a central coordinator or by exchange of overhead information among SUs which may cause complexity and result in an un-scalable system. Consequently, we present an OSA algorithm in which each SU adjusts its activity factors independently by learning from the locally available information. In the proposed OSA algorithm, each SU learns to respond optimally to its environment and adapts its activity factors to the optimal values over time. This fully distributed learning-based OSA algorithm distinguishes this work in coordinating spectrum access among SUs from the previously proposed channel assignment schemes for SUs with support of a central controller (e.g., [34]) or exploiting a common control channel (e.g., [39]).

The implementation of the proposed learning-based OSA depends on the estimation of the

sum of activity factors of all SUs in each channel. Since estimation with limited samples suffers from random errors, the proposed learning-based OSA algorithm can be cast in the framework of stochastic gradient descent optimization. We analytically investigate its convergence and convergence rate to characterize its asymptotic behavior and efficiency. The main difficulty in analyzing its convergence properties lies in the fact that the estimation errors are biased.

The remainder of this chapter is organized as follows. Section 3.2 presents an overview of the system model and problem formulation. In Section 3.3, the proposed OSA scheme using adaptive hopping-based transmission strategy is developed and the corresponding optimization problem is formulated to derive the optimum activity factors for SUs. Next, in Section 3.4, we develop a fully distributed learning-based OSA algorithm, which can be formulated as a stochastic gradient descent method. Subsequently, in Section 3.5, its convergence behavior and convergence rate are analyzed in consideration of biased noisy feedbacks. Illustrative results are provided in Section 3.6. Finally, Section 3.7 presents the concluding remarks.

3.2 System Model and Problem Formulation

We consider a frequency band licensed to PUs, which is divided into N_p non-overlapping frequency slots (or channels), each with bandwidth B^i . The frequency channels are chosen such that multipath fading can be considered constant (i.e., flat fading) over each channel (e.g., orthogonal frequency-division multiplexing (OFDM) narrowband subcarriers). Furthermore, we consider an ad-hoc secondary network with N_s SUs looking for temporal spectrum opportunities in these N_p channels. SUs are assumed to follow a slotted transmission scheme. Each time-slot of equal duration T consists of two periods: *sensing* of duration τ and *transmission* of duration $(T - \tau)$. In this work, we assume sufficiently accurate sensing with negligible PU miss-detection. Perfect sensing could be a sensible assumption in certain scenarios, e.g., applications in which SUs are located inside the service area of the PU transmitter (e.g., [71]).

Let $\mathcal{N}_a := \{1, \dots, N_a\}$ denote the set of N_a channels that are detected idle at the beginning of each time-slot, and hence, can be utilized by N_s SUs. In this work, we assume that SUs are able to perform full spectrum sensing of N_p channels to find the idle channels in each time-slot. Furthermore, let C_k^i reflect channel quality (i.e., bits per second) for the SU k in the channel i and $g_{k,k}^i$ denote the power gain of the SU link k in the channel i . Consider a block flat fading situation in which $g_{k,k}^i$ remains unchanged during a given time-slot but independently varies from one time-slot to another. Thus, the transmission capacity of SU k in channel i is $B^i \log(1 + P_k^i g_{k,k}^i / n_k^i)$

where P_k^i and n_k^i represent the signal power and the noise power for the SU k in the channel i , respectively. In this work, without loss of generality, we consider the transmission capacity of SU k in channel i as a measure for C_k^i .

In general, the PU can use a time frame different from that of SUs. From the SU viewpoint, the PU activity in a given channel can be modeled as a two-state continuous-time random process with the ON (1) and OFF (0) states representing the *busy* and *idle* periods of the PU, respectively.

Given that channel i is detected idle in the sensing slot, the conditional probability that it becomes busy t seconds later is denoted by $\pi_{01}^i(t)$ which is an increasing function of time. Note that, by properly designing transmission slot duration (i.e., $T - \tau$), the increase of instantaneous PU return probability over a transmission slot can be kept negligible. Subsequently, the probability—that the PU reoccupies channel i in a transmission slot given that channel i is detected idle in the sensing slot at the beginning of that time-slot—is defined as the average of instantaneous probability of PU return over the whole transmission time, i.e., $\alpha_i = \frac{1}{T-\tau} \int_{t=0}^{T-\tau} \pi_{01}^i(t) dt$. As a result, α_i is a time-independent function, however, it is still a function of spectrum usage statistics of the primary users. On one hand, the PU return causes collision for the PU. In order to protect the PU transmission quality, α_i can be kept smaller than a required level by designing proper transmission duration (i.e., $T - \tau$). For instance, in [72, 73], it is demonstrated that by selecting a suitable spectrum sensing time and a transmission time, the SU can maximize its achievable throughput under the constraint that PUs are adequately protected.

On the other hand, the PU return may destroy the entire on-going SU transmission in the channel i . To avoid such a serious data loss due to the PU return, we propose an adaptive transmission strategy for SUs in which a SU dynamically hops over *multiple idle* channels, each with an unequal sojourn time (called activity factor) to be determined, so that possible PU return in a channel may destroy only a small fraction of the SU transmission that can be recovered by erasure-correction coding. Let β_k^i ($0 \leq \beta_k^i \leq 1$) denote the activity factor of SU k in channel $i \in \mathcal{N}_a$ during a transmission slot. The activity-factor matrix of all β_k^i of all N_s SUs in N_a idle

channels can be presented as $\beta = \begin{bmatrix} \beta_1^1 & \dots & \beta_1^{N_a} \\ \vdots & \ddots & \vdots \\ \beta_{N_s}^1 & \dots & \beta_{N_s}^{N_a} \end{bmatrix}$.

Note that β_k^i is restricted to a binary value in previous studies [22–26, 74, 75], such that $\beta_k^i = 0$ expresses that the SU k does not transmit in the channel i and $\beta_k^i = 1$ represents that the SU k transmits in the channel i for the entire transmission slot. Therefore, the proposed transmission scheme with $0 \leq \beta_k^i \leq 1$ generalizes the existing schemes. Figure 3.1 illustrates an example of a

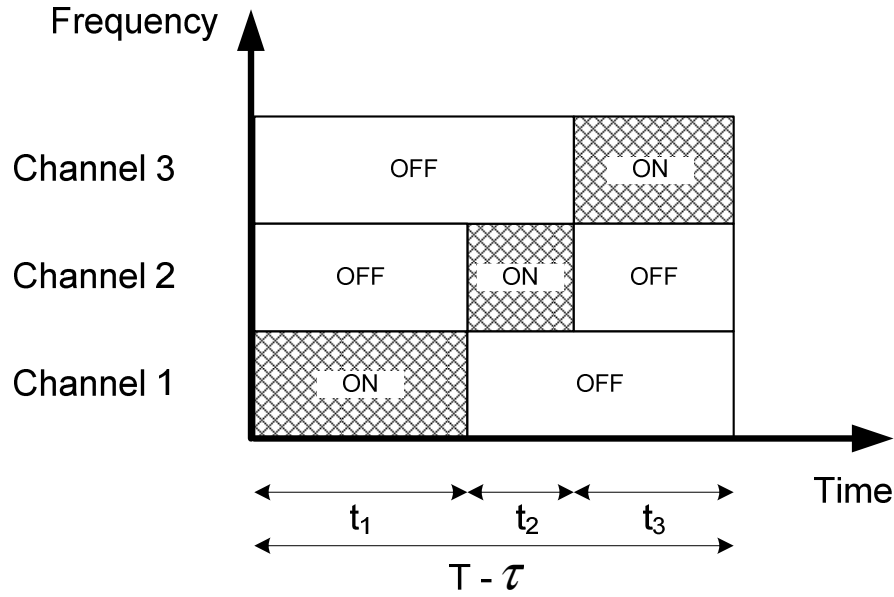


Fig. 3.1 An example of a SU activity in three idle channels with different activity factors during a transmission slot.

SU activity according to the proposed hopping transmission strategy during a single transmission slot. In this example, assuming that the SU needs one channel for its transmission and $N_a = 3$, the activity factors of the SU in the different channels can be calculated as $\beta_k^i = \frac{t_i}{T - \tau}$, $i = 1, 2, 3$.

To coordinate spectrum access among SUs, we assume that SUs share an idle channel orthogonally in time domain, and hence, there is no mutual interference between SUs. Since one SU can exclusively use an idle channel at a certain point of time during each transmission slot, it is needed to assure that the total activity factors of different SUs in each idle channel remains smaller than 1. This constraint guarantees possible orthogonal sharing in time for each idle channel. Thus, $\sum_{k=1}^{N_s} \beta_k^i \leq 1, i = 1, \dots, N_a$.

Consider that the SU k needs a fixed number of channels, R_k , for its transmission during a single transmission slot. It follows that the sum of all activity factors of each SU k over all idle channels must equal its required number of channels, i.e., $\sum_{i=1}^{N_a} \beta_k^i = R_k$.

The normalized transmission rate of SU k in channel i is $\beta_k^i C_k^i$ since it transmits partially with activity factor β_k^i . Taking into account the possible loss in SU transmission due to PU return in each idle channel i with probability of α_i , the throughput of SU k in the idle channel i is defined

as its *successful* transmission rate

$$f_k^i = \beta_k^i C_k^i (1 - \beta_k^i \alpha_i) \quad (3.1)$$

where $\beta_k^i \alpha_i$ expresses the probability that the SU k experiences transmission loss due to the PU return. In other words, the PU return probabilities, α_i , enable modeling the effect of dynamic PU activities on SU performance.

The goal of this work is to develop a resource allocation scheme that determines the optimal activity factors for N_s SUs in N_a idle channels in a single transmission slot to maximize the overall throughput of all SUs (i.e., $f = \sum_{k=1}^{N_s} \sum_{i=1}^{N_a} f_k^i$) under constraints of ensuring possible orthogonal time sharing in each idle channel (i.e., $\sum_{k=1}^{N_s} \beta_k^i \leq 1$) and fixed channel requirements for SUs (i.e., $\sum_{i=1}^{N_a} \beta_k^i = R_k$).

3.3 Optimal Hopping-Based Opportunistic Spectrum Access

In this section, we study optimization problems which offer optimum activity factors considering the adaptive hopping-based transmission strategy for SUs. First, the activity factor optimization problem is developed for a single SU to find the best solution for each SU without consideration of the spectrum sharing with the other SUs. Then, the activity factor optimization problem formulation and algorithm development are discussed for multiple SUs.

3.3.1 Single-User Opportunistic Spectrum Access

We first consider the activity factor optimization problem for a single SU. The index of SU k is set to 1 without loss of generality in this section. In this case, the optimization problem can be formulated as

$$\max_{\beta_1} \sum_{i=1}^{N_a} \beta_1^i C_1^i (1 - \beta_1^i \alpha_i) \quad (3.2a)$$

$$\text{subject to } \sum_{i=1}^{N_a} \beta_1^i = R_1 \quad (3.2b)$$

$$0 \leq \beta_1^i \leq 1, \quad i = 1, \dots, N_a. \quad (3.2c)$$

Note that the objective function in (3.2a) expresses the overall SU throughput over all idle channels and R_1 in (3.2b) represents the channel requirement of the SU. Based on (3.1), the overall throughput of the SU k over all idle channels can be simply presented by $\sum_{i=1}^{N_a} f_k^i$ due to independent activity of the SU k over different idle channels. Note that there are no specific assumptions on the joint distribution of the PU activities to formulate the overall throughput in (3.2a).

Since the objective function in (3.2a) is concave (i.e., the negative of objective function is convex) and the equality constraint in (3.2b) is a linear function of $\beta_1 = [\beta_1^1, \dots, \beta_1^{N_a}]$, this problem is a convex optimization with a coupling constraint in (3.2b). A dual decomposition is an appropriate approach to solve the convex problem with zero duality gap when the problem has coupling constraints. By relaxing the coupling constraints, the optimization problem decouples into several sub-problems [76]. To relax the coupling constraint in (3.2b), it makes sense to write the Lagrangian function of (3.2) as

$$\mathcal{L}(\lambda, \beta_1) = \sum_{i=1}^{N_a} \beta_1^i C_1^i (1 - \beta_1^i \alpha_i) - \lambda \left(\sum_{i=1}^{N_a} \beta_1^i - R_1 \right) \quad (3.3)$$

where λ denotes the Lagrange multiplier corresponding to (3.2b). The optimization problem can be separated into two levels of optimization. At the lower level, there are N_a sub-problems for each idle channel with Lagrangian $\mathcal{L}(\lambda, \beta_1^i) = \beta_1^i C_1^i (1 - \beta_1^i \alpha_i) - \lambda \beta_1^i$ assuming λ is fixed. Subsequently, it can be solved by writing the the Karush-Kuhn-Tucker (KKT) conditions

$$\frac{\partial \mathcal{L}(\lambda, \beta_1^i)}{\partial \beta_1^i} = C_1^i - 2C_1^i \beta_1^i \alpha_i - \lambda = 0. \quad (3.4)$$

Then, considering $0 \leq \beta_1^i \leq 1$, we obtain $\beta_1^i(\lambda) = \left[\frac{C_1^i - \lambda}{2C_1^i \alpha_i} \right]_0^1$ where $[x]_a^b = \min(b, \max(a, x))$. At the higher level, there is the master dual problem responsible for updating the dual variable (i.e., λ) by solving the dual problem. Then, λ can be found iteratively with the help of the following gradient method

$$\lambda^{n+1} = \lambda^n + \varepsilon \left(\sum_{i=1}^{N_a} \beta_1^i(\lambda^n) - R_1 \right) \quad (3.5)$$

where n is the iteration index, ε is a sufficiently small positive step-size. Since the proposed transmission strategy generalizes the existing approaches, the non-binary optimal activity factors

prove the benefit of the proposed approach over the existing schemes in offering throughput improvement. This can be explained by the fact that using more idle channels, each of them for a fraction of transmission slot, helps the SU to decrease transmission loss due to the collision caused by the PU return.

Assuming that there is a λ such that $0 \leq \frac{C_1^i - \lambda}{2C_1^i \alpha_i} \leq 1$, $\forall i \in \mathcal{N}_a$, then, $\beta_1^i = \frac{C_1^i - \lambda}{2C_1^i \alpha_i}$, and, according to the equality constraint (3.2b),

$$\sum_{i=1}^{N_a} \frac{C_1^i - \lambda}{2C_1^i \alpha_i} = R_1 \Rightarrow \lambda = \frac{\sum_{i=1}^{N_a} \frac{1}{2\alpha_i} - R_1}{\sum_{i=1}^{N_a} \frac{1}{2C_1^i \alpha_i}}. \quad (3.6)$$

Therefore, the optimum activity factor in the channel i can be represented as

$$\beta_1^i = \frac{R_1 + C_1^i \sum_{i=1}^{N_a} \frac{1}{2C_1^i \alpha_i} - \sum_{i=1}^{N_a} \frac{1}{2\alpha_i}}{2C_1^i \alpha_i \sum_{i=1}^{N_a} \frac{1}{2C_1^i \alpha_i}}. \quad (3.7)$$

3.3.2 Multi-User Opportunistic Spectrum Access

Considering multiple SUs in a secondary network, the problem of spectrum sharing affects the design of OSA. To coordinate the spectrum access among SUs, we assume that SUs share an idle channel orthogonally in time domain, and hence, there is no mutual interference between SUs. The goal is to maximize the overall throughput of SUs (i.e., $\sum_{k=1}^{N_s} \sum_{i=1}^{N_a} f_k^i$) under constraints of ensuring possible orthogonal time sharing in each idle channel and fixed channel requirements for SUs. More specifically, the optimization problem can be formulated as

$$\max_{\boldsymbol{\beta}} \sum_{k=1}^{N_s} \sum_{i=1}^{N_a} \beta_k^i C_k^i (1 - \beta_k^i \alpha_i) \quad (3.8a)$$

$$\text{subject to } \sum_{k=1}^{N_s} \beta_k^i \leq 1, \quad i = 1, \dots, N_a \quad (3.8b)$$

$$\sum_{i=1}^{N_a} \beta_k^i = R_k, \quad k = 1, \dots, N_s \quad (3.8c)$$

$$0 \leq \beta_k^i \leq 1, \quad i = 1, \dots, N_a, \quad k = 1, \dots, N_s. \quad (3.8d)$$

It is worth mentioning that the feasibility criterion for the above optimization problem is $\sum_{k=1}^{N_s} R_k \leq N_a$. In other words, when the demand of all SUs combined (i.e., $\sum_{k=1}^{N_s} R_k$) is larger than the

number of accessible idle channels (i.e., N_a), it is not possible to select a matrix of activity factors (i.e., β) which satisfies all constraints.

This problem is a convex optimization with coupling constraints in (3.8b) and (3.8c). In order to decouple this problem, first, a dual decomposition with respect to (3.8b) and then, for the sub-problem, another dual decomposition with respect to (3.8c) are applied. This offers a two-level optimization decomposition including a master dual problem, a secondary master dual problem, and the sub-problems [76]. By taking a relaxation of the coupling constraints in (3.8b), the Lagrangian function of the optimization problem in (3.8) becomes

$$\max_{\beta} \sum_{k=1}^{N_s} \sum_{i=1}^{N_a} \beta_k^i C_k^i (1 - \beta_k^i \alpha_i) - \sum_{i=1}^{N_a} \mu_i \left(\sum_{k=1}^{N_s} \beta_k^i - 1 \right) \quad (3.9)$$

where $\mu_i \geq 0$ is the Lagrange multiplier associated with (3.8b). Therefore, at the lower level, for fixed μ_i , there are N_s sub-problems with the following objective function for each SU

$$\max_{\beta_k} \sum_{i=1}^{N_a} \beta_k^i C_k^i (1 - \beta_k^i \alpha_i) - \sum_{i=1}^{N_a} \mu_i \beta_k^i \quad (3.10a)$$

$$\text{subject to } \sum_{i=1}^{N_a} \beta_k^i = R_k \quad (3.10b)$$

$$0 \leq \beta_k^i \leq 1, \quad i = 1, \dots, N_a \quad (3.10c)$$

where $\beta_k = [\beta_k^1, \dots, \beta_k^{N_a}]$. The Lagrangian function of (3.10) for fixed $\mu = [\mu_1, \dots, \mu_{N_a}]$ is

$$\begin{aligned} \mathcal{L}(\lambda_k, \mu, \beta_k) &= \sum_{i=1}^{N_a} \beta_k^i C_k^i (1 - \beta_k^i \alpha_i) \\ &\quad - \sum_{i=1}^{N_a} \mu_i \beta_k^i - \lambda_k \left(\sum_{i=1}^{N_a} \beta_k^i - R_k \right) \end{aligned} \quad (3.11)$$

where λ_k is the Lagrange multiplier associated with (3.10b). This optimization problem can also be separated into two levels of optimization. At the lower level, there are N_a sub-problems for each idle channel with Lagrangian $\mathcal{L}(\lambda_k, \mu_i, \beta_k) = \beta_k^i C_k^i (1 - \beta_k^i \alpha_i) - \mu_i \beta_k^i - \lambda_k \beta_k^i$ assuming λ_k

is fixed. Subsequently, it can be solved by writing the KKT conditions

$$\frac{\partial \mathcal{L}(\lambda_k, \mu_i, \beta_k)}{\partial \beta_k^i} = C_k^i - 2C_k^i \beta_k^i \alpha_i - \mu_i - \lambda_k = 0. \quad (3.12)$$

Then, considering $0 \leq \beta_k^i \leq 1$,

$$\beta_k^i(\lambda_k, \mu_i) = \left[\frac{C_k^i - \mu_i - \lambda_k}{2C_k^i \alpha_i} \right]_0^1 \quad (3.13)$$

where $[x]_a^b = \min(b, \max(a, x))$. At the higher level, there exists the secondary master dual problem responsible for updating the dual variable λ_k by solving the secondary dual problem. Then, λ_k can be found iteratively with the help of the following gradient method

$$\lambda_k^{n+1} = \lambda_k^n + \nu_n \left(\sum_{i=1}^{N_a} \beta_k^i(\lambda_k^n, \mu_i^n) - R_k \right) \quad (3.14)$$

where n is the iteration index and $\nu_n > 0$ is a sequence of scalar step-sizes. λ_k (called SU k price) is updated until satisfying the channel requirement for the SU k . Then, at the highest level, μ_i (called channel i price) is updated with a slower rate until satisfying $\sum_{k=1}^{N_s} \beta_k^i \leq 1$. The μ_i can be found iteratively with the help of gradient approach. The following gradient method can be used

$$\mu_i^{n+1} = \left[\mu_i^n + \gamma_n \left(\sum_{k=1}^{N_s} \beta_k^i(\lambda_k^n, \mu_i^n) - 1 \right) \right]^+ \quad (3.15)$$

where $\gamma_n > 0$ is a sequence of scalar step-sizes. Also, $[\cdot]^+$ denotes the projection onto the non-negative space. The dual variables will converge to the dual optimals as long as ν_n and γ_n are chosen to be sufficiently small. Some popular choices include constant value $\delta > 0$ or diminishing functions of time as an^{-c} for some constants $a > 0$ and $0 < c \leq 1$. Since the duality gap is zero due to the convex optimization, the primal variable β_k^i will also converge to the optimal value as well.

Based on the above derivations, we present the optimal OSA scheme in Algorithm 1, with an inner loop to update the SU prices (i.e., λ_k) and an outer loop to update the channel prices (i.e., μ_i). Algorithm 1 needs to be performed at the beginning of every time-slot of duration T to find the optimal activity factors of SUs. However, considering slowly varying statistics of PU activity

Algorithm 1 Optimal OSA

-
- 1 Set $n = 0$, μ_i^0 equal to some non-negative value for all i and λ_k^0 equal to some value for all k .
 - 2 β_k^i is computed for all k and i according to (3.13).
 - 3 Fast price updating: each SU price λ_k is updated with the gradient iteration (3.14).
 - 4 Set $n \leftarrow n + 1$ and go to step 2 (until satisfying termination criterion).
 - 5 Slow price updating: each channel price μ_i is updated according to the gradient iteration (3.15).
 - 6 Go to step 2 (until satisfying termination criterion).
-

and slow fading, the frequency that optimization problem needs to be solved will decrease. In Algorithm 1, it is noted that a central coordinator is responsible to manage the sequence of access of different users in different channels based on their optimal activity factors.

Apparently, Algorithm 1 (i.e., the optimal OSA) can be potentially performed in a distributed manner by each SU. However, from (3.15), it is obvious that each SU needs to know the sum of activity factors of all N_s SUs in the idle channel i , $\beta^i = \sum_{k=1}^{N_s} \beta_k^i(t)$, to update the channel price μ_i . Such information can be obtained with the aid of a central coordinator or heavy exchange of overhead information which causes complexity and results in an un-scalable system. It is thus crucial that SUs learn this information to update channel prices independently which will be used to adjust their activity factors. It is noted that perfect knowledge of channel gains are required to update β_k^i based on (3.13). However, in the potential distributed implementation, each SU needs only the channel state information of its own link (i.e., the channel state information of other SU links are not required).

3.4 Learning-Based Distributed Opportunistic Spectrum Access

In this section, to enable distributed implementation of the optimal OSA scheme, an adaptive carrier sensing multiple access (CSMA) scheme is devised as a decentralized mechanism to access an idle channel for SUs based on their activity factors. Then, we discuss how to use the capturing status feedbacks of the proposed adaptive CSMA scheme to estimate the sum of activity factors of all SUs in each idle channel, which will be employed to update the channel prices (i.e., μ_i). Subsequently, we model channel price updating as a stochastic gradient descent method

considering erroneous estimations of β^i .

It is proposed that SUs share idle channels by means of an adaptive CSMA based on their activity factors without a central coordinator. In the adaptive CSMA scheme, each transmission slot is divided into S equal sub-slots with length $\frac{T-\tau}{S}$, labeled t_1, \dots, t_S . In each sub-slot t_j in channel i , the SU k performs the following steps:

- 1- Generate a Bernoulli random variable $x_k^i(t_j)$ with the success probability β_k^i to be determined. If $x_k^i(t_j) = 0$, the SU k will not transmit in the subslot t_j . If $x_k^i(t_j) = 1$, the SU k will proceed to the next step.
- 2- Generate a backoff time $W_k^i(t_j)$ according to a uniform distribution in the interval $(0, W)$.
- 3- After expiry of the backoff time, sense the channel i , if it is idle, transmit.

In this proposed adaptive CSMA scheme, one SU with the smallest backoff time among the SUs who compete for the same sub-slot (i.e., $x_k^i(t_j) = 1$) will succeed and transmit in this sub-slot. Let $y_k^i(t_j)$ be a binary random variable representing the capturing status: $y_k^i(t_j) = 1$ if the SU k captures the channel i in sub-slot t_j ; otherwise, $y_k^i(t_j) = 0$.

Assuming that each SU k keeps track of its capturing status feedbacks, $y_k^i(t_j)$, the *achieved* activity factor of SU k in the channel i (i.e., the average time proportion of a transmission slot that an SU *successfully* occupies the channel i , given the competition among SUs) can be obtained as

$$\bar{\beta}_k^i = \frac{\text{E} \left[\sum_{j=1}^S x_k^i(t_j) y_k^i(t_j) \right]}{S}. \quad (3.16)$$

Then,

$$\begin{aligned} \bar{\beta}_k^i &= \text{Prob} [y_k^i(t_j) = 1, x_k^i(t_j) = 1] \\ &= \beta_k^i \text{Prob} [y_k^i(t_j) = 1 | x_k^i(t_j) = 1] \end{aligned} \quad (3.17)$$

where $\beta_k^i = \text{Prob}[x_k^i = 1]$ represents the *intended* activity factor of SU k in channel i . The probability of getting the smallest backoff time to capture the channel is inversely proportional to the number of SUs actively competing to capture the same channel, i.e.,

$$\text{Prob} [y_k^i(t_j) = 1 | x_k^i(t_j) = 1] = \text{E} \left[\frac{1}{1 + \sum_{\bar{k}=1, \bar{k} \neq k}^{N_s} x_{\bar{k}}^i(t_j)} \right]. \quad (3.18)$$

Applying the Jensen's inequality, $\text{Prob}[y_k^i(t_j) = 1 | x_k^i(t_j) = 1] \geq \frac{1}{1 + \sum_{\bar{k}=1, \bar{k} \neq k}^{N_s} \beta_{\bar{k}}^i}$. In order to find a closed-form expression, $\text{Prob}[y_k^i(t_j) = 1 | x_k^i(t_j) = 1]$ is approximated with the lower-bound, i.e.,

$$\bar{\beta}_k^i \simeq \frac{\beta_k^i}{1 + \sum_{\bar{k}=1, \bar{k} \neq k}^{N_s} \beta_{\bar{k}}^i}. \quad (3.19)$$

Note that (3.19) shows that the *achieved* activity factor of each SU using the proposed CSMA scheme depends on the *intended* activity factor of other SUs. However, by keeping $\sum_{k=1}^{N_s} \beta_k^i \leq 1$, it can be guaranteed that the *achieved* activity factor is always larger than the half of *intended* activity factor (i.e., $\bar{\beta}_k^i \geq \frac{\beta_k^i}{2}$). Thus, to reduce computational complexity, here, we consider the similar utility function as in (3.8), along with $\sum_{k=1}^{N_s} \beta_k^i \leq 1$ to manage competition among SUs. Note that this helps to alleviate *achieved* activity factor (i.e., $\bar{\beta}_k^i$) degradation due to the crowding effects.

Apparently, in Algorithm 1, each SU k needs the sum of the activity factors of all N_s SUs in channel i , $\sum_{k=1}^{N_s} \beta_k^i$, to update the channel price μ_i in (3.15). From (3.19), the SU k can estimate $\sum_{\bar{k}=1, \bar{k} \neq k}^{N_s} \beta_{\bar{k}}^i \simeq \left(\frac{\beta_k^i}{\bar{\beta}_k^i} - 1\right)$ where its *achieved* activity factor $\bar{\beta}_k^i$ can be updated after a window of S' sub-slots, based on the available observations of $y_k^i(t_l)$, $l = f, \dots, f + S'$ where $0 \leq f \leq S - S'$, as $\bar{\beta}_k^i = \sum_{l=f}^{f+S'} y_k^i(t_l) / S'$. Hence, $\beta_k^i = \sum_{k=1}^{N_s} \beta_k^i$ can be updated after each S' sub-slots as

$$\hat{\beta}^i \simeq \beta_k^i + \frac{S' \cdot \beta_k^i}{\sum_{l=f}^{f+S'} y_k^i(t_l)} - 1. \quad (3.20)$$

Note that if $\beta_k^i = 0$, the SU k can estimate $\sum_{\bar{k}=1, \bar{k} \neq k}^{N_s} \beta_{\bar{k}}^i$ by keeping track of its capturing status feedbacks, $y_k^i(t_j)$, while assuming a virtual activity factor $\tilde{\beta}_k^i = 1$, i.e., $\sum_{\bar{k}=1, \bar{k} \neq k}^{N_s} \beta_{\bar{k}}^i \simeq \left(\frac{\tilde{\beta}_k^i}{\tilde{\beta}_k^i} - 1\right)$. In other words, the SU k performs the proposed CSMA scheme with $\tilde{\beta}_k^i = 1$ and sets $y_k^i(t_j) = 1$ if it achieves the smallest back-off time. However, since the actual activity factor is zero, the SU k does not transmit in order to avoid affecting other SUs' estimation process.

Since the estimator $\hat{\beta}^i$ is a non-linear function of $\bar{\beta}_k^i = \frac{\sum_{l=f}^{f+S'} y_k^i(t_l)}{S'}$, it can be proved that the bias and the variance of $\hat{\beta}^i$ are of $\mathcal{O}((S')^{-1})$ [77]. In other words, considering $\hat{\beta}^i = \beta^i + w =$

Algorithm 2 Learning-based OSA

- 1 Set $n = 0$, μ_i^0 equal to some non-negative value for all i and λ_k^0 equal to some value.
- 2 Each SU k computes β_k^i for all i according to (3.13).
- 3 Fast price updating: each SU k updates λ_k price with the gradient iteration (3.14).
- 4 Set $n \leftarrow n + 1$ and go to step 2 (until satisfying termination criterion).
- 5 According to the selected β_k^i in different channels, each SU k starts transmission for S' sub-slots based on the proposed CSMA procedure.
- 6 Slow price updating after each S' sub-slots: Each SU k updates $\sum_{k=1}^{N_s} \beta_k^i$ according to (3.20) and μ_i according to the gradient iteration (3.22).
- 7 Go to step 2 (until satisfying the termination criterion).

$\sum_{k=1}^{N_s} \beta_k^i + w$ where w denotes the random error, we have

$$\mathbb{E}[w] \leq K_e (S')^{-1} \text{ and } \text{var}[w] \leq K_v (S')^{-1}. \quad (3.21)$$

From (3.15), in the optimal OSA scheme, the channel price μ_i is updated using a gradient method with $\nabla g(\mu_i) = 1 - \sum_{k=1}^{N_s} \beta_k^i = 1 - \beta^i$. However, in the learning-based OSA, only noisy measurements of $\nabla g(\mu_i)$ are available for SUs. Based on (3.15), using the estimation of $\beta^i = \sum_{k=1}^{N_s} \beta_k^i$, channel price μ_i can be updated independently by each SU as

$$\begin{aligned} \mu_i^{n+1} &= \left[\mu_i^n + \gamma_n (\hat{\beta}^i - 1) \right]^+ \\ &= \left[\mu_i^n + \gamma_n (-\nabla g(\mu_i^n) + w_n) \right]^+. \end{aligned} \quad (3.22)$$

Comparing to (3.15), the channel price updating in (3.22) involves stochastic errors (i.e., w_n), and hence, the popular stochastic gradient descent method [78, 79] is exploited to study the convergence of the proposed learning-based OSA algorithm.

Based on the above derivations, we present the fully-distributed OSA scheme in Algorithm 2, which can be separately performed by each SU to determine its optimal activity factors. Each SU needs to perform Algorithm 2 at the beginning of every time-slot of duration T to update its own activity factors iteratively until convergence to the optimal values. It is noted that the average time

scale of SU activity (i.e., being on and off) is a sub-slot in which a successful transmission could happen. Thus, on one hand, a sub-slot has to be large enough to accommodate a transmission with all overheads and collision avoidance signaling. On the other hand, it should be short enough that S sub-slots (i.e., the whole transmission duration) can be smaller than the coherence time since a block flat fading situation is considered.

3.5 Convergence Analysis

In this section, our goal is to prove that if each SU autonomously deploys (3.22) to update the channel prices, then the network performance converges to the optimal value. Thus, we investigate the convergence and convergence rate, which characterize the asymptotic behavior and efficiency of the proposed OSA algorithm while it is formulated as a stochastic gradient descent method. To study the convergence, we adopt the following assumptions on the step size γ_n and learning window size S' .

Assumption 1 γ_n is assumed as a deterministic positive step size satisfying $\gamma_n > 0, \gamma_n \rightarrow 0, \sum_{n=0}^{\infty} \gamma_n \rightarrow \infty, \sum_{n=0}^{\infty} \gamma_n^2 < \infty$.

Note that Assumption 1 is widely used in the stochastic gradient search literature [79–81]. This is because, these conditions ensure a balance to have the step size decay neither too slow nor too fast. In particular, the step size should approach zero sufficiently slow ($\gamma_n \rightarrow 0, \sum_{n=0}^{\infty} \gamma_n \rightarrow \infty$) to avoid false convergence while approaching zero at a sufficiently fast rate ($\gamma_n \rightarrow 0, \sum_{n=0}^{\infty} \gamma_n^2 < \infty$) to diminish the noise effects as the iteration gets close to the optimal solution. A common generalization of step size sequence is $\gamma_n = an^{-c}$ for $a > 0$ and $0.5 < c \leq 1$ [79].

Assumption 2 The size of learning window (i.e., S') is assumed as an increasing function of time $S' = K_b n^b, K_b \geq 1, b > 0$ such that $b + c > 1$. The condition $b + c > 1$ forces sufficiently fast decay of estimation bias.

Remark 1 Based on (3.21), Assumption 2 guarantees that the bias and variance of gradient estimator are diminishing functions of time. Specifically, $E[w_n] \leq K_e n^{-b}$ and $\text{var}[w_n] \leq K_v n^{-b}$.

Remark 2 $\nabla g(\mu_i)$ has Lipschitz continuity, i.e., there exists a positive real constant D_0 such that $|\nabla g(\mu_i) - \nabla g(\mu'_i)| \leq D_0 |\mu_i - \mu'_i|$ for all positive μ_i and μ'_i . This can be explained by the fact that $\nabla g(\mu_i)$ is a continuous and linear function of μ_i based on (3.13), and also bounded (i.e., $1 - N_s \leq \nabla g(\mu_i) = 1 - \sum_{k=1}^{N_s} \beta_k^i \leq 1$).

In the following proposition, we establish the convergence of $\mu_i^{n+1} = \mu_i^n + \gamma_n (-\nabla g(\mu_i^n) + w_n)$ which guarantees the convergence of (3.22), and hence, the activity factors of all SUs. This result is an extension of Theorem 1 in [82, page 51] in consideration of biased errors.

Proposition 1 (Convergence with probability of 1) *Under Assumption 1 and Assumption 2, the sequence $\{\mu_i^n\}$ converges to the optimal value with probability of 1.*

Proof: See Appendix A.1 for the proof.

Remark 3 *If S' is fixed, $\lim_{n \rightarrow \infty} [(g(\mu_i^n) - g(\mu_i^*)) - \mathbb{E}[w_n](\mu_i^n - \mu_i^*)] = 0$. It implies that $\frac{g(\mu_i^n) - g(\mu_i^*)}{\mu_i^n - \mu_i^*} \rightarrow \mathbb{E}[w_n]$. Since $\{|\mu_i^n - \mu_i^*|^2\}$ is convergent, if S' is chosen sufficiently large (i.e., sufficiently small $\mathbb{E}[w_n]$), $g(\mu_i^n) - g(\mu_i^*)$ becomes sufficiently small. This explains that iterations (i.e., μ_i^n) converge in a neighborhood of the optimal value as moving in the direction of the optimal point.*

Remark 4 *For some positive real constants D_1 and D_2 , and for all μ_i^n ,*

$$D_1 |\mu_i^n - \mu_i^*| \leq |\nabla g(\mu_i^n) - \nabla g(\mu_i^*)| \leq D_2 |\mu_i^n - \mu_i^*|. \quad (3.23)$$

This is because $\nabla g(\mu_i^n) = 1 - \sum_{k=1}^{N_s} \beta_k^i$ is a continuous and linear function of μ_i^n based on (3.13), and also bounded.

Next, we present our second main result on the convergence rate of the learning-based algorithm. It reveals that the convergence rate is attached by how rapidly the learning window size increases and how fast the step size diminishes. The proof of the following proposition is built on the result for the convergence rate considering unbiased random errors in [83].

Proposition 2 (Convergence rate) *Let Assumption 1 and Assumption 2 hold. Then, for $0.5 < c < 1$, there exists an N_0 such that for all $n > N_0$, the following is true:*

$$\begin{aligned} \mathbb{E} \left[|\mu_i^{n+1} - \mu_i^*|^2 \right] &\leq \frac{aD_3K_e^2q^{-1}}{1 - D_5q^{-1}} n^{-2b} + \frac{D_4q^{-1}}{1 - D_5q^{-1}} n^{-b-c} \\ &\quad + \mathcal{O}(n^{-2b-1} + n^{-b-c-1}) \end{aligned} \quad (3.24)$$

which implies $\mathbb{E} \left[|\mu_i^{n+1} - \mu_i^|^2 \right] = \mathcal{O}(n^{-\min(2b, b+c)})$. And for $c = 1$,*

$$\mathbb{E} \left[|\mu_i^{n+1} - \mu_i^*|^2 \right] \leq D_8 n^{-D_1 a} + D_6 n^{-2b} + D_7 n^{-b-1} \quad (3.25)$$

which implies $E \left[\left| \mu_i^{n+1} - \mu_i^* \right|^2 \right] = \mathcal{O} \left(n^{-\min(D_1 a, 2b, b+1)} \right)$. Note that $D_3, D_4, D_5, D_6, D_7, D_8$ and q are positive real constants.

Proof: See Appendix A.2 for the proof.

Remark 5 Based on Proposition 2, by adjusting the values of b and c , we can control the convergence rate properly when $0.5 < c < 1$. If $c = 1$, the magnitude of step size (i.e., a) is another parameter which needs to be designed accurately to achieve the desired convergence rate.

3.6 Numerical Results

In this section, we present three numerical examples including one on the performance of the optimal OSA with hopping strategy, the second on the convergence of the learning-based OSA algorithm, and the third on the robustness of the optimal OSA under perturbations of PU return probability. In these examples, we assume independent channels with the same bandwidth $B^i = 1$ and same α_i . We set the same SNR $= \frac{P_k^i}{n_k^i}$ and same channel requirement (i.e., $R_k = 1$) for individual SUs.

3.6.1 Performance of the Optimal Opportunistic Spectrum Access

First, we present numerical results to evaluate the performance of the optimal hopping-based OSA. To better understand the proposed approach with $0 \leq \beta_k^i \leq 1$, we compare it with existing OSA approaches (e.g., [22–26, 74, 75]) in which β_k^i is restricted to a binary value. In this example, SU power gains $g_{k,k}^i$ are randomly generated according to the Rayleigh distribution assuming $E[g_{k,k}^i] = 1$.

Figure 3.2 illustrates the overall throughput of all SUs versus number of idle licensed channels (i.e., N_a) for $N_s = 1$ and $N_s = 2$ assuming fixed $\alpha_i = 0.3$ and SNR = 10dB. It is shown that the proposed hopping-based OSA strategy offers a significant system improvement in comparison with the existing OSA approaches. Furthermore, this improvement is an increasing function of N_s . It also demonstrates that the throughput of the SU increases with N_a because distributing the channel requirement into more channels reduces the SU transmission loss due to the PU return and takes advantage of the channel diversity.

On the other hand, with a fixed N_a of 10, Figure 3.3 shows that the proposed hopping-based OSA strategy offers an overall throughput that is a decreasing function of α_i with a remarkably

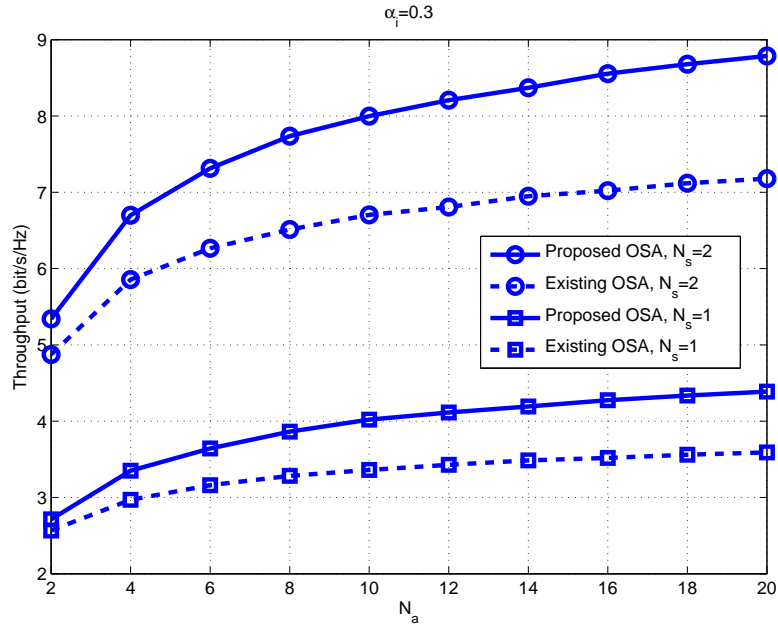


Fig. 3.2 Performance comparison of the proposed OSA and conventional OSA versus the number of idle channels N_a for fixed $\alpha_i = 0.3$ and SNR = 10dB.

lower slope in comparison with the existing OSA approaches. It confirms the advantage of the proposed strategy over the existing OSA schemes, especially at high α_i . In addition, Figure 3.4 illustrates the overall throughput of all SUs versus SNR of SUs assuming fixed $\alpha_i = 0.3$ and $N_a = 10$. It is shown that throughput improvement increases as the SNR of an individual SU increases.

3.6.2 Convergence of the Learning-Based Opportunistic Spectrum Access Algorithm

Here, we investigate the performance of the learning-based OSA algorithm by presenting numerical results which confirm convergence of SUs' activity factors to the optimal values. In this example, we assume $N_s = 3$, $N_a = 3$, $\alpha_i = 0.1$ and SNR = 10dB. Figure 3.5 and Figure 3.6 illustrate the convergence process of the activity factors of three different SUs in one of the idle licensed channels for two different sets of power gains (i.e., $g_{k,k}^i$). As can be observed, the learning-based scheme takes merely around 100 iterations to quickly converge to optimum solutions. Moreover, it depicts that although activity factors of SUs do not converge by using a fixed learning window, they stay in a close vicinity of the optimal values which is explained by Remark 3.

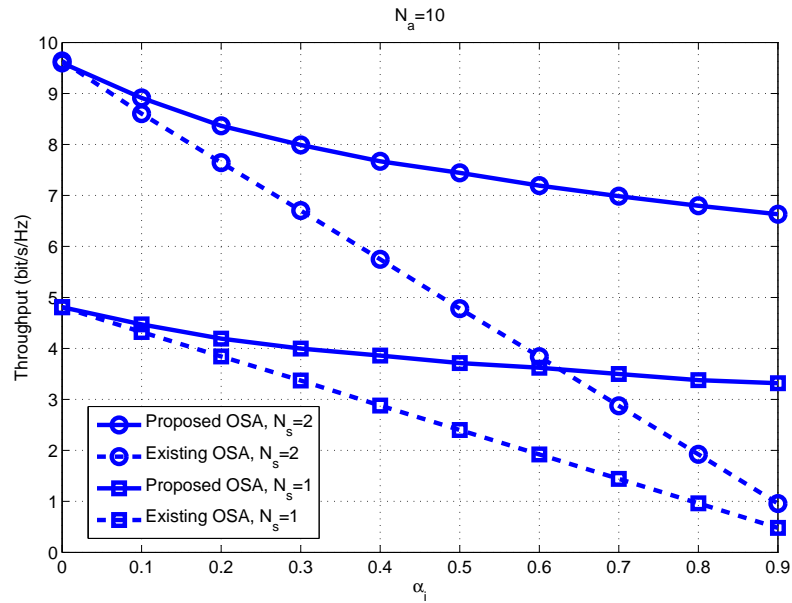


Fig. 3.3 Performance comparison of the proposed OSA and conventional OSA versus the PU return probability α_i for fixed $N_a = 10$ and SNR = 10dB.

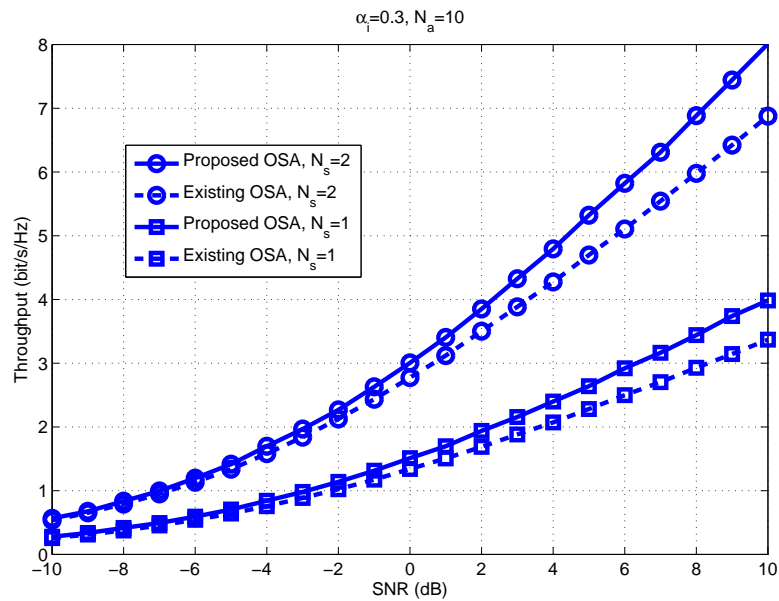


Fig. 3.4 Performance comparison of the proposed OSA and conventional OSA versus SNR for fixed $N_a = 10$ and $\alpha_i = 0.3$.

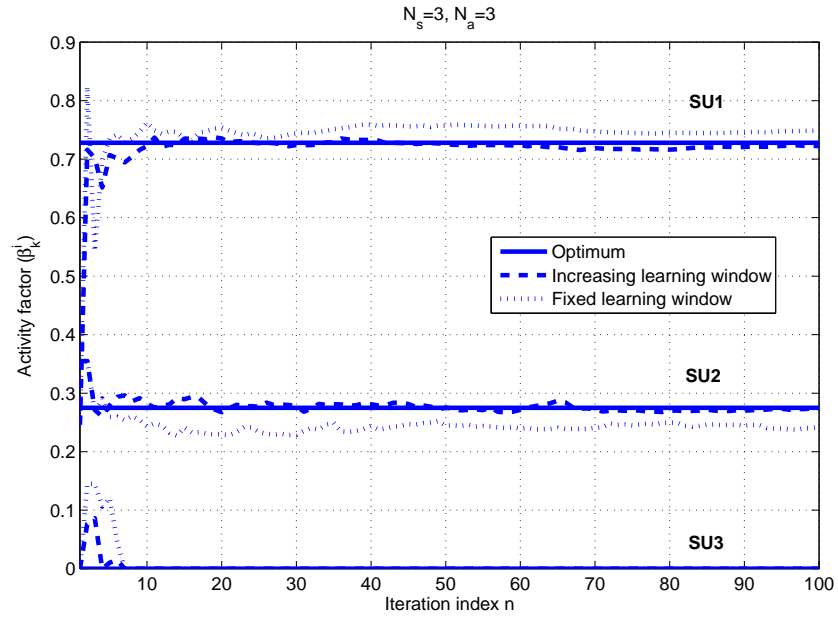


Fig. 3.5 Convergence of the proposed distributed learning-based OSA.

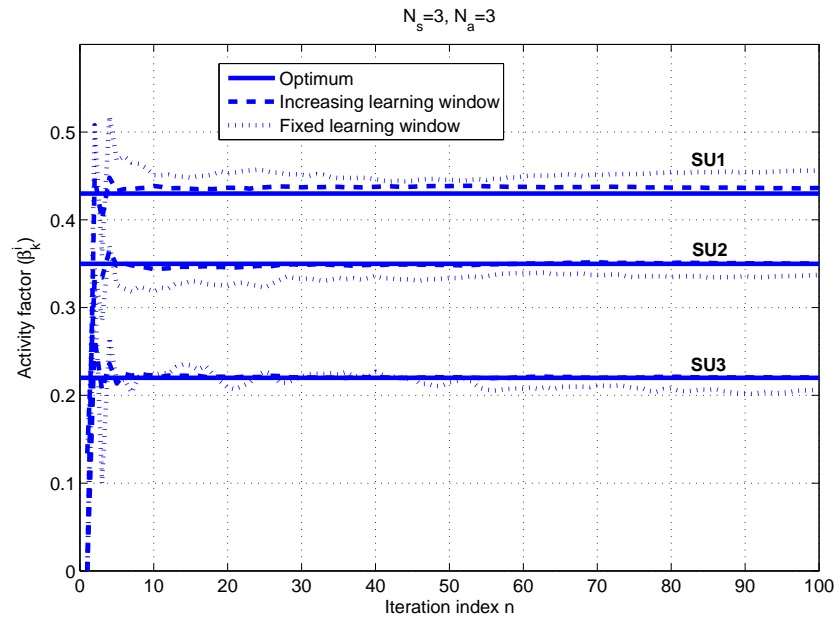


Fig. 3.6 Convergence of the proposed distributed learning-based OSA.

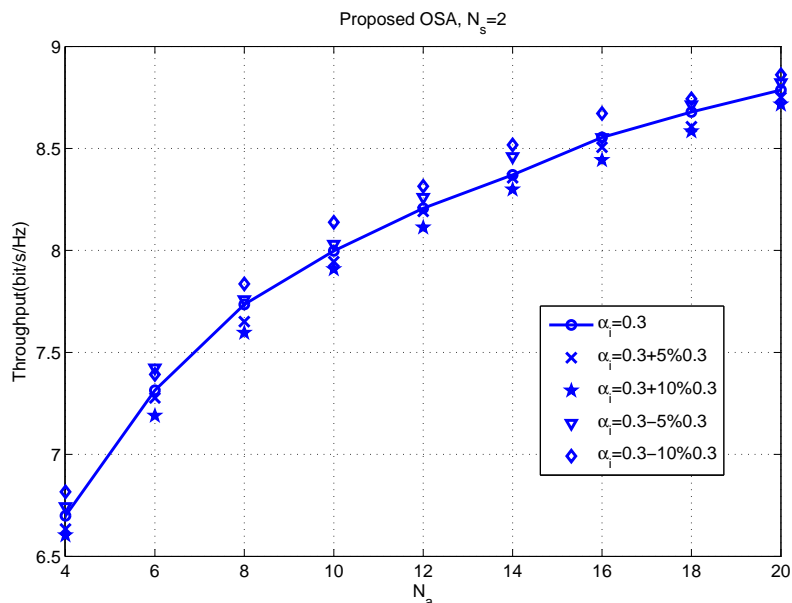


Fig. 3.7 Effect of the PU return probability change on the SU throughput.

3.6.3 Robustness to the Perturbations of Primary User Return Probability

Finally, we evaluate the robustness of the optimal OSA while the PU return probability deviates from its assumed norms. In this example, we assume $N_s = 2$, $\text{SNR} = 10\text{dB}$ and $\alpha_i = 0.3$ and also we allow $\pm 5\%$ and $\pm 10\%$ deviations of α_i . Figure 3.7 shows the overall SU throughput versus number of idle channels (i.e., N_a). It is shown that the overall SU throughput only varies slightly as the PU return probability α_i slightly increases or decreases.

3.7 Concluding Remarks

In this chapter, we have presented an adaptive hopping transmission strategy for OSA, in which the SU transmits over multiple idle channels, each with an adaptive activity factor to alleviate the effects of collision caused by the PU return. Based on the dual decomposition method, we have provided an algorithm which can be implemented in a distributed manner to determine the optimal activity factors. The optimal values for activity factors reveal the benefits of the proposed approach relative to the existing schemes in which a SU selects one channel to transmit for the entire transmission. Illustrative results confirm performance gains offered by the proposed adaptive hopping access strategy in comparison with the existing schemes. In addition, we have presented

a learning-based algorithm which enables each SU to adapt its activity factors autonomously by learning the other SUs' behavior. Via stochastic gradient search analysis, we have established that the updated activity factors by SUs converge with probability of 1 to the optimal points. Also, the study on the convergence rate demonstrates that the increasing rate of the learning window size and the decreasing rate of the step size affect how fast the proposed OSA algorithm tracks the optimal values. Illustrative results confirm the validity of the analytical convergence study.

Chapter 4

Distributed Opportunistic Spectrum Access via Adaptive Carrier Sensing in Cognitive Radio Networks: Game-Theoretic Approaches

4.1 Introduction

In Chapter 3, we have presented an adaptive CSMA scheme to autonomously coordinate spectrum sharing among SUs in the proposed OSA design. In the proposed CSMA-based OSA scheme, adaptive access probabilities (called activity factors) are adopted and optimized for SUs by taking into account channel qualities, PU return probabilities and spectrum sharing incentives. Using the proposed adaptive CSMA scheme, in this chapter¹, we study the SU activity factor allocation problem in a game-theoretic framework. There are three key reasons for using a game-theoretic approach. First, since game theory explicitly recognizes interactions among autonomous SUs, it enables the development of distributed algorithms. Second, game-theoretic algorithms empower us to accelerate the convergence compared to the distributed OSA algorithm proposed in Chapter 3. Third, game theory offers a useful tool to predict, analyze and characterize the long-run behavior of the system, specifically in comparison with the globally optimal solution.

¹Parts of Chapter 4 have been presented at the 2012 IEEE Vehicular Technology Conference (VTC-Fall) in Quebec City, QC, Canada [84] and the 2012 IEEE Global Communications Conference (GLOBECOM) in Anaheim, CA, USA [85], and submitted for possible publication in the IEEE Transactions on Vehicular Technology [86].

In the proposed game-theoretic algorithm, activity factor selections are made independently and dynamically by each SU which aims to satisfy its own demand despite the imposed sharing incentives. More specifically, we formulate the activity factor optimization problem as an exact potential game and analyze the existence, feasibility, and optimality of the Nash equilibrium (NE). To address incomplete information about the game structure, we study learning approaches, which can respond optimally to the history information and achieve NE points, in terms of information requirements and convergence properties. In light of having perfect information, we establish the convergence of the best-response iterations to a pure NE that is not essentially Pareto-optimal. Aiming to enable equilibrium selection, we introduce the log-linear learning process that assures convergence to the most efficient NE. By introducing noise into the decision making process, the log-linear iterations diverge from the suboptimal NE, while moving in the direction toward the Pareto-optimal NE which is robust to noisy perturbations [87, 88].

Inspired by how the log-linear learning works, we propose a fully-distributed algorithm based on best-response dynamics in which each SU adjusts its activity factors independently by learning from the locally available information. Taking advantage of the noisy observations, we show that the best-response iterations will finally stay in a neighborhood of the Pareto-optimal NE with probability of 1. This can be explained by the fact that the Pareto-optimal NE of the formulated game is the single stochastically stable NE. It is noteworthy that, in comparison with the learning-based algorithm offered in Chapter 3, the proposed game-theoretic algorithm in this chapter appears to have much faster convergence.

Furthermore, in order to address competition among SUs in the adaptive CSMA-based access scheme, we introduce an alternative design objective based on the *achieved* activity factors of SUs instead of *intended* activity factors. Then, the problem of finding optimal activity factors of SUs is cast in a game-theoretic framework to highlight the issues of competition and cooperation among SUs. Subsequently, the existence and characteristics including the uniqueness and efficiency of the NE are investigated. To improve the efficiency of the unique NE in the competitive design, the game is transformed into a more cooperative framework by exploiting a pricing mechanism. Finally, an algorithm based on the best-response dynamics is developed in which each SU independently updates its activity factors until convergence to the unique NE.

The remainder of this chapter is organized as follows. Section 4.2 presents an overview of the system model under consideration. In Section 4.3, the OSA design is formulated as an exact potential game. Then, the existence, feasibility and efficiency of the NE for the formulated game are analyzed. Section 4.4 investigates the convergence properties of learning approaches including

the best-response dynamics in the presence of perfect information and noisy estimations, and the log-linear dynamics. In Section 4.5, the competition among SUs is addressed by introducing an alternative optimization problem in the OSA design. Finally, Section 4.6 presents the concluding remarks.

4.2 System Model

The system model considered in this chapter is similar to the Chapter 3. In particular, we study a cognitive radio network with N_s SUs looking for temporal spectrum availabilities in N_p frequency slots (or channels), licensed to PUs. SUs are assumed to follow a time-slotted transmission aiming to sense the channel before transmission. Each time-slot of equal duration T consists of two periods: sensing of duration τ and transmission of duration $(T - \tau)$. Let $\mathcal{N}_a := \{1, \dots, N_a\}$ denote the set of N_a channels that are detected idle at the beginning of each time-slot, and hence, can be utilized by N_s SUs.

Regarding the spectrum sharing, it is assumed that SUs share idle channels using the proposed adaptive CSMA approach in Chapter 3, Section 3.4. In the proposed CSMA, the SU k enters a competition to access the idle channel $i \in \mathcal{N}_a$ during a transmission slot with a certain probability (called activity factors), $\beta_k^i (0 \leq \beta_k^i \leq 1)$. The activity factors of SUs need to be determined based on the channel qualities, PU return probabilities and sharing incentives. Adaptive activity factors enable prioritizing SUs who gain most from using a channel, and hence, improving channel utilization in comparison with a simple random access scheme.

In a highly dynamic environment such as cognitive radio networks, it is practically essential to find a reasonably good solution which can be obtained in a sufficiently fast manner. To this end, in this work, we study the activity factor optimization problem in (3.8) from a game-theoretic learning perspective which enables distributed implementation and fast convergence to a reasonably good solution.

4.3 Game-Theoretic Design of Hopping-Based Opportunistic Spectrum Access

In this section, we formulate the access design for SUs from a game-theoretic perspective aiming to present a distributed scheme. More specifically, we consider a strategic non-cooperative game in which the players are SUs.

According to the optimization problem in (3.8), each SU could simply maximize its transmission rate (i.e., $\sum_{i=1}^{N_a} \beta_k^i C_k^i (1 - \beta_k^i \alpha_i)$). However, SUs cannot select activity factors which violate the coupling constraints in (3.8b). Since it is difficult for SUs to identify feasible activity factors in advance, we construct an alternative payoff function for SU k as

$$u_k = \sum_{i=1}^{N_a} \beta_k^i C_k^i (1 - \beta_k^i \alpha_i) - \sum_{i=1}^{N_a} \mu_i \Theta \left(\sum_{j=1}^{N_s} \beta_j^i - 1 \right) \quad (4.1)$$

where $\Theta(x) = \begin{cases} x, & x \geq 0 \\ 0, & x < 0 \end{cases}$ and μ_i 's are positive scalars. The second term of (4.1) represents the coupling constraints in (3.8b) by severely punishing the SU who violates each of them.

Let $\boldsymbol{\beta}_k = [\beta_k^1, \dots, \beta_k^{N_a}]$ be the strategy at SU k and $\boldsymbol{\beta}_{-k}$ be the strategy of all SUs excluding the SU k . Furthermore, the admissible strategies of SU k is defined as

$$\mathcal{B}_k = \left\{ \boldsymbol{\beta}_k : \beta_k^i \in \left\{ 0, \frac{1}{S}, \frac{2}{S}, \dots, 1 \right\}, \forall i \in \mathcal{N}_a, \sum_{i=1}^{N_a} \beta_k^i = R_k \right\}. \quad (4.2)$$

Note that β_k^i takes discrete values in the proposed CSMA-based algorithm. Then, we can define the non-cooperative game for the spectrum access design of SUs as

$$\mathcal{G} = [\mathcal{N}_s, \{\mathcal{B}_k\}_{k \in \mathcal{N}_s}, \{u_k\}_{k \in \mathcal{N}_s}] \quad (4.3)$$

where $\mathcal{N}_s = \{1, \dots, N_s\}$ is the set of players of the game (i.e. SUs), \mathcal{B}_k is the activity factor strategy set of the SU k and u_k is the corresponding payoff function of the SU k defined on the set of pure-strategy profiles $\mathcal{B} = \mathcal{B}_1 \times \dots \times \mathcal{B}_{N_s}$.

An exact potential game is a strategic game in which the incentive of all players to change their strategies can be expressed in a global potential function. The potential games are easy to analyze since improving each player's utility also increases the value of a potential function [89]. In the following theorem, we demonstrate that the game \mathcal{G} falls into the framework of exact potential games.

Theorem 1 \mathcal{G} is an exact potential game with the potential function,

$$\Phi = \sum_{j=1}^{N_s} \sum_{i=1}^{N_a} \beta_j^i C_j^i (1 - \beta_j^i \alpha_i) - \sum_{i=1}^{N_a} \mu_i \Theta \left(\sum_{j=1}^{N_s} \beta_j^i - 1 \right). \quad (4.4)$$

Proof: It is clear that the game \mathcal{G} satisfies the exact potential game definition [89],

$$u_k(\beta_k, \beta_{-k}) - u_k(\beta'_k, \beta_{-k}) = \Phi(\beta_k, \beta_{-k}) - \Phi(\beta'_k, \beta_{-k}), \forall \beta_k, \beta'_k \in \mathcal{B}_k, \forall k \in \mathcal{N}_s. \quad (4.5)$$

Thus, \mathcal{G} is an exact potential game and Φ is the potential function of \mathcal{G} . ■

Conceptually, a strategic game can reach a steady-state NE point, if it exists, from which no player can improve its utility by changing its own strategy unilaterally [90]. In other words, a strategy profile $\beta^* = \{\beta_k^*\}_{k=1}^{N_s} \in \mathcal{B}$ is a NE if and only if

$$u_k(\beta_k^*, \beta_{-k}^*) \geq u_k(\beta'_k, \beta_{-k}^*), \forall \beta'_k \in \mathcal{B}_k, \forall k \in \mathcal{N}_s. \quad (4.6)$$

We are interested to investigate the existence and characteristics including the feasibility and efficiency of NE for the game \mathcal{G} .

4.3.1 Existence of the Nash Equilibrium

First of all, we study the existence of NE of the game \mathcal{G} in the following theorem based on the properties of the potential games.

Theorem 2 The game \mathcal{G} admits at least one pure-strategy NE.

Proof: This theorem comes directly from Corollary 4 in [91], which states every finite potential game \mathcal{G} has at least one pure-strategy NE. ■

Remark 6 In general, the pure-strategy NE of game \mathcal{G} may not be unique.

4.3.2 Feasibility of the Nash Equilibrium

Since the optimization problem in (3.8) has the coupling constraints in (3.8b) which are merged in the payoff functions in the formulated game \mathcal{G} , it is required to verify if an arbitrary pure-strategy NEs is feasible, i.e., satisfying the constraints $\sum_{k=1}^{N_s} \beta_k^i \leq 1, i = 1, \dots, N_a$. Thus, the following theorem presents conditions that assure the feasibility of pure-strategy NEs.

Theorem 3 *All pure-strategy NEs of the game \mathcal{G} must be feasible if*

$$\mu_i > \mu_{th}, \forall i \in \mathcal{N}_a \quad (4.7)$$

where

$$\mu_{th} = \max_{k \in \mathcal{N}_s, \beta_k \in \mathcal{B}_k} \left(S \sum_{i=1}^{N_a} \beta_k^i C_k^i (1 - \beta_k^i \alpha_i) \right). \quad (4.8)$$

Proof: See Appendix B.1 for the proof.

Theorem 3 ensures that, by properly designing μ_i 's, the payoff functions in (4.1) can guarantee the feasibility of the steady states of the system.

4.3.3 Efficiency of the Nash Equilibrium

The other aspect that we study is how efficient the NE of game \mathcal{G} is in comparison with the optimal solution of (3.8). The following theorem specifies the relationship between the optimal solution and the NE of the game \mathcal{G} .

Theorem 4 *The optimal solution of (3.8) is the Pareto-optimal pure-strategy NE of \mathcal{G} if $\mu_i > \mu_{th}, \forall i \in \mathcal{N}_a$.*

Proof: See Appendix B.2 for the proof.

Remark 7 *In the next section, learning-based iterative algorithms are proposed which enable the convergence to the Pareto-optimal pure-strategy NE.*

4.4 Iterative Learning-Based Access Algorithms with Perfect and Noisy Observations

Assuming that the rationality of players and the structure of the game are common knowledge, equilibrium can be observed as a result of analysis and introspection of the players. Otherwise, under assumption of bounded rationality or partial information, equilibrium may arise as a consequence of a long-run learning process [92]. In this section, aiming to achieve an equilibrium of the game \mathcal{G} , we discuss learning approaches in terms of information requirements and convergence properties.

4.4.1 Best-Response Dynamics with Perfect Observations

To reach an equilibrium of the game \mathcal{G} , first, we present a simple learning algorithm for activity factor selection, based on the asynchronous best-response dynamics [92]. In particular, at each time $t \in \{0, 1, 2, \dots\}$, exactly one SU $k \in \mathcal{N}_s$, is randomly selected to revise its activity factors based on the best-response dynamics defined as

$$\beta_k[t] = \arg \max_{\beta'_k \in \mathcal{B}_k} u_k(\beta'_k, \beta_{-k}[t-1]). \quad (4.9)$$

Under the perfect knowledge of current strategies of the other SUs (i.e., $\beta_{-k}[t-1]$), the convergence of the proposed game-theoretic algorithm is established in the following theorem.

Theorem 5 *The learning algorithm under asynchronous best-response dynamics converges with probability of 1 to a pure-strategy NE of the game \mathcal{G} from any initial strategy point.*

Proof: Based on Theorem 19 in [90], in a finite exact potential game, best-response dynamics will converge with probability of 1 to a pure-strategy NE in finite steps. Accordingly, in game \mathcal{G} , the best-response iterations will converge to a pure-strategy NE. ■

To verify convergence of the best-response dynamics, we provide a numerical result. In this example, we assume independent channels with the same bandwidth $B^i = 1$ and the same α_i . We set the same SNR $= \frac{P_k^i}{n_k^i} = 10\text{dB}$ and $R_k = 1$ for individual SUs. Furthermore, we assume $N_s = 3$, $N_a = 3$ and $\alpha_i = 0.1$. Note that we use the same example for all simulation results in this chapter.

Figure 4.1 demonstrates the convergence process of the activity factors of three SUs in the first idle licensed channel for a certain channel realization. All SUs start by setting their initial values of their activity factors to zero. In each iteration, they sequentially play to optimize their own payoff functions, and update their activity factors based on the best-response dynamics in (4.9) (e.g., in the following order: SU3, SU2, SU1). Note that each SU updates its activity factors in three different channels simultaneously. However, the simulation results for only channel 1 are demonstrated.

In iteration 1, SU3 plays followed by SU2 and SU1 to obtain $\beta_3^1[1] = 0.5$, $\beta_2^1[1] = 0.33$, and $\beta_1^1[1] = 0.53$, which result in $\sum_{k=1}^3 \beta_k^1 \geq 1$. In iteration 2, SU3 is penalized for this excessive amount, and, for its specific channel realization, Figure 4.1 indicates that the SU3 is forced to reduce its activity factor to $\beta_3^1[2] = 0.14$ in order to keep $\sum_{k=1}^3 \beta_k^1 \leq 1$. Subsequently, SU2 and

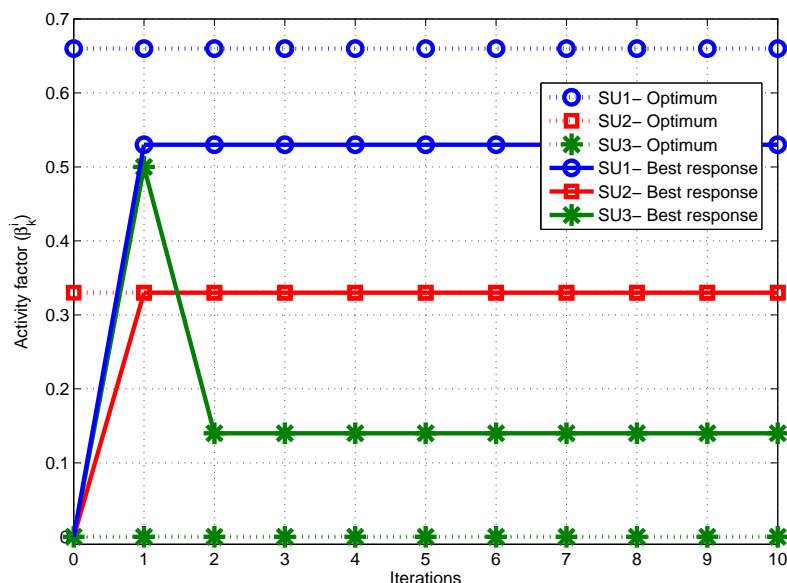


Fig. 4.1 Convergence of the SU activity factors with best-response dynamics.

SU1 do not need to change their strategies, and maintain $\beta_2^1[2] = 0.33$, and $\beta_1^1[2] = 0.53$. From iteration 3, since $\sum_{k=1}^3 \beta_k^1 \leq 1, i = 1, \dots, 3$, SUs actually optimize their own throughput, i.e., their own payoff functions become $u_k = \sum_{i=1}^3 \beta_k^i C_k^i (1 - \beta_k^i \alpha_i)$. Thus, their strategies do not change any more. Note that, for different channel realizations, it is possible that all SUs change their activity factors to satisfy $\sum_{k=1}^{N_s} \beta_k^i \leq 1$ in iteration 2. Furthermore, the process of reducing $\sum_{k=1}^{N_s} \beta_k^i$ may take more than two iterations.

Additionally, Figure 4.2 shows the convergence of the potential function. As evident from Figures 4.1 and 4.2, in less than 10 iterations, the activity factor selection algorithm converges to a NE which is not essentially Pareto-optimal. Note that each iteration corresponds to a complete update by all the SUs.

According to Theorem 5, the best-response iterations will converge to a pure-strategy NE which is not necessarily the maximizer of the potential function Φ (i.e., the globally optimal solution of (3.8)). Since NE could be highly inefficient with regards to the network-level objective, it is thus crucial to find a learning process to reach the socially optimum solution.

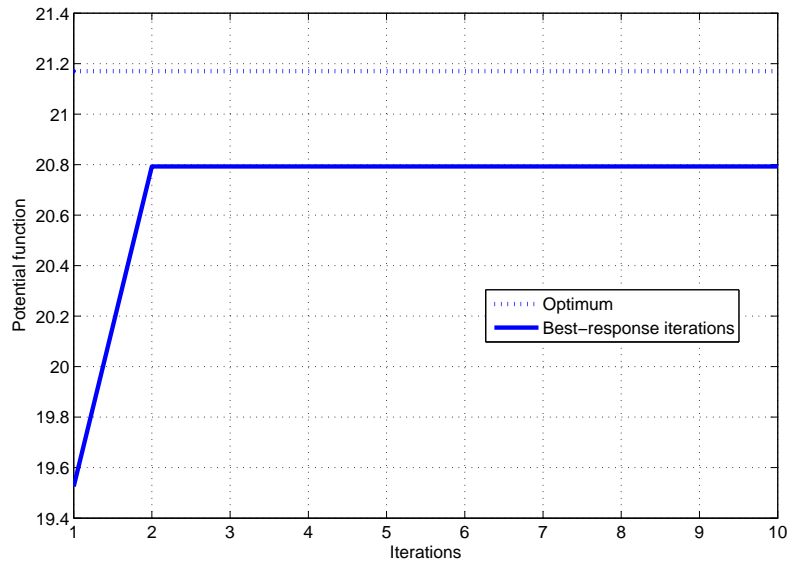


Fig. 4.2 Convergence of the potential function with best-response dynamics.

4.4.2 Log-Linear Dynamics with Perfect Observations

Since the basic best-response dynamics suffer from multiple rest points (e.g., any pure-strategy NE), it is essential to introduce a learning process that can select an appropriate equilibrium. Aiming to enable equilibrium selection, log-linear learning has been proposed as a perturbed best-response process which guarantees convergence to the most efficient NE for potential games [87, 88]. The basic idea behind the equilibrium selection in the log-linear learning is to introduce noise into decision making process which enables categorizing equilibria based on their stability characteristics. This noise allows players to select suboptimal actions with a certain probability which is attached with the magnitude of the payoff difference of the best response and the suboptimal action.

In the log-linear learning, SUs are assumed to be myopic and boundedly rational. At each time $t > 0$, exactly one SU $k \in \mathcal{N}_s$ is randomly selected to update its action, using a probability distribution over its strategy set in response to the current strategy profile. Let k be the player chosen at time t to revise its action. Then, the SU k will choose action β_k given the current

strategy profile $\beta_{-k}[t-1]$ with a probability based on the log-linear choice rule

$$\pi_k^{\beta_k}[t] = \frac{e^{\frac{1}{\epsilon} u_k(\beta_k, \beta_{-k}[t-1])}}{\sum_{\beta'_k \in \mathcal{B}_k} e^{\frac{1}{\epsilon} u_k(\beta'_k, \beta_{-k}[t-1])}} \quad (4.10)$$

where $0 < \frac{1}{\epsilon} < \infty$. The scalar $\frac{1}{\epsilon}$ can be interpreted as the level of rationality of the SUs. In other words, ϵ shows the level of noise in the SUs' decisions and determines how often SUs choose their best responses. The described rule is called log-linear since the log-likelihood ratio of selecting between two actions is linearly proportional to the difference of corresponding payoffs, given other SUs' actions [93]. As $\epsilon \rightarrow 0$, the log-linear rule approaches to the best-response rule. However, the SU k will choose any action $\beta_k \in \mathcal{B}_k$ with equal probability as $\epsilon \rightarrow \infty$. Thus, for any $0 < \epsilon < \infty$, SUs explore non-best responses with non-zero probabilities which are exponentially smaller for actions yielding smaller payoffs [87, 88].

Our goal is to characterize the long-run behavior of asynchronous log-linear learning process for game \mathcal{G} . To this end, the log-linear dynamic adjustment process is represented as an irreducible and aperiodic Markov chain $\{X_t^\epsilon\}_{t \in \mathbb{N}}$ on the set of strategy profiles of the game [87, 88]. Subsequently, the stationary distribution, i.e., limiting distribution in a Markov chain, is studied to explain the long-run behavior of this update rule. In [87], the stationary distribution of asynchronous log-linear learning process in game \mathcal{G} is presented as

$$\mathcal{P}^\epsilon(\beta) = \frac{e^{\frac{1}{\epsilon} \Phi(\beta)}}{\sum_{\beta \in \mathcal{B}} e^{\frac{1}{\epsilon} \Phi(\beta)}}. \quad (4.11)$$

According to (4.11), $\mathcal{P}^\epsilon(\beta)$ (i.e., the probability that $X_t^\epsilon = \beta$ for sufficiently large times $t > 0$) can be expressed as an explicit function of the potential function. A strategy profile $\beta = \{\beta_k\}_{k=1}^{N_s}$ is said to be stochastically stable if $\lim_{\epsilon \rightarrow 0} \mathcal{P}^\epsilon(\beta) > 0$. Consequently, the stochastically stable strategy can be computed based on (4.11).

Corollary 1 *In game \mathcal{G} , the only stochastically stable strategy profile of asynchronous log-linear learning process is the maximizer of potential function Φ which is the NE of the potential game \mathcal{G} based on Theorem 2 in [89]. Assuming $\mu_i > \mu_{th}, \forall i \in \mathcal{N}_a$, the optimal solution of (3.8) is equal to the maximizer of the potential function. As a result, the optimal solution of (3.8) is the only stochastically stable NE of the game \mathcal{G} assuming $\mu_i > \mu_{th}, \forall i \in \mathcal{N}_a$.*

The importance of this Corollary—which comes directly from Corollary 1 in [87] for exact po-

tential games—is two-fold, i.e., convergence and equilibrium selection. In particular, it explains that the asynchronous log-linear learning guarantees convergence to a set of Nash equilibria and more specifically enables equilibrium refinement. In other words, the log-linear learning assures convergence to the potential maximizer which is equal to the globally optimal solution in the game \mathcal{G} assuming $\mu_i > \mu_{th}, \forall i \in \mathcal{N}_a$.

To verify the convergence properties of log-linear learning, Figures 4.3 and 4.4 show the convergence process of the activity factors of three SUs in the first idle licensed channel for a certain channel realization and the convergence of the potential function, respectively. They confirm that the log-linear iterations lead to the globally optimal solution despite the best-response dynamics. As can be observed, it takes merely around 20 iterations to quickly converge to the optimum solution.

The other aspect which affects the practicality of a learning process is the convergence speed. From Proposition 152 in [94], assuming $\mu_i > \mu_{th}$, the convergence time of the log-linear learning to be η -close to the optimal solution is in the order of

$$N_s \log \log(N_s) + \log \left(\frac{1}{\eta} \right) \quad (4.12)$$

for any initial condition if the rationality level (i.e., $\frac{1}{\epsilon}$) is sufficiently large. According to (4.12), the convergence time is linearly proportional to the number of SUs using the log-linear learning in game \mathcal{G} .

Up to this point, we study the best-response dynamics and the log-linear dynamics assuming the perfect knowledge of the sum of activity factors of all N_s SUs in an idle channel, i.e., $\sum_{k=1}^{N_s} \beta_k^i$. Such information can be obtained with the aid of a central coordinator or heavy exchange of overhead information, which causes high complexity and results in an un-scalable system. It is thus crucial that SUs learn this information to adjust their activity factors.

4.4.3 Best-Response Dynamics with Noisy Observations

In Chapter 3, Section 3.4, we have studied how to use the capturing status feedbacks of the proposed adaptive CSMA scheme, $y_k^i(t_j)$, to estimate the sum of activity factors of all SUs in each channel. It is shown that $\beta^i = \sum_{k=1}^{N_s} \beta_k^i$ can be updated after each window of S' sub-slots as $\hat{\beta}^i \simeq \beta_k^i + \left(\frac{S' \cdot \beta_k^i}{\sum_{l=f+1}^{f+S'} y_k^i(t_l)} \right) - 1$. Since estimation with a limited number of samples suffers from random errors, it is shown that $\hat{\beta}^i = \beta^i + w$ where $E[w]$ and $\text{var}[w]$ are of $\mathcal{O}((S')^{-1})$.

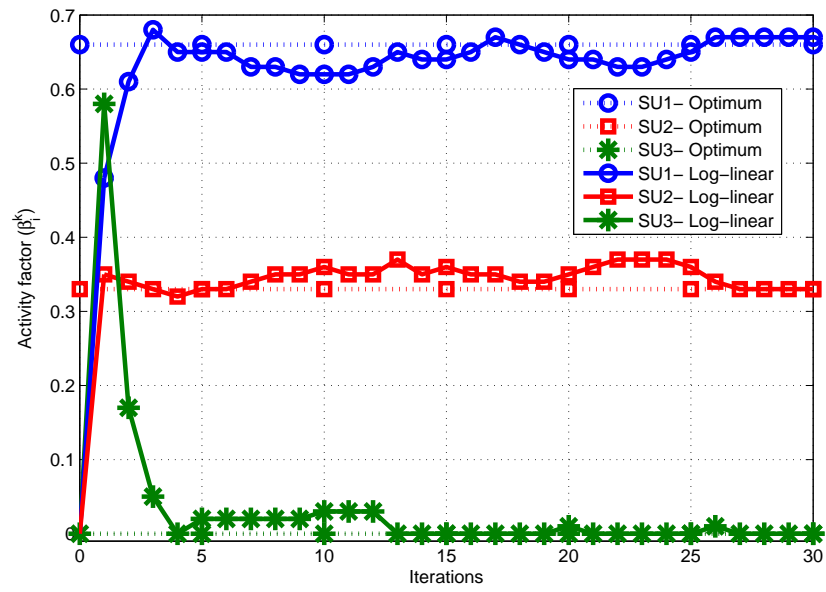


Fig. 4.3 Convergence of the SU activity factors with log-linear dynamics.

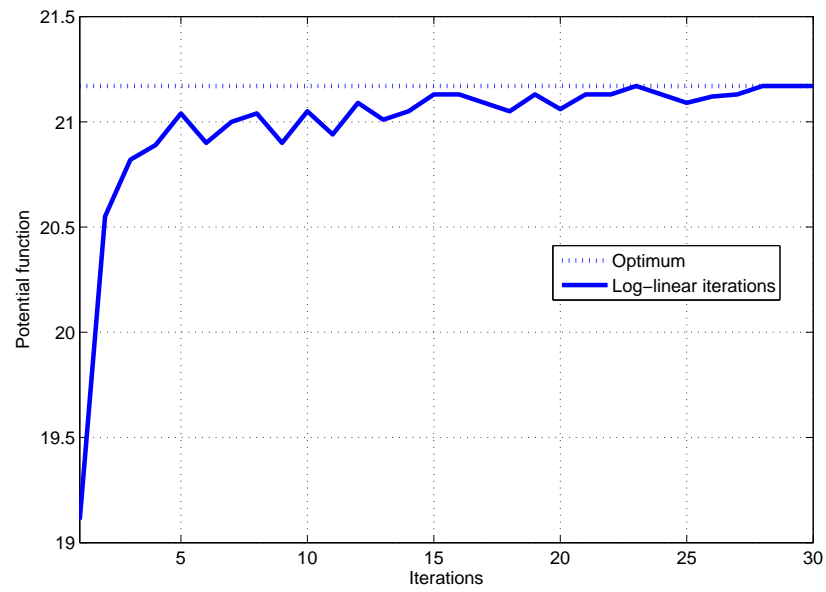


Fig. 4.4 Convergence of the potential function with log-linear dynamics.

From (4.1), it is clear that the estimation noise of β^i will cause a bias b ($|b| \leq |w|$) in u_k , and hence, best-response iterations in (4.9) will also involve random errors. Since the first derivative of u_k is finite, the bias and variance of the random noise in the best-response iterations should be also of $\mathcal{O}((S')^{-1})$.

As shown in the log-linear learning, adding noise to the decision making process enables equilibrium selection, taking advantage of the fact that the Pareto-optimal NE is the only stochastically stable NE in potential games. Accordingly, in Theorem 3 of [95], it is shown that a bounded noise will asymptotically ensure the convergence of the best-response iterations to a neighborhood of the globally optimal solution in potential games. That is because suboptimal NE points are less stable than the Pareto-optimal NE (i.e., the global optimum) in a sense that a small noise can cause the best-response iterations diverge from the suboptimal NE while moving in the direction toward the Pareto-optimal NE.

Similarly, in the proposed algorithm, best-response iterations involve errors although they are random with bounded bias and variance. With a sufficiently large or increasing estimation window (i.e., S'), the random noise can be approximated as a bounded noise. Therefore, it is expected that the best-response iterations converge to the global optimum. Mathematically, this can be presented as the following claim.

Claim 1 $\forall \xi > 0$, an estimation window size can be selected (i.e., $\exists S' > 0$) such that $\lim_{t \rightarrow \infty} \inf \Phi(\beta[t]) \geq \Phi_{\max} - \xi$ with probability of 1.

This claim declares that, by properly designing an estimation window size (i.e., S'), the best-response iterations can get arbitrarily close to the globally optimal solution of (3.8) which is also the maximizer of the potential function (i.e., Φ), assuming $\mu_i > \mu_{th}, \forall i \in \mathcal{N}_a$.

To confirm convergence of the noisy best-response iterations to the global optimum, Figure 4.5 demonstrates the convergence process of the activity factors of three SUs in the first idle licensed channel. In addition, the convergence process based on the proposed learning-based non-game-theoretic algorithm in Chapter 3, Section 3.4 is illustrated in Figure 4.5. It is clear that the game-theoretic algorithm accelerate the convergence in comparison with the algorithm proposed in Chapter 3, Section 3.4. Furthermore, Figure 4.6 shows the convergence of the potential function. They confirm that the best-response iterations will stay in a neighborhood of the global optimum.

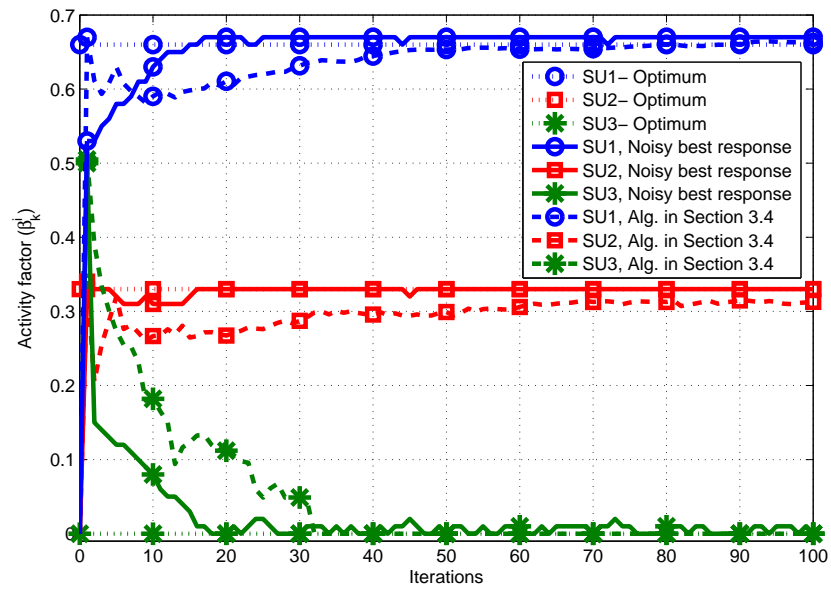


Fig. 4.5 Convergence of the SU activity factors with noisy best-response dynamics.

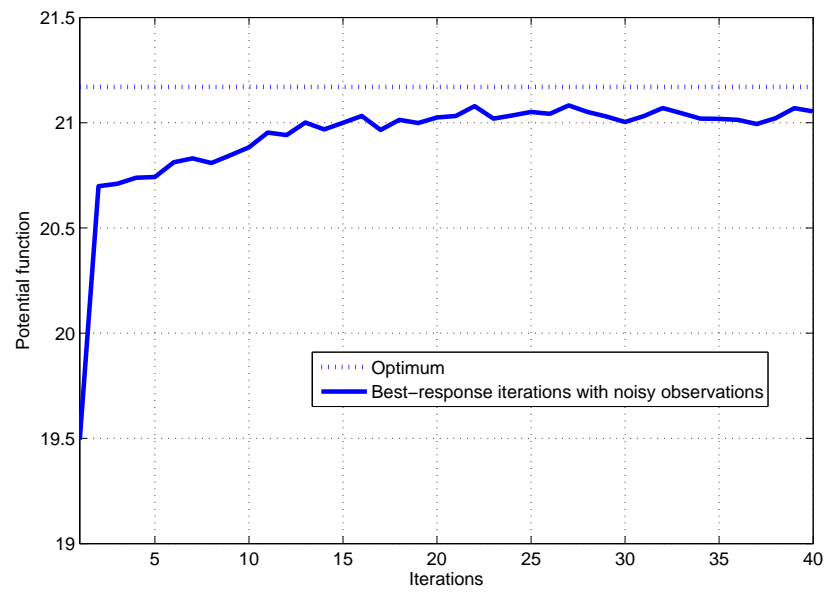


Fig. 4.6 Convergence of the potential function with noisy best-response dynamics.

4.5 Competition and Cooperation in Opportunistic Spectrum Access via Adaptive Carrier Sensing

As previously discussed in Chapter 3, Section 3.4, by adopting adaptive CSMA scheme as a decentralized mechanism among SUs, the *achieved* activity factor of each SU depends on the *intended* activity factors of the other SUs, i.e., $\bar{\beta}_k^i \simeq \frac{\beta_k^i}{1 + \sum_{\bar{k}=1, \bar{k} \neq k}^{N_s} \beta_{\bar{k}}^i}$. This is due to the congestion nature of channel contention in carrier sensing. Accordingly, we consider an alternative utility function based on *achieved* activity factor of SUs for the CSMA-based OSA design, aiming to reflect the crowding effects in the activity factor optimization problem.

4.5.1 Problem Formulation

We formulate the activity factor optimization problem to maximize the overall throughput of all SUs which reflects the competition among SUs under constraints of fixed channel requirements for SUs. Different from the optimization problem in (3.8), we set the utility function as $\sum_{k=1}^{N_s} \sum_{i=1}^{N_a} \bar{\beta}_k^i C_k^i (1 - \bar{\beta}_k^i \alpha_i)$ instead of $\sum_{k=1}^{N_s} \sum_{i=1}^{N_a} \beta_k^i C_k^i (1 - \beta_k^i \alpha_i)$. Note that the orthogonal time sharing constraints (i.e., $\sum_{k=1}^{N_s} \beta_k^i \leq 1$, $i = 1, \dots, N_a$) are not required in this problem since SUs share the idle channels using the adaptive CSMA scheme. Furthermore, since the contention among SUs is reflected in the utility function, there is no need to keep $\sum_{k=1}^{N_s} \beta_k^i \leq 1$, $i = 1, \dots, N_a$ for contention control among SUs as well. More specifically, the activity optimization problem is given by

$$\max_{\boldsymbol{\beta}} \sum_{k=1}^{N_s} \sum_{i=1}^{N_a} \frac{\beta_k^i C_k^i}{1 + \sum_{\bar{k}=1, \bar{k} \neq k}^{N_s} \beta_{\bar{k}}^i} \left(1 - \frac{\beta_k^i \alpha_i}{1 + \sum_{\bar{k}=1, \bar{k} \neq k}^{N_s} \beta_{\bar{k}}^i} \right) \quad (4.13a)$$

$$\text{subject to } \sum_{i=1}^{N_a} \beta_k^i = R_k, \quad k = 1, \dots, N_s \quad (4.13b)$$

$$0 \leq \beta_k^i \leq 1, \quad i = 1, \dots, N_a, \quad k = 1, \dots, N_s. \quad (4.13c)$$

Based on (4.13), we aim to develop a resource allocation scheme which determines the optimal activity factors. Since the optimization problem in (4.13) is generally non-convex, and hence, suffers from highly computational complexity, we study the OSA design in a game-theoretic framework which enables us to model interactions between competing SUs and subsequently present a distributed scheme. More specifically, we consider a strategic non-cooperative game in

which the players are SUs.

4.5.2 Game-Theoretic Design

We consider the case where SUs simply choose their activity factors to maximize their individual utilities. Therefore, the payoff function of SU k becomes

$$u'_k = \sum_{i=1}^{N_a} \frac{\beta_k^i C_k^i}{1 + \sum_{\bar{k}=1, \bar{k} \neq k}^{N_s} \beta_{\bar{k}}^i} \left(1 - \frac{\beta_k^i \alpha_i}{1 + \sum_{\bar{k}=1, \bar{k} \neq k}^{N_s} \beta_{\bar{k}}^i} \right). \quad (4.14)$$

Let $\beta_k = [\beta_k^1, \dots, \beta_k^{N_a}]$ be the strategy at SU k and β_{-k} be the strategy of all SUs excluding the SU k . Furthermore, the admissible strategies of SU k is defined as

$$\mathcal{D}_k = \left\{ \beta_k : 0 \leq \beta_k^i \leq 1, \forall i \in \mathcal{N}_a, \sum_{i=1}^{N_a} \beta_k^i = R_k \right\}. \quad (4.15)$$

Then, we can define the non-cooperative game for the OSA design in cognitive radio networks as

$$\mathcal{G}' = \left[\mathcal{N}_s, \{\mathcal{D}_k\}_{k \in \mathcal{N}_s}, \{u'_k\}_{k \in \mathcal{N}_s} \right] \quad (4.16)$$

where $\mathcal{N}_s = \{1, \dots, N_s\}$ is the set of players of the game (i.e., SUs), \mathcal{D}_k is the activity factor strategy set of the SU k , and u'_k is the corresponding payoff function of the SU k defined on the set of pure-strategy profiles $\mathcal{D} = \mathcal{D}_1 \times \dots \times \mathcal{D}_{N_s}$.

Existence of the Nash Equilibrium

Although the NE concept predicts a stable outcome of a non-cooperative game, such a point does not necessarily exist. Thus, first, we study the existence of NE of the game \mathcal{G}' in the following theorem.

Theorem 6 *The game \mathcal{G}' admits at least one pure-strategy NE.*

Proof: This comes directly from Theorem 1 in [96], which presents sufficient conditions for the existence of NE for games with continuous payoff functions. Accordingly, since \mathcal{D}_k 's are compact and convex sets, and u'_k is a continuous function and also concave in \mathcal{D}_k (definition of a concave game), the game \mathcal{G}' has at least one pure-strategy NE. ■

Uniqueness of the Nash Equilibrium

To investigate the convergence issues, after ensuring the NE existence, it is important to know whether the NE of the game \mathcal{G}' is unique or not. The following theorem investigates the uniqueness of NE of the game \mathcal{G}' .

Theorem 7 *The pure-strategy NE of the game \mathcal{G}' is unique for non-zero α_i values.*

Proof: Theorem 2 in [96] guarantees NE uniqueness for the concave games if a certain condition, called diagonally strict concavity (DSC), is met. Based on this theorem, we establish the uniqueness for the game \mathcal{G}' . A game with strictly concave payoff functions satisfies DSC. Accordingly, since u'_k is a strictly concave function in \mathcal{D}_k under assumption of non-zero α_i 's, it can be concluded that \mathcal{G}' has a unique pure-strategy NE. ■

Efficiency of the Nash Equilibrium

The other aspect which is important to characterize is the equilibrium efficiency in a game-theoretic design, since it is the state at which the network will spontaneously operate. In other words, we are interested to study how efficient the NE of game \mathcal{G}' is as compared to the optimal solution of (4.13). To this end, numerical results are provided to compare the overall throughput of SUs which can be obtained from the globally optimal solution of (4.13) to that which can be reached from the NE of game \mathcal{G}' .

In this example, we assume independent channels with the same bandwidth $B^i = 1$ and the same α_i . We set the same SNR = $\frac{P_k^i}{n_k^i} = 10\text{dB}$ and same channel requirement (i.e., $R_k = 1$) for individual SUs. Figure 4.7 shows that the unique NE of \mathcal{G}' may be inefficient in terms of total profit for all SUs. However, the throughput decrease is small while the globally optimal solution can only be achieved at the cost of high complexity. Furthermore, it demonstrates the overall throughput of SUs while β_k^i are restricted to binary values. Apparently, the proposed hopping-based OSA strategy (with non-binary β_k^i) improves the performance comparing to the existing OSA approaches (with binary β_k^i). For the higher range of α_i , even the overall throughput obtained in NE of game \mathcal{G}' with non-binary β_k^i is larger than which can be obtained from globally optimal solution of (4.13) with binary β_k^i .

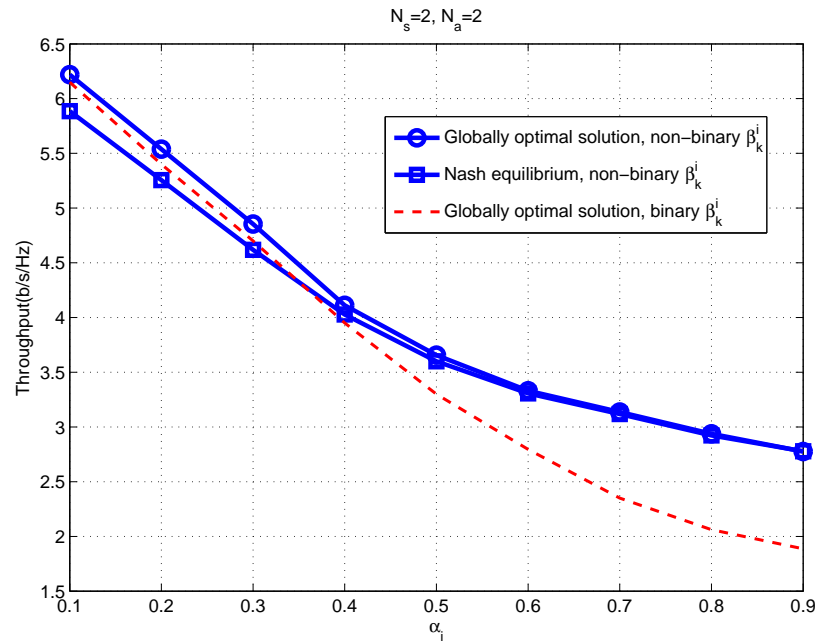


Fig. 4.7 Performance comparison of the NE of game \mathcal{G}' (with non-binary β_k^i) and the globally optimal solution (with non-binary and binary β_k^i) versus the PU return probability α_i for fixed $N_s = 2$, $N_a = 2$ and SNR = 10dB.

4.5.3 Cooperative Design with Dynamic Pricing

In the non-cooperative game \mathcal{G}' , each SU acts self-interestedly, and hence, ignores the cost imposed to the other SUs. Thus, a key challenge is how to modify the payoff function of each SU to deal with NE inefficiency by inducing cooperation, while maintaining the non-cooperative game framework. Pricing has been used as an effective tool to motivate users in a non-cooperative game to adopt a more cooperative behavior [97]. By adding a pricing mechanism to the payoff functions, each SU pays a price for using the resources, and hence, voluntarily cooperates with other SUs.

Therefore, we develop a non-cooperative game with pricing (i.e., \mathcal{G}'') which is practically the same game as \mathcal{G}' with different payoff functions, as given below,

$$\mathcal{G}'' = \left[\mathcal{N}_s, \{\mathcal{D}_k\}_{k \in \mathcal{N}_s}, \{u_k''\}_{k \in \mathcal{N}_s} \right]. \quad (4.17)$$

In the game \mathcal{G}'' , considering a linear usage-based pricing scheme, the payoff functions are constructed as

$$u_k'' = \sum_{i=1}^{N_a} \frac{\beta_k^i C_k^i}{1 + \sum_{\bar{k}=1, \bar{k} \neq k}^{N_s} \beta_{\bar{k}}^i} \left(1 - \frac{\beta_k^i \alpha_i}{1 + \sum_{\bar{k}=1, \bar{k} \neq k}^{N_s} \beta_{\bar{k}}^i} \right) - \sum_{i=1}^{N_a} \bar{\mu}_k^i \beta_k^i \quad (4.18)$$

where $\bar{\mu}_k^i \geq 0$ represents the pricing factor of the SU k in channel i .

Remark 8 Since payoff functions with pricing (i.e., u_k'') are also strictly concave for non-zero α_i values, similar to Theorem 6 and 7, it is clear that the game \mathcal{G}'' owns a unique pure-strategy NE.

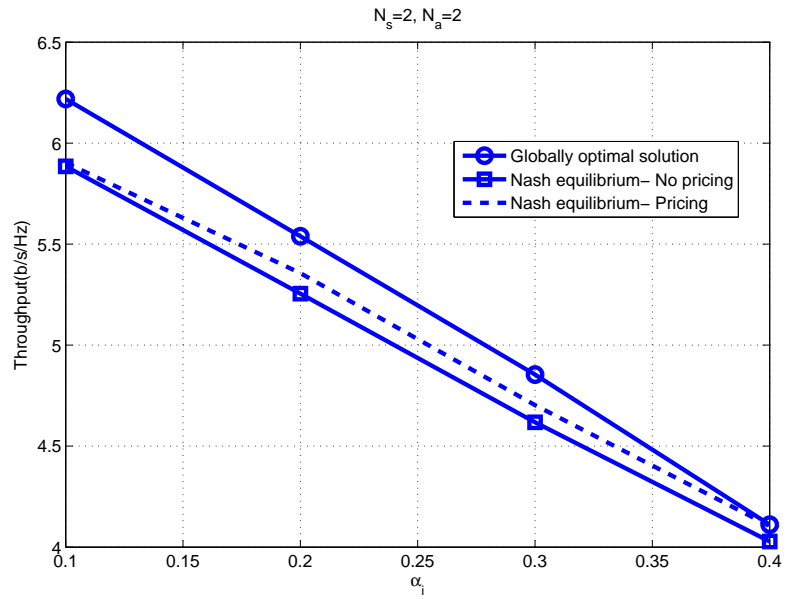
In general, the pricing factors need to be adjusted in such a way that it offers the largest possible enhancement in the overall throughput. In this work, we consider a game with dynamic pricing factors by defining $\bar{\mu}_k^i = \alpha_i \sum_{\bar{k}=1, \bar{k} \neq k}^{N_s} \beta_{\bar{k}}^i$. This implies that each SU pays a penalty for each channel proportional to the crowdedness and the PU return probability of the corresponding channel. As a result, each SU may avoid channels in which the other SUs have already high activity. Thus, this setting can facilitate to resolve contention among SUs in the crowded channels and subsequently improve the NE efficiency in comparison with the game \mathcal{G}' with no pricing.

To investigate the NE efficiency of the game \mathcal{G}'' , we present numerical results which evaluate the overall throughput of SUs obtained from the NE of game \mathcal{G}'' . With the same setting as Figure 4.7, Figure 4.8 shows that pricing mechanism offers improvement in terms of the total profit for all SUs compared to the game \mathcal{G}' with no pricing. Particularly, for higher α_i , the performance of the NE with pricing is close to the optimal solution.

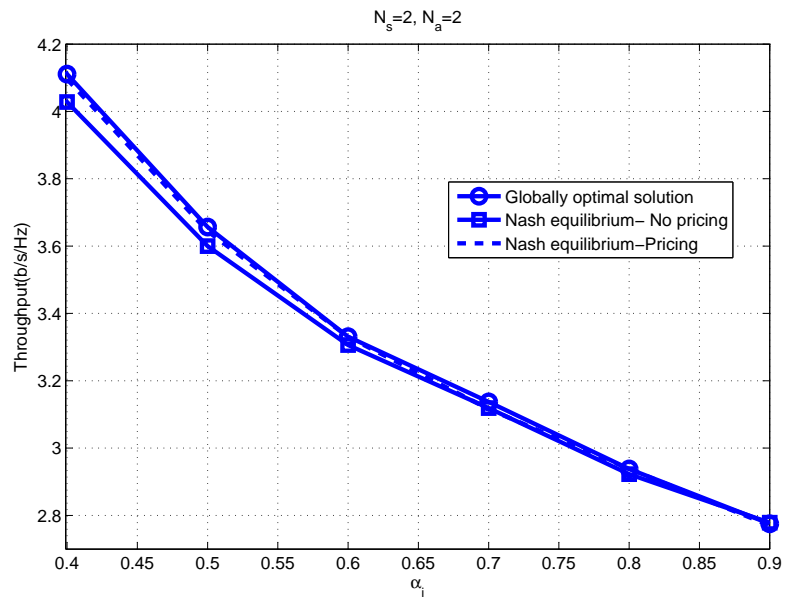
4.5.4 Learning Equilibrium

In this section, we explore how to reach the unique NE of the formulated games as a consequence of a long-run learning process. The key idea is to present an iterative algorithm in which each SU could update its strategy independently while terminating with the unique NE.

One reasonable dynamic learning process is called the continuous best-response dynamics in which each player changes its strategy at a rate proportional to the gradient of its payoff function [96]. Assuming that $\bar{\lambda}_k$ denotes the proportionality constant for the SU k , the differential



(a) low range of α_i



(b) high range of α_i

Fig. 4.8 Performance comparison of the NE of game \mathcal{G}'' and the globally optimal solution versus the PU return probability α_i for fixed $N_s = 2, N_a = 2$ and SNR = 10dB.

equations for updating the activity factors β_k become

$$\frac{\partial \beta_k}{\partial t} = \bar{\lambda}_k \nabla_k u'_k, k = 1, \dots, N_s \quad (4.19)$$

where $\nabla_k u'_k$ denotes the gradient with respect to β_k of u'_k . The following theorem ensures the convergence of the continuous best-response dynamics in (4.19) for the games \mathcal{G}' and \mathcal{G}'' .

Theorem 8 *The continuous best-response dynamics converge to the unique pure-strategy NE considering either the game \mathcal{G}' or game \mathcal{G}'' from any feasible initial strategy point for non-zero α_i values.*

Proof: This comes directly from Theorem 8 in [96] in which it is shown that for a game satisfying DSC, the system in (4.19) is globally asymptotically stable with respect to the unique NE of the game. Since a game with strictly concave payoff functions satisfies DSC, the continuous best-response dynamics converge to the unique NE for both the strictly concave game \mathcal{G}' and the strictly concave game \mathcal{G}'' . ■

Consequently, we present iterative game-theoretic algorithms for activity factor selection to reach the unique equilibrium of both game \mathcal{G}' and game \mathcal{G}'' , based on the best-response dynamics. In particular, in a round robin fashion, SUs iteratively update their activity factors based on the best-response dynamics defined as

$$\beta_k[t] = \arg \max_{\beta'_k \in \mathcal{B}_k} u_k(\beta'_k, \beta_{-k}[t-1]). \quad (4.20)$$

To verify the convergence of the iterative algorithm based on (4.20), numerical results are also provided. Figure 4.9 demonstrates the convergence process of the activity factors of three SUs in one of the idle licensed channels considering the game \mathcal{G}' . Similarly, Figure 4.10 shows the convergence for the game \mathcal{G}'' with pricing. They confirm that the best-response iterations will converge to the unique NE. As can be observed, the OSA scheme takes merely around 10 iterations to converge to the NE. Note that each iteration corresponds to a complete round-robin update by all the SUs. Furthermore, comparing Figure 4.10 with Figure 4.9, it is clear that using the pricing scheme keeps $\sum_{k=1}^{N_s} \beta_k^i$ smaller that means less contention among SUs in the channel i . By decreasing contention among SUs in a specific channel and distributing SUs' activity over different channels, the pricing scheme improves the total throughput.

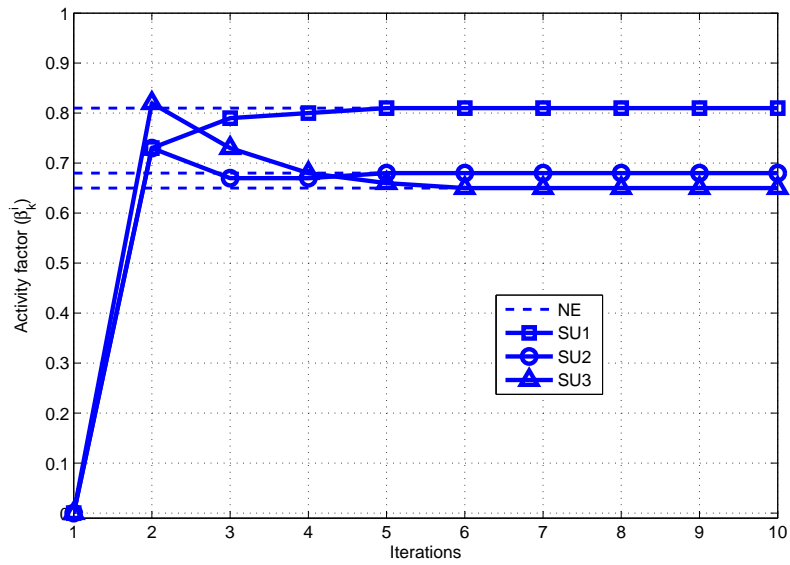


Fig. 4.9 Convergence of the SU activity factors in the proposed iterative algorithm considering the game \mathcal{G}' .

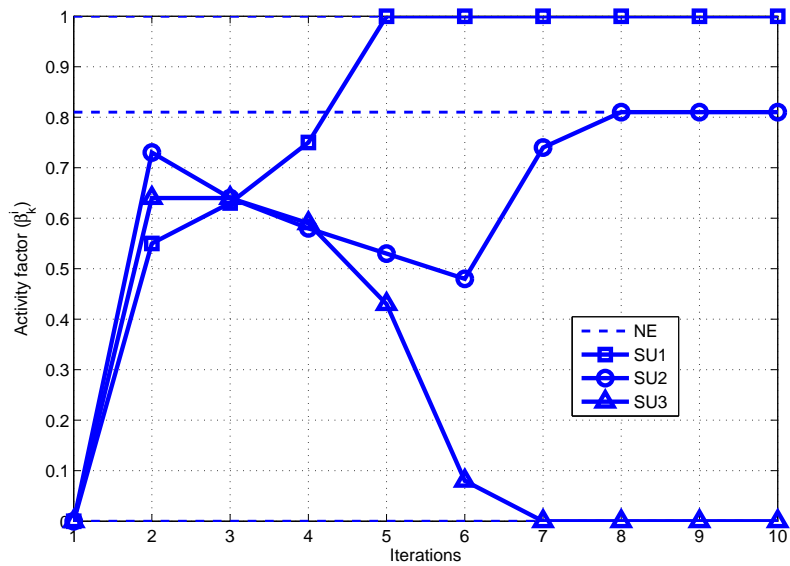


Fig. 4.10 Convergence of the SU activity factors in the proposed iterative algorithm considering the game \mathcal{G}'' .

4.6 Concluding Remarks

In this chapter, we have developed a distributed game-theoretic CSMA-based OSA scheme in which activity factors of SUs over multiple idle channels are adaptively adjusted. Via potential game framework, it is established that the formulated game admits at least one pure-strategy NE. In consideration of coupling constraints among SUs, sufficient conditions are presented to ensure the feasibility of the pure-strategy NE. In addition, it is proved that the globally optimal solution is the Pareto-optimal NE.

Furthermore, we have investigated the convergence properties of the best-response dynamics and log-linear dynamics of the formulated game. Assuming that the perfect knowledge of moves previously made by all SUs is available for each SU, we have proved that best-response iterations converge to a pure-strategy NE which is not essentially the global solution. However, the log-linear process enables equilibrium refinement and convergence to the most socially desirable solution. Subsequently, in a game with noisy observations, we have shown that best-response iterations also converge with probability of 1 to a neighborhood of the global optimum.

Moreover, we have presented an alternative design objective for SUs which reflects competition among SUs and formulated the problem in the game-theoretic framework. Via concave game framework, we have established that the formulated game admits a unique pure-strategy NE which is not necessarily efficient. With the aid of a dynamic pricing mechanism, we have improved the NE efficiency by inducing cooperation in the non-cooperative game. Furthermore, we have proved that the iterative algorithms based on the best-response dynamics converge to the unique pure-strategy NE.

Chapter 5

Throughput Analysis for Adaptive Carrier Sense Multiple Access

5.1 Introduction

In Chapter 3 and Chapter 4, we have presented an adaptive CSMA scheme, aiming to present fully-distributed OSA algorithms (including non-game-theoretic and game-theoretic approaches) for SUs. In the proposed adaptive CSMA, each SU that has a new packet for transmission enters a competition (i.e., backoff mechanism) to access an idle channel with a certain probability (called activity factor). Activity factors of different SUs need to be optimized based on channel qualities, PU return probabilities and sharing incentives. By assigning adaptive access probabilities to different SUs, the proposed adaptive CSMA prioritizes SUs that will gain most from using a channel, and hence, improves channel utilization compared to a simple random access scheme. Although the proposed random access scheme (i.e., adaptive CSMA) aims to minimize the collision probability among SUs, the contention among users is inherent in any random access scheme. Thus, in this chapter¹, we develop an analytical model to compute the system throughput and evaluate the performance of the adaptive CSMA in the presence of inevitable collisions.

More specifically, we analyze the collision probability among competing users and the saturation throughput of the proposed adaptive CSMA in a single idle channel. In [100], the saturation throughput of a CSMA scheme is defined as the fraction of opportunities which are used success-

¹Parts of Chapter 5 have been submitted to the 2013 IEEE Global Communications Conference (GLOBECOM) in Atlanta, GA, USA [98], and submitted for possible publication in the IEEE Transactions on Wireless Communications [99].

fully to transmit data, assuming users always have data to transmit. Comparing to the conventional CSMA, we show that the adaptive CSMA significantly decreases the collision probability and increases the saturation throughput, specifically in networks with larger number of users. Furthermore, we investigate the effects of the network configuration-based adaptations on the saturation throughput.

To study the saturation throughput of the adaptive CSMA, we design a MAC layer which can be backward compatible with distributed coordination function (DCF), IEEE 802.11 CSMA-based MAC mechanism. However, the random backoff mechanism is slightly modified to mitigate the contention among users and improve the throughput performance. Similar to DCF, we consider the binary exponential backoff rules and the collision avoidance operations to manage retransmission of collided packets.

In the IEEE 802.11 MAC enhancement studies, there are works that focus on optimizing the backoff algorithm of CSMA to reduce the collision probability, and hence, to maximize the overall throughput. For instance, [55], which is the closest in spirit with our proposed adaptive CSMA, has proposed an opportunistic CSMA scheme for a WLAN to improve throughput by exploiting the multi-user diversity gain. The proposed opportunistic CSMA prioritizes the users with high-SNRs by granting earlier access to those users. Since the priority is given by earlier access, there is a conflict between users with high-SNRs and users who are newly arrived with smaller contention window sizes. To address this issue, it is assumed that all users share the same contention window size. By enforcing same contention window size among different users, backoff operation needs to be performed centrally at the AP and the resulting backoff window size needs to be broadcasted to all users. However, in our work, prioritizing users with a good channel quality is based on granting higher access probability, instead of earlier access as in [55]. Consequently, the proposed adaptive CSMA can support fully distributed and asynchronous operation with the exponential backoff mechanism on the user-side.

The remainder of this chapter is organized as follows. Section 5.2 presents an overview of the IEEE 802.11 CSMA-based MAC mechanism. In Section 5.3, the system model and problem formulation under consideration are provided. Next, Section 5.4 analyzes the saturation throughput of the proposed adaptive CSMA. Furthermore, in Section 5.5, numerical results are provided to validate the throughput analysis and illustrate throughput improvement compared to the conventional CSMA. Finally, Section 5.6 presents the concluding remarks.

5.2 IEEE 802.11 Distributed Coordination Function Review

In IEEE 802.11 standard, the MAC mechanism has two different operation modes including, distributed coordination function (DCF) and optional point coordination function (PCF). PCF is a centralized MAC protocol in which a centralized scheduler at the AP coordinates access among users by sending polling messages, aiming to support collision-free services. However, DCF is a contention-based access scheme, based on CSMA using binary exponential backoff rules to manage retransmission of collided packets [100]. In this section, we briefly review DCF operation, as standardized by 802.11 protocol.

DCF requires a user, with a new packet for transmission, to sense the channel activity prior to transmission. If the channel is sensed idle for a time interval equal to a distributed inter-frame space (DIFS), the user transmits. Otherwise, if the user senses a transmission either immediately or during the DIFS, it continues monitoring the channel. When the channel is measured idle for a DIFS, the user backoffs for a random period of time. The backoff mechanism enables collision avoidance by minimizing the probability of collision with other users. Furthermore, a user must go through the backoff mechanism between two consecutive packet transmissions to avoid the channel capture [100].

DCF uses a discrete-time backoff mechanism, i.e., the time following a DIFS is slotted. The backoff time-slot length needs to be designed equal to the time a user requires to detect the transmission of a packet from any other user. At each packet transmission, the backoff time is selected according to a uniform distribution in the interval $(0, W - 1)$ where W represents the contention window which is a function of the number of transmissions already failed for the packet. Each user starts the packet transmission by setting W equal to the minimum contention window size (i.e., CW_{\min}). According to the binary exponential backoff rules, W is doubled after each unsuccessful transmission. Each user increases W up to the maximum contention window size $CW_{\max} = 2^m CW_{\min}$ where m represents the maximum backoff stage [100].

The backoff time counter is decremented and a user transmits when the backoff time counter reaches zero. Once the data packet is received successfully, the receiver waits for a period of time called short inter-frame space (SIFS) and then sends an acknowledgement (ACK). By sensing the ACK, the receiver informs the transmitter about the successful reception of the transmitted packet. If the ACK is not received by the transmitter, it retransmits that packet according to the exponential backoff rules [100].

To improve the throughput performance of CSMA in IEEE 802.11, in addition to the basic ac-

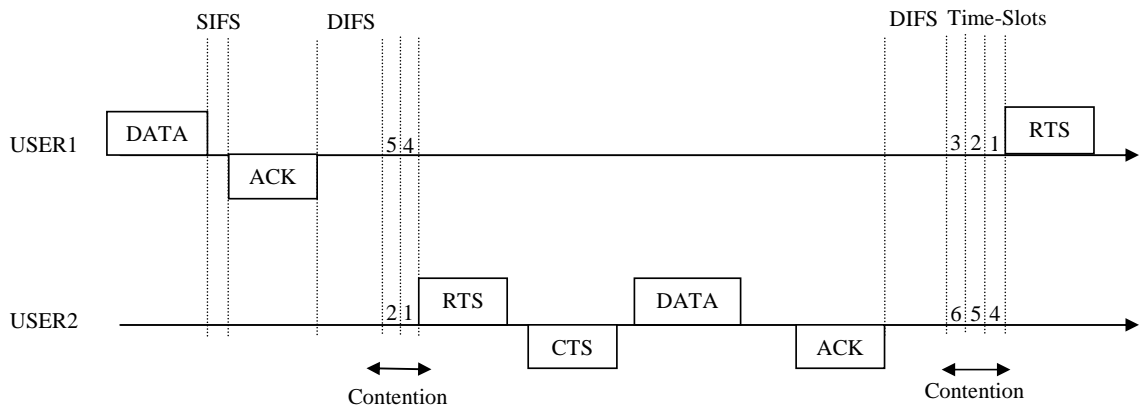


Fig. 5.1 Example of the channel-access procedure of two users using CSMA with the RTS/CTS access mechanism in time domain.

cess mechanism, an optional four-way handshaking technique, i.e., request-to-send/clear-to-send (RTS/CTS), has been proposed for a packet transmission. In the RTS/CTS access mechanism, a user who is ready to transmit, after waiting for a DIFS and passing the backoff process, has to transmit a special short frame called request-to-send (RTS) before transmitting its packet. After detection of the RTS frame by the receiver, it responds by transmitting a clear-to-send (CTS) frame after a SIFS. If the CTS frame is correctly detected by the transmitter, it is allowed to transmit its packet afterwards. The RTS/CTS access mechanism effectively reduces the average collision time because collisions can be early detected by the transmitters when the CTS is not received [100].

Figure 5.1 illustrates an example of the channel-access procedure of two users using CSMA with the RTS/CTS access mechanism. At the end of the packet transmission of user 1, both users wait for a DIFS and pick their backoff times. Since the backoff time of user 2 is shorter, it wins the competition and starts the packet transmission, while user 1 is still in the middle of its backoff procedure. When user 1 senses the channel busy because of the transmitted RTS, it stops its backoff mechanism. When the channel is measured idle again for a DIFS, user 1 joins the competition and sets its backoff time to 3 without resetting its backoff counter. However, user 2 randomly picks a new backoff time (i.e., 6).

Although the binary exponential backoff mechanism is effective in controlling collision among users, the throughput of a network using DCF still decreases by increasing the number of users due to the collision probability increase. However, the large number of users potentially could be an opportunity to improve the overall throughput of a network by creating the multi-user diversity.

5.3 System Model and Problem Formulation

Different from DCF, the proposed adaptive CSMA attempts to manage the contention among users prior to entering the backoff mechanism. To enable such contention management, it assigns a certain probability (called activity factor) to each user with a new packet for transmission and allows it to enter the backoff competition to access a specific idle channel (e.g., i) based on its own activity factor, β_k^i ($0 \leq \beta_k^i \leq 1$). Adaptive activity factors enable prioritizing users who gain most from using a channel, and hence, improving the channel utilization in comparison with a simple random access scheme.

More specifically, in the adaptive CSMA, the user k —which already sensed the channel i idle for a DIFS and is ready to transmit a packet—performs the following steps:

1. Generate a Bernoulli random variable x_k^i with the success probability β_k^i . If $x_k^i = 0$, the user k will not transmit and defer its transmission for a period of time called long inter-frame space (LIFS). If $x_k^i = 1$, the user k will proceed to the next step.
2. Generate a backoff time according to a uniform distribution in the interval $(0, W - 1)$.
3. After expiry of the backoff time, sense the channel i , if it is idle, continue to transmit using the basic access or the RTS/CTS access mechanism rules.

Note that LIFS is a newly-defined inter-frame space parameter in the adaptive CSMA scheme. We assume that LIFS is properly designed such that the user with $x_k^i = 0$ could skip the current competition and retry after the on-going packet transmission process. For instance, LIFS can be set equal to W for each user, to ensure that the corresponding user with $x_k^i = 0$ would not capture the channel.

According to the activity factor optimization problem in (3.8), it is not possible to derive the closed-form expressions of the optimal activity factors based on the channel qualities, the PU return probabilities and the number of SUs. Thus, to study the throughput performance of the adaptive CSMA, we consider a specific case in which the adaptive CSMA attempts to take advantage of the channel diversity among different users and give higher chance of access to the users with better channel qualities. To this end, inspired by (3.13), the activity factor of each user in each channel is defined as an increasing function of its channel transmission capacity as

follows,

$$\beta_k^i = \left[1 - \frac{\tilde{\mu}_k^i}{C_k^i} \right]_0^1 \quad (5.1)$$

where $[x]_a^b = \min(b, \max(a, x))$, C_k^i represents the channel transmission capacity for the user k in the channel i , and $\tilde{\mu}_k^i$ denotes the threshold for the user k in the channel i which is a positive scalar. Note that the derived analytical results on the saturation throughput—presented in the next section—are generally developed as functions of β_k^i , and are not dependent on the specific definitions of β_k^i . The reason for the specific definition of β_k^i in (5.1) is to be used in the numerical results to illustrate the throughput performance.

Similar to Chapters 3 and 4, the channel transmission capacity of the user k in the channel i is represented by $C_k^i = B^i \log(1 + P_k^i g_{k,k}^i / n_k^i)$ where B^i denotes the bandwidth in the channel i , $\frac{P_k^i}{n_k^i}$ is the signal-to-noise ratio (SNR) for the user k in the channel i , and $g_{k,k}^i$ is the channel power gain for the user k in the channel i . In this work, a block-fading model is assumed in which $g_{k,k}^i$ remains unchanged within the coherence time but independently varies of the previous channel realization. To make sure that $g_{k,k}^i$ does not change during a packet transmission, the coherence time is assumed sufficiently long in this work. Furthermore, the channel power gains $g_{k,k}^i$ are considered independent for different users.

To support the distributed operation by each user and allow the fair access among different users, we assume that each user updates its activity factor in each channel relative to its own average channel transmission capacity. Then, we define the threshold for the user k in the channel i as

$$\tilde{\mu}_k^i = \rho_k^i \text{E}_g[C_k^i] \quad (5.2)$$

where ρ_k^i is a positive scalar and $\text{E}_g[\cdot]$ denotes the expectation with respect to the channel power gain distribution. In practice, this expected value (i.e., $\text{E}_g[C_k^i]$) can be empirically estimated by each user. By adjusting the threshold based on (5.2), each user gets a higher chance of transmission if its channel transmission capacity (i.e., C_k^i) is relatively higher than its own average (i.e., $\text{E}_g[C_k^i]$). In other words, each user is compared with itself, and hence obtains the fair access over a long time.

In particular, to enable a long-term fairness for different users with different channel conditions (i.e., different SNR = $\frac{P_k^i}{n_k^i}$ and/or different probability distribution for $g_{k,k}^i$), we select ρ_k^i for

each user in each channel such that the same average access probability (i.e., $E_g[\beta_k^i] = \beta$) can be achieved for all users. More specifically,

$$E_g[\beta_k^i] = E_g \left\{ \left[1 - \frac{\rho_k E_g[C_k^i]}{C_k^i} \right]_0^1 \right\} = \beta. \quad (5.3)$$

According to (5.1), (5.2) and (5.3), it is clear that each user can update its activity factor in each channel based on the locally available information and does not need to know the knowledge on other users. Thus, the proposed adaptive CSMA can be implemented in a fully-distributed manner.

Furthermore, aiming to enhance the efficiency of the proposed adaptive CSMA, ρ_k^i can be tuned dynamically depending on the network-configuration parameters. Some network parameters such as the number of users in the network have a significant impact on the system throughput. Assuming that users have the perfect knowledge of the number of users in the network, ρ_k^i can be defined as an increasing function of N_s to control $\sum_{k=1}^{N_s} \beta_k^i$ (i.e., the sum of all activity factors in the channel i) as N_s increases. In other words, by increasing the thresholds (i.e., ρ_k^i) in the larger networks, the adaptive CSMA attempts to reduce the activity factors of users. Such dynamic threshold setting helps to control the contention among users, and decreases the collision probability. For instance, assuming that users have same SNR, ρ_k^i can be chosen as $1 - \frac{1}{N_s}$. In the next section, we investigate the effects of choosing different ρ_k^i on the throughput by the numerical results.

5.4 Throughput Analysis

In this section, we study the saturation throughput of the proposed adaptive CSMA in a single idle channel (e.g., i), assuming a constant packet size L_P . In [100], the saturation throughput for CSMA-based DCF is defined and calculated as the number of successfully delivered information bits per second, while the transmission queue of each user is assumed to be always nonempty. Accordingly, considering that the activity factors of different users are channel dependent, we define the saturation throughput of the adaptive CSMA as

$$T_{\text{saturation}} = E_g \left[\frac{P_s L_P}{(1 - P_{\text{tr}})T_b + \sum_{k=1}^N P_{s,k} T_{s,k} + (P_{\text{tr}} - P_s)T_c} \right] \quad (5.4)$$

where T_b is the duration of a backoff time-slot, $P_s = \sum_{k=1}^N P_{s,k}$ is the probability that a successful transmission happens in a generic (i.e., randomly chosen) backoff time-slot, $P_{s,k}$ is the probability of a successful transmission by the user k in a generic backoff time-slot, P_{tr} is the probability that at least one transmission, either successful or not, happens in a generic backoff time-slot, $T_{s,k}$ is the average time that the channel is sensed busy because of a successful transmission by the user k , and T_c is the average time that the channel is sensed busy by each user because of a collision.

In the saturation throughput expression (5.4), the numerator represents the average number of information bits that successfully transmitted in a backoff time-slot, i.e., $P_s L_P$. In the denominator, the average length of a backoff time-slot is presented. In particular, the back-off time-slot is empty with probability $(1 - P_{tr})$, it contains a successful transmission with probability P_s , and it contains a collision with probability $P_c = P_{tr} - P_s$ [100]. To analyze the saturation throughput in (5.4), first, we need to derive the probability (called access probability) that a single user transmits a packet in a generic backoff time-slot. Then, by defining P_s and P_{tr} , we can express the throughput as a function of access probability.

For the *conventional CSMA* scheme, in [100], the access probability P_a of a user has been studied by analyzing the behavior of a single user with a Markov model. The proposed Markov chain models the binary exponential backoff rules and the collision avoidance operations of a single user. Assuming that each transmitted packet collides and fails with a constant and independent probability (P_f), the access probability of a user is computed as a function of P_f , the contention window W and the maximum backoff stage m as follows

$$P_a = \frac{2(1 - 2P_f)}{(1 - 2P_f)(W + 1) + P_f W(1 - (2P_f)^m)}. \quad (5.5)$$

On the other hand, the probability that a transmitted packet in a generic backoff time-slot encounters a collision is equal to the probability that at least one of the remaining users transmits. Thus,

$$P_f = 1 - (1 - P_a)^{N_s - 1} \quad (5.6)$$

where N_s denotes the number of competing users [100]. By solving the nonlinear system of (5.5) and (5.6), P_a can be obtained as a function of N_s , W and m . In [100], it is proved that the nonlinear system of P_a and P_f has a unique solution.

In the proposed *adaptive CSMA* scheme, the access probability of the user k is different and

can be calculated as $\beta_k^i P_a$ in consideration of the adaptive access scheme based on the activity factors. Then, since there are N_s users in the network attempting to transmit on the channel, each with different access probability $\beta_k^i P_a$, the probability that there is at least one transmission in a generic backoff time-slot (i.e., P_{tr}) is

$$P_{tr} = 1 - \prod_{k=1}^{N_s} (1 - \beta_k^i P_a). \quad (5.7)$$

A transmitted packet will be received successfully, if exactly one user transmits on the channel. Thus, the probability of successful transmission (i.e., P_s) becomes

$$P_s = \sum_{k=1}^{N_s} P_{s,k} = \sum_{k=1}^{N_s} \beta_k^i P_a \prod_{k'=1, k' \neq k}^{N_s} (1 - \beta_{k'}^i P_a). \quad (5.8)$$

Based on (5.4), to specifically compute the saturation throughput, it is required to specify the values of $T_{s,k}$ and T_c . Consider that H represents the size of PHY and MAC header and δ denotes the propagation delay. In the basic access mechanism, we have

$$T_{s,k}^{\text{bas}} = H + \frac{L_P}{C_k^i} + \text{SIFS} + \delta + \text{ACK} + \text{DIFS} + \delta, \quad (5.9)$$

$$T_c^{\text{bas}} = H + L_P^* + \text{DIFS} + \delta \quad (5.10)$$

where $\frac{L_P}{C_k^i}$ represents the transmission duration of the user k and L_P^* represents the average time of the longest packet transmission involved in a collision. Consider a case that different users have the same SNR and same probability distribution for $g_{k,k}^i$. In this case, assuming that the collision probability of three or more packets is negligible, L_P^* can be approximated as

$$L_P^* \simeq E_g \left[\max \left\{ \frac{L_P}{C_k^i}, \frac{L_P}{C_{k'}^i} \right\} \right]. \quad (5.11)$$

On the other hand, by using the RTS/CTS access mechanism, collision can happen only during

Table 5.1 IEEE 802.11 MAC parameters used in the numerical results.

Packet Payload (L_P)	2400 bytes
Backoff Time-Slot (T_b)	9 μs
PHY and MAC Header (H)	65 μs
Propagation Delay (δ)	1 μs
SIFS	10 μs
DIFS	28 μs
ACK	40 μs
RST	48 μs
CTS	40 μs
CW_{\min}	16
CW_{\max}	1024

the RTS frames, and hence, $T_{s,k}$ and T_c can be represented as

$$\begin{aligned}
T_{s,k}^{\text{rts}} = & \text{RTS} + \text{SIFS} + \delta + \text{CTS} + \text{SIFS} + \delta + \text{H} + \frac{L_P}{C_k^i} \\
& + \text{SIFS} + \delta + \text{ACK} + \text{DIFS} + \delta,
\end{aligned} \tag{5.12}$$

$$T_c^{\text{rts}} = \text{RTS} + \text{DIFS} + \delta. \tag{5.13}$$

Consequently, based on (5.7), (5.8), (5.9), (5.10), (5.12) and (5.13), the saturation throughput can be obtained using (5.4).

5.5 Numerical Results

In this section, we discuss a numerical example on the throughput of the adaptive CSMA scheme based on the analytical and the simulation results. Such numerical example helps us to validate the throughput analysis of the adaptive CSMA, in comparison with the simulation results. Furthermore, it illustrates the throughput improvement offered by the adaptive CSMA relative to the conventional CSMA scheme. For the simulation results, we used a simplified MAC layer simulator which is implemented in Matlab.

The set of parameters used in the numerical results, by both analysis and simulation, are summarized in Table 5.1 based on the IEEE 802.11g MAC specifications [101]. The channel bandwidth is assumed equal to $B^i = 20\text{MHz}$. Unless otherwise specified, we consider the same

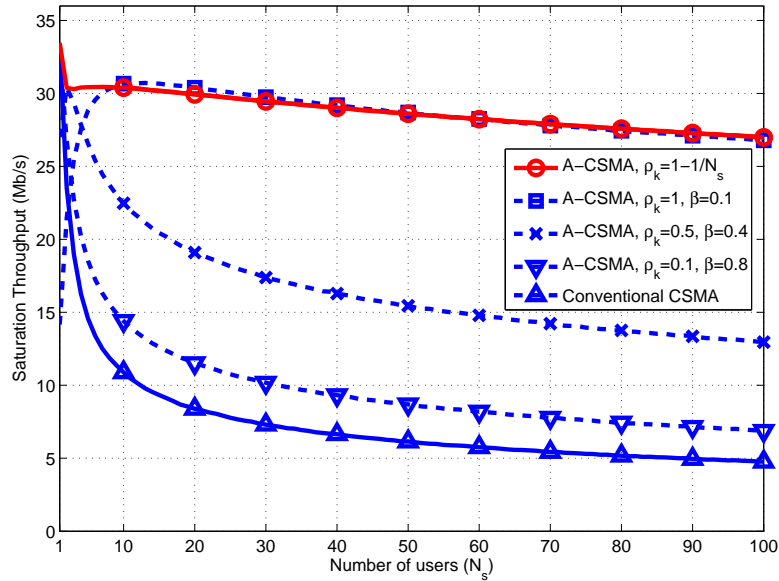


Fig. 5.2 Saturation throughput versus number of users using the basic access mechanism.

average signal-to-noise ratio (i.e., $\text{SNR} = \frac{P_k^i}{n_k^i} = 10\text{dB}$) for all users. Furthermore, in all the presented results, the channel power gains $g_{k,k}^i$ are randomly generated according to the Rayleigh distribution assuming $E_g[g_{k,k}^i] = 1$.

Using the basic access mechanism, Figure 5.2 demonstrates the saturation throughput (i.e., $T_{\text{saturation}}$) of the adaptive CSMA scheme versus the number of users in the network (i.e., N_s). In this figure, the throughput performance of the adaptive CSMA is shown considering different threshold settings (i.e., ρ_k^i). Comparing to the conventional CSMA scheme, it is shown that the adaptive CSMA offers a significant throughput improvement for networks with more than 5 users. As evident from Figure 5.2, the adaptive CSMA with the dynamic threshold $\rho_k^i = 1 - \frac{1}{N_s}$ outperforms the conventional CSMA for any number of users.

Using the RTS/CTS access mechanism, Figure 5.3 illustrates the saturation throughput of the adaptive CSMA scheme versus the number of users in the network for different threshold settings. As can be observed, the adaptive CSMA with the dynamic threshold $\rho_k^i = 1 - \frac{1}{N_s}$ achieves the multi-user diversity gain using the RTS/CTS access mechanism. In other words, the adaptive CSMA improves the throughput as N_s increases, while the throughput of the conventional CSMA decreases with the number of users due to the more frequent collisions. Comparing to

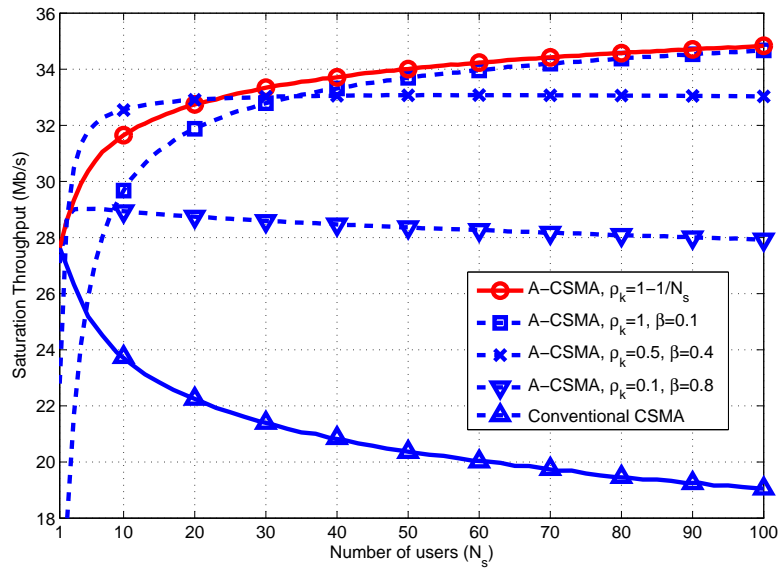


Fig. 5.3 Saturation throughput versus number of users using the RTS/CTS access mechanism.

Figure 5.2, it is clear that the RTC/CTS technique improves the throughput performance relative to the basic access scheme. This can be explained by the fact that the RTC/CTS technique effectively reduces the collision time (i.e., T_c). Figure 5.2 and Figure 5.3 confirm the precision of the analytical results on the saturation throughput (lines) as they closely match the simulation results (the symbols), for both the basic access and the RTS/CTS access mechanisms.

Figure 5.4 shows the collision probability (i.e., $P_c = P_{tr} - P_s$) of the adaptive CSMA scheme versus the number of users for different threshold settings. It is clear that the adaptive CSMA significantly decreases the collision probability. In agreement with the throughput results in Figure 5.3, it also demonstrates that the adaptive CSMA with $\rho_k^i = 1 - \frac{1}{N_s}$ provides the largest decrease as compared to the conventional CSMA, except for $\rho_k^i = 1$. Despite the smaller collision probability for $\rho_k^i = 1$, the adaptive CSMA with $\rho_k^i = 1 - \frac{1}{N_s}$ provides a higher throughput. According to Figure 5.5, this can be explained with the larger probability of successful transmission for the adaptive CSMA with $\rho_k^i = 1 - \frac{1}{N_s}$ comparing to the adaptive CSMA with $\rho_k^i = 1$, specifically for smaller N_s .

To investigate the effects of the packet length on the throughput performance, Figure 5.6 illustrates the saturation throughput of the adaptive CSMA scheme with $\rho_k^i = 1 - \frac{1}{N_s}$ versus the packet length for $N_s = 20$. Apparently, the saturation throughput improves when the packet

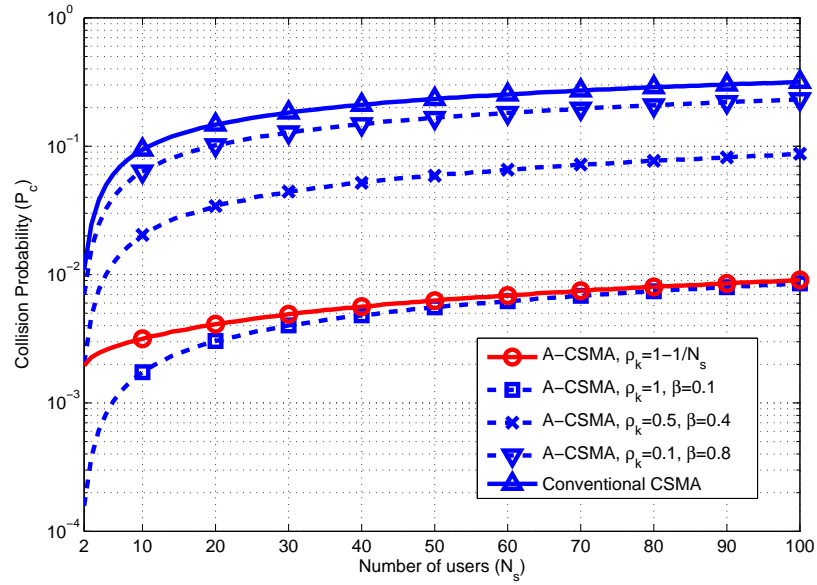


Fig. 5.4 Collision probability versus number of users using the RTS/CTS access mechanism.

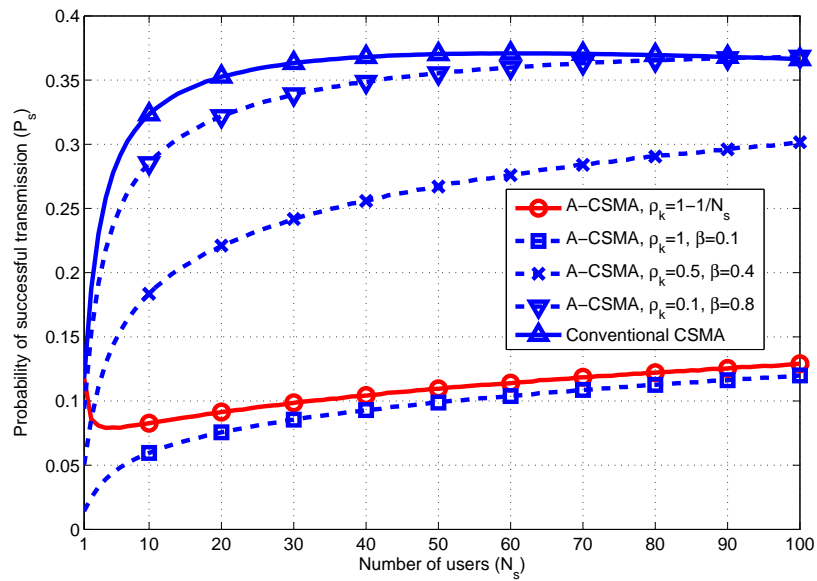


Fig. 5.5 Probability of successful transmission versus number of users using the RTS/CTS access mechanism.

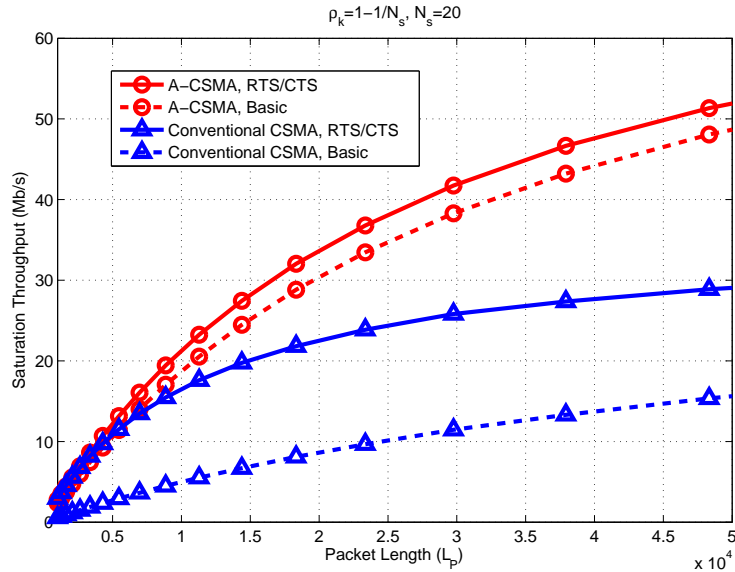


Fig. 5.6 Saturation throughput versus packet length with $N_s = 20$.

length increases. This happens because the MAC overhead is constant, while the packet length is increasing. Furthermore, it is shown that the throughput improvement offered by the adaptive CSMA comparing to the conventional CSMA is an increasing function of the packet length.

Figure 5.7 and Figure 5.8 explore the dependency of the saturation throughput of the adaptive CSMA scheme on the minimum contention window size CW_{\min} , using the basic access and the RTS/CTS access mechanisms. In both figures, we assume the maximum backoff stage equal to 6 (i.e., $m = 6$). In addition, in each figure, two different threshold settings ($\rho_k^i = 0.1$ and $\rho_k^i = 1 - \frac{1}{N_s}$) are investigated for three different network sizes ($N_s = 5$, $N_s = 25$ and $N_s = 50$).

Using the basic access mechanism, Figure 5.7 shows that the throughput is highly dependent on the minimum contention window size. To achieve the maximum throughput, it is clear that CW_{\min} needs to be designed as a function of the number of users in the network. For instance, the optimal value of CW_{\min} is around 16 for a network with 5 users, while $CW_{\min} = 128$ gives a better throughput performance when $N_s = 50$. Furthermore, for a certain number of users, it is shown that using a fixed ρ_k reduces the maximum achievable throughput comparing to the dynamic threshold setting $\rho_k = 1 - \frac{1}{N_s}$.

Figure 5.8 shows the behavior of the saturation throughput of the adaptive CSMA scheme with the RTS/CTS access mechanism for different values of CW_{\min} . Apparently, in this case, the saturation throughput is less sensitive to the minimum contention window size for the lower

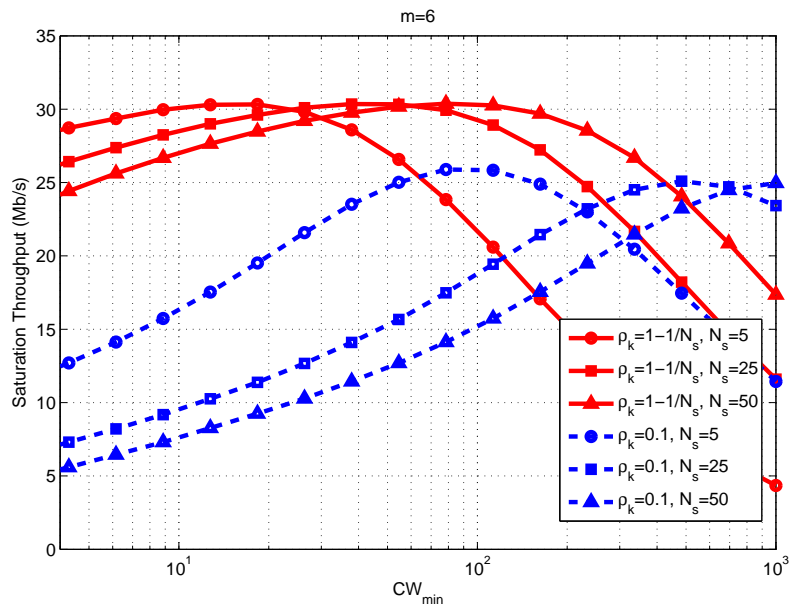


Fig. 5.7 Saturation throughput versus minimum contention window size using the basic access mechanism.

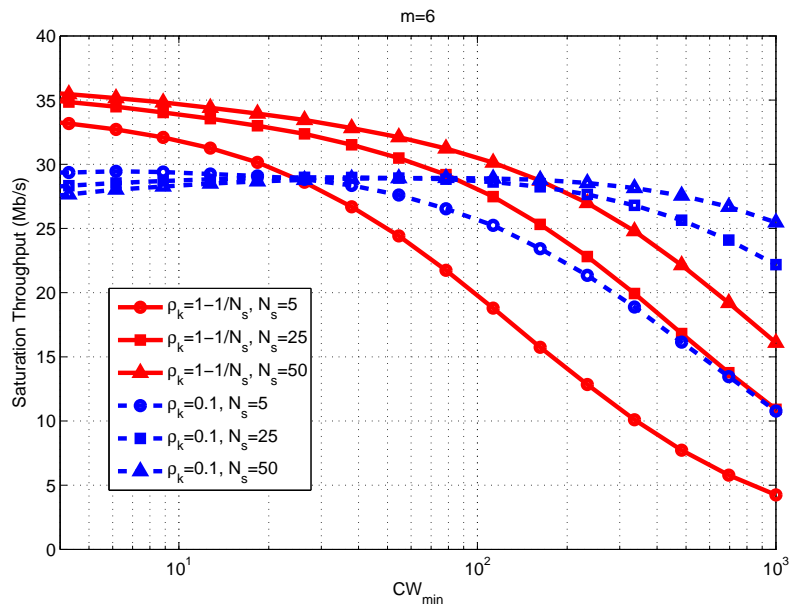


Fig. 5.8 Saturation throughput versus minimum contention window using the RTS/CTS access mechanism.

Table 5.2 Percentage of successfully transmitted packets for different users with different SNR s , assuming $\beta = 0.8$.

User Index	1	2	3	4	5	6	7	8	9	10
SNR (dB)	0	2.5	5	7.5	10	12.5	15	17.5	20	25
Percentage (%)	9.96	9.95	9.97	9.93	9.97	9.99	9.96	9.97	9.96	10

range of CW_{\min} . For instance, using $\rho_k^i = 0.1$, the saturation throughput is almost independent of the minimum contention window size for $CW_{\min} < 64$. Comparing two different threshold settings, it is shown that the maximum achievable throughput is higher for $\rho_k^i = 1 - \frac{1}{N_s}$.

To confirm that the proposed adaptive CSMA gives fair access to different users, Table 5.2 shows the distribution of successfully transmitted packets among 10 users, each with a different SNR between 0dB to 25dB. It is shown that the successfully transmitted packets are fairly distributed among users.

5.6 Concluding Remarks

In this chapter, we have presented a study on the throughput performance of the proposed adaptive CSMA in a single idle channel. The effects of network configuration parameters (e.g., the number of users in the network, the minimum contention window, and the packet length) have been investigated on the saturation throughput. In the adaptive CSMA, users go through a refinement process based on their adaptive activity factors, before participating in the backoff competition. As a result, we have shown that the collision probability is decreased due to the smaller number of competitors. Furthermore, the saturation throughput is improved since users with better channel qualities are given higher chance to stay in the competition. Numerical results confirm the performance gains, i.e., high throughput as well as long-term fairness, offered by the proposed adaptive CSMA-based access strategy in comparison with the conventional CSMA scheme.

Chapter 6

Aggregate Interference and Capacity-Outage Analysis in Cognitive Radio Networks

6.1 Introduction

When studying the OSA design in a cognitive radio network, one of the key design issues is sufficiently protecting PUs' communications from the interference caused by SUs, while optimizing the spectrum utilization of SUs. In Chapter 3, we have proposed an adaptive transmission strategy for SUs to reduce the effects of collision between PU and SU. Assuming the proposed access scheme, in Chapter 3 and Chapter 4, we have developed SU access algorithms, focusing on the SU access optimization. To be able to support QoS requirements for PUs, in this chapter¹, we look into the problem from a PU perspective and evaluate the PU performance in the presence of interference from SUs. More specifically, we present a study on the aggregate interference imposed by SUs to a PU and introduce the capacity-outage probability of PU as a measure to keep the level of interference below a prescribed tolerance level.

To guarantee a certain level of QoS for PUs, different approaches are considered in the OSA design literature. In [22, 29], the proposed OSA schemes limit the probability of collision of

¹Parts of Chapter 6 have been presented at the 2010 25th Queen's Biennial Symposium on Communications (QBSC) in Kingston, ON, Canada [102], the 2010 IEEE Vehicular Technology Conference (VTC-Fall) in Ottawa, ON, Canada [103] and the 2011 IEEE Canadian Conference on Electrical and Computer Engineering (CCECE) in Niagara Falls, ON, Canada [104], and published in the IEEE Transactions on Vehicular Technology [105].

SUs with PUs. However, the collision probability is not a precise measure to protect PUs since the effects of propagation channel gains from SUs to PUs are not considered. Another proposed approach is to keep the aggregate interference level caused by SUs below a prescribed tolerable threshold for PUs assuming perfect knowledge of instantaneous channel gains from SU transmitters to PU receivers [106, 107]. However, knowing and tracking the instantaneous channel gains from SU transmitters to PU receivers might be difficult in practice.

Recognizing such practical limitations, in this chapter, we present a statistical model on the aggregate interference caused by SUs to a PU due to miss-detection errors. In particular, the probabilistic properties of the aggregate interference is investigated in consideration of random SU locations and their propagation characteristics. Based on the developed statistical model, we subsequently derive the PU capacity-outage probability (i.e., the probability that the PU capacity falls below a prescribed level). This will help to examine the effects of various system parameters on the performance of the PU in the presence of interference from SUs. Consequently, PU capacity-outage probabilities are introduced as a measure to maintain QoS for PUs in designing OSA schemes for SUs.

In cognitive radio networks, beacon signaling can be used by PUs in order to help SUs in the detection of spectrum holes [108–110]. In a cognitive network using a beacon, different locations are considered for the beacon transmitter to study the aggregate interference. The beacon transmitter could be located at the PU receiver [64, 110] or at the PU transmitter [65]. Accordingly, we analyze the effects of the beacon transmitter location on the aggregate interference caused by SUs and the performance of the PU dealing with such aggregate interference. In addition, we study the effects of applying cooperative sensing [111–116] in a cognitive radio network on the mitigation of interference. More specifically, we look into the interference distribution and the capacity-outage probability of the PU, while SUs use OR (logical OR operation) and maximum likelihood (ML) cooperative techniques to detect the spectrum holes.

The remainder of this chapter is organized as follows. After a brief overview of the system configuration and modeling in Section 6.2, Section 6.3 provides the probability density function (PDF) of the aggregate interference over Nakagami fading channels and the closed-form expression for the capacity-outage probability when the beacon transmitter is at the PU receiver. Section 6.4 presents the interference distribution and closed-form expression for the capacity-outage probability for the case in which the beacon transmitter is at the PU transmitter. In addition, the performance comparison is provided to study the beacon transmitter placement effect. In Section 6.5, the interference and capacity-outage analysis of a network with cooperative sensing are

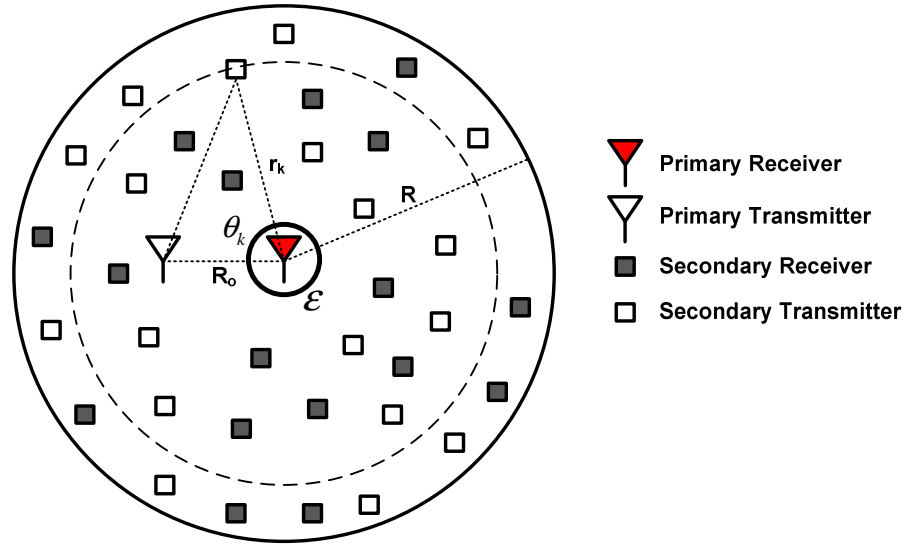


Fig. 6.1 Network model.

studied. Finally, Section 6.6 presents the concluding remarks.

6.2 System Configuration and Modeling

To model the aggregate interference caused by SUs to a PU in a single licensed channel, we consider a PU communications link of distance R_0 surrounded by N_s SUs. According to the proposed transmission strategy for SUs in Chapter 3, we assume that each SU has an activity factor of β , which is the probability that the SU is actively transmitting. Furthermore, we assume that the SUs are uniformly located with a density of λ_d SUs per unit area in a ring centered at the PU receiver with the inner radius ϵ and the outer radius of R , where $\epsilon < R_0$. In other words, ϵ represents the minimum allowable distance between a transmitter and a receiver. Under these assumptions, the distance between the SU transmitter k and the PU receiver, r_k , is a random variable with PDF $f_{r_k}(r_k) = 2r_k(R^2 - \epsilon^2)^{-1}$, where $\epsilon \leq r_k \leq R$. Moreover, the angle θ_k , which the SU transmitter k makes to the line connecting the PU transmitter and receiver, is uniformly distributed between 0 and 2π (see Figure 6.1).

The wireless channel model includes the path loss and the small-scale fading, i.e., the channel response can be expressed as $h = \tilde{h}Ad^{-\frac{\alpha}{2}}$, where d is the distance between the transmitter and the receiver under consideration, $\alpha \geq 2$ is the path-loss exponent, A is a constant dependent

on the frequency and transmitter/receiver antenna gain, and \tilde{h} represents the small-scale fading component. Since such a model is valid for $d \neq 0$, we assume that transmitters cannot be located closer than an arbitrarily small distance $\varepsilon > 0$ (i.e., a minimum allowable distance between a transmitter and a receiver). For simplicity, without loss of generality, we normalize $A = 1$ in the following discussion. The channel response of the PU transmitter-receiver link is denoted as h_0 , whereas that of the interference link from the SU transmitter k to the PU receiver is denoted as h_k .

To indicate the presence of PU transmission, we assume that a beacon signal is transmitted on an out-of-band control channel. If a SU correctly detects the beacon, it will be silent for the whole PU transmission period. In the case that it miss-detects the beacon, the SU transmits concurrently with the PU with a probability that is its activity factor β . As a result, it may introduce interference to the PU. Different approaches are proposed in literature for the spectrum sensing in cognitive radio networks such as the direct spectrum sensing (i.e., sensing the PU signal) [117] and spectrum sensing through beacon signals [108]. In this work, we consider the spectrum sensing through beacons in order to study the effects of beacon transmitter placement on the aggregate interference. However, the aggregate interference analysis for the direct sensing is similar to the case when the beacon transmitter is located at the PU transmitter. Therefore, the results can be applied for the direct sensing as well.

Assume an energy detection scheme in which the SU declares the beacon presence if its received power from the beacon is larger than a threshold. The received beacon signal at the SU transmitter k can be presented as $y_{B,k} = \tilde{g}_k d_{B,k}^{-\frac{\alpha}{2}} x_B + z_B$ where x_B is the transmitted beacon signal with power P_B , $d_{B,k}$ is the distance between the beacon transmitter and the SU transmitter k , \tilde{g}_k represents the small-scale fading over the link between the beacon transmitter and the SU transmitter k , and $z_B \sim \mathcal{N}(0, \sigma_B^2)$ is the additive white Gaussian noise (AWGN). Hence, the received signal-to-noise ratio (SNR) of the beacon signal at the SU transmitter k is $\eta_k = \frac{P_B |\tilde{g}_k|^2 d_{B,k}^{-\alpha}}{\sigma_B^2}$.

In [118], the exact detection probability of an energy detector is derived as a function of η_k . In particular, $P_d(\eta_k) = Q\left(\frac{Q^{-1}(P_{fa}) - \sqrt{\nu}\eta_k}{\sqrt{1+2\eta_k}}\right)$ where P_{fa} is the false alarm probability and ν is the product of the energy detector's integration time and the channel bandwidth. In [64], it is shown that for a small P_{fa} (e.g., $P_{fa} < 0.01$), the detection probability can be approximated as
$$P_d(\eta_k) \simeq \begin{cases} 0, & \eta_k < \eta_0 \\ 1, & \eta_k \geq \eta_0 \end{cases}, \text{ where } \eta_0 = \frac{Q^{-1}(P_{fa})}{\sqrt{\nu}}.$$
 Hence, the average beacon miss-detection

probability of the SU k can be approximated as

$$P_{m,k} \simeq \text{Prob}(\eta_k < \eta_0). \quad (6.1)$$

Assuming $\gamma = \frac{\sigma_B^2 \eta_0}{P_B}$, then

$$P_{m,k} \simeq \text{Prob} \left(|\tilde{g}_k|^2 < \frac{\sigma_B^2 \eta_0}{P_B} d_{B,k}^\alpha \right) = \text{Prob}(|\tilde{g}_k|^2 < \gamma d_{B,k}^\alpha). \quad (6.2)$$

Let x_0 and x_k be the transmitted signals from the PU and the SU k with power of P_0 and P , respectively. The received signal at the PU receiver can be written as

$$y_0 = h_0 x_0 + \sum_{k=1}^{N_s} F_k h_k x_k + z_0 \quad (6.3)$$

where $z_0 \sim \mathcal{N}(0, \sigma_0^2)$ is AWGN and F_k , which indicates the coincident transmission of the SU k with the PU transmission, is a Bernoulli random variable, i.e.,

$$F_k = \begin{cases} 1, & \text{with probability } P_{m,k} \beta \\ 0, & \text{with probability } 1 - P_{m,k} \beta \end{cases}. \quad (6.4)$$

Since x_k in (6.3) are independent and zero-mean signals with power P , according to (6.3) and (6.4), the aggregate interference caused by SUs becomes

$$I_0 = \sum_{k=1}^{N_s} I_k, \quad I_k = P_{m,k} L_k = P_{m,k} \beta P |\tilde{h}_k|^2 r_k^{-\alpha} \quad (6.5)$$

where $L_k = P \beta |\tilde{h}_k|^2 r_k^{-\alpha}$ denotes the level of interference that the SU k causes to the PU receiver if it miss-detects the beacon signal. According to (6.5), the contribution level of the SU k to the aggregate interference depends on the product $P_{m,k} L_k$.

6.3 Beacon Transmitter at the Primary User Receiver

6.3.1 Interference Model

In this section, we study the probabilistic properties of aggregate interference in small-scale fading channels when the beacon transmitter is located at the PU receiver.

Rayleigh fading

In a Rayleigh fading channel, $|\tilde{g}_k|^2$ has an exponential distribution with parameter 1. Therefore, according to (6.2), the beacon miss-detection probability is given by

$$P_{m,k} \simeq 1 - e^{-\gamma d_{B,k}^\alpha}. \quad (6.6)$$

The beacon miss-detection probability must be kept low, typically lower than 3% for good operation, and in this range, it can be further approximated as

$$P_{m,k} \simeq 1 - e^{-\gamma d_{B,k}^\alpha} \simeq 1 - (1 - \gamma d_{B,k}^\alpha) = \gamma d_{B,k}^\alpha. \quad (6.7)$$

When the beacon transmitter is located at the primary receiver, $d_{B,k} = r_k$, and from (6.5) and (6.7), $I_k = P\beta\gamma|\tilde{h}_k|^2$. Since $|\tilde{h}_k|^2$ has an exponential distribution with parameter 1, I_k , $k = 1, \dots, N_s$ are i.i.d. random variables and have the exponential distribution with parameter $\frac{1}{P\beta\gamma}$. As a result, $I_0 = \sum_{k=1}^{N_s} I_k$ has a Gamma distribution with shape parameter N_s , scale parameter $P\beta\gamma$ and $E[I_0] = N_s P\beta\gamma$, i.e.,

$$f_{I_0}(i_0; N_s, P\beta\gamma) = \frac{i_0^{N_s-1} e^{-\frac{i_0}{P\beta\gamma}}}{(P\beta\gamma)^{N_s} \Gamma(N_s)}, \quad i_0 > 0. \quad (6.8)$$

Figure 6.2 illustrates the plot of the cumulative distribution function (CDF) of aggregate interference. The plot confirms that the Gamma distribution with the calculated parameters has an accurate fit for the interference distribution².

² $\beta = 0.01$, $\lambda_d = 0.01$, $\gamma = 10^{-6}$, $P = 1$, $\varepsilon = 1$, $R_0 = 5$ and $R = 50$ are used for numerical results shown in Figures 6.2-6.15 unless specified otherwise.

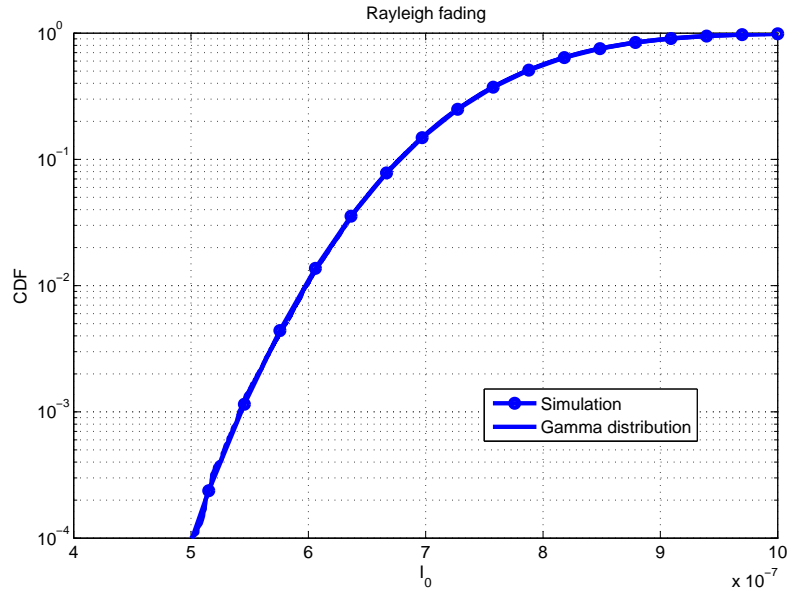


Fig. 6.2 CDF of the aggregate interference in a Rayleigh fading channel for the beacon transmitter at the PU receiver.

Nakagami fading

In a Nakagami fading channel parameterized by the average received power P_{avg} and the fading parameter m , the channel power (i.e., $|\tilde{h}_k|^2$ and $|\tilde{g}_k|^2$) has a Gamma distribution with the shape parameter $\zeta = m$ and the scale parameter $\theta = \frac{1}{m}$ assuming $P_{\text{avg}} = 1$. Considering the CDF of the Gamma distribution, according to (6.2), the miss-detection probability is

$$P_{m,k} = \text{Prob}(|\tilde{g}_k|^2 < \gamma r_k^\alpha) = \frac{\Gamma(\zeta, \gamma r_k^\alpha / \theta)}{\Gamma(\zeta)} = \frac{\Gamma(m, m\gamma r_k^\alpha)}{\Gamma(m)} \quad (6.9)$$

where $\Gamma(s) = \int_0^{+\infty} t^{s-1} e^{-t} dt$ is the Gamma function and $\Gamma(s, x) = \int_0^x t^{s-1} e^{-t} dt$ is the lower incomplete Gamma function. For small $\gamma \ll 1$, $\Gamma(m, m\gamma r_k^\alpha) \approx \frac{(m\gamma r_k^\alpha)^m}{m}$. Therefore, according to (6.5), the aggregate interference is

$$I_0 = \sum_{k=1}^{N_s} I_k, \quad I_k = P\beta \frac{(m\gamma)^m}{m\Gamma(m)} |\tilde{h}_k|^2 r_k^{\alpha(m-1)}. \quad (6.10)$$

To present a statistical model for the interference, the mean and variance of the aggregate interference are calculated. Since $f_{r_k}(r_k) = 2r_k(R^2 - \varepsilon^2)^{-1}$, where $\varepsilon \leq r_k \leq R$, then for $\varepsilon \ll R$,

$E[r_k^{\alpha(m-1)}] \simeq \frac{2R^{\alpha(m-1)}}{\alpha(m-1)+2}$. Note that $E[.]$ and $\text{var}[.]$ denote expectation and variance respectively. Therefore, the mean of aggregate interference becomes

$$E[I_0] \simeq N_s P \beta \frac{(m\gamma)^m}{m\Gamma(m)} \frac{2R^{\alpha(m-1)}}{\alpha(m-1)+2}. \quad (6.11)$$

Since $\text{var} \left[|\tilde{h}_k|^2 r_k^{\alpha(m-1)} \right] \simeq \frac{R^{2\alpha(m-1)}}{m} \left[\frac{2-\alpha(m-1)^2}{(\alpha(m-1)+1)(\alpha(m-1)+2)} \right]$, then

$$\text{var}[I_0] \simeq N_s \left(P \beta \frac{(m\gamma)^m}{m\Gamma(m)} \right)^2 \frac{R^{2\alpha(m-1)}}{m} \left[\frac{2-\alpha(m-1)^2}{(\alpha(m-1)+1)(\alpha(m-1)+2)} \right]. \quad (6.12)$$

By using mean squared-error curve-fitting for different numbers of SUs, the Gamma distribution is found to have a good agreement with the simulation results. For a given set of $\{r_k\}$, I_k , $k = 1, \dots, N_s$ are Gamma random variables. As a sum of Gamma random variables, I_0 (conditioned on $\{r_k\}$) is a Gamma random variable as well with $E[I_0|\{r_k\}] \simeq P\beta \frac{(m\gamma)^m}{m\Gamma(m)} \sum_{k=1}^{N_s} r_k^{\alpha(m-1)}$ and $\text{var}[I_0|\{r_k\}] = \left(P\beta \frac{(m\gamma)^m}{m\Gamma(m)} \right)^2 \sum_{k=1}^{N_s} \frac{r_k^{2\alpha(m-1)}}{m}$. For a large number of SUs independently and identically distributed uniformly in the circular area with $\varepsilon \leq r_k \leq R$, I_0 (unconditioned) can be approximated as a Gamma random variable with $E[I_0] \simeq N_s P\beta \frac{(m\gamma)^m}{m\Gamma(m)} E[r_k^{\alpha(m-1)}]$ and $\text{var}[I_0] = N_s \left(P\beta \frac{(m\gamma)^m}{m\Gamma(m)} \right)^2 \text{var} \left[|\tilde{h}_k|^2 r_k^{\alpha(m-1)} \right]$ in (6.11) and (6.12).

According to (6.11) and (6.12), the shape parameter ζ and the scale parameter θ of Gamma distribution can be derived as

$$\begin{aligned} \zeta &= \frac{E^2[I_0]}{\text{var}[I_0]} = N_s m \frac{4(\alpha(m-1)+1)}{(\alpha(m-1)+2)(2-\alpha(m-1)^2)}, \\ \theta &= \frac{\text{var}[I_0]}{E[I_0]} = P\beta \frac{(m\gamma)^m}{m\Gamma(m)} \frac{R^{\alpha(m-1)}}{m} \frac{2-\alpha(m-1)^2}{2(\alpha(m-1)+1)}. \end{aligned} \quad (6.13)$$

Figure 6.3 compares the simulations results with Gamma distribution with the calculated parameters for different m . It shows that the Gamma approximation matches closely with the simulation results.

6.3.2 Capacity-Outage Probability

In the presence of interference from SUs, the instantaneous capacity of the PU is $C_{I_0} = \log_2 \left(1 + |h_0|^2 \frac{P_0}{I_0 + \sigma_0^2} \right)$. Given a required PU threshold rate C_0 , the capacity-outage probability can be

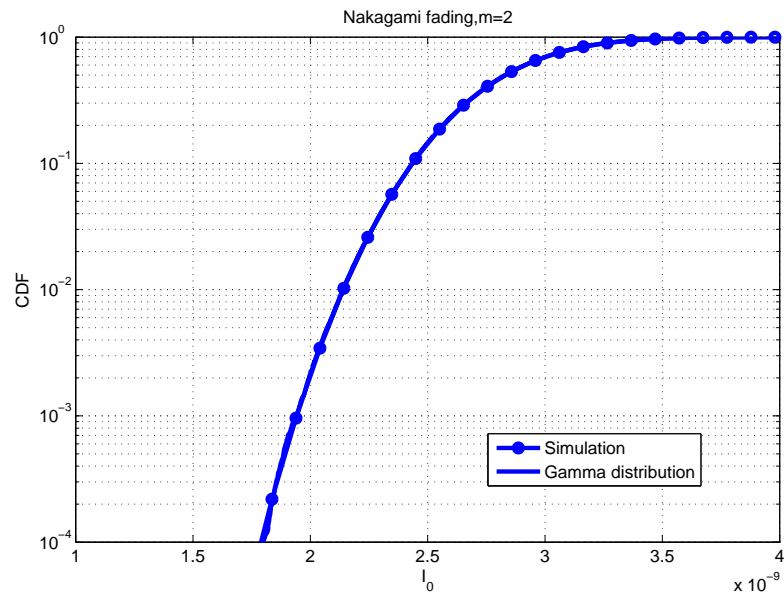
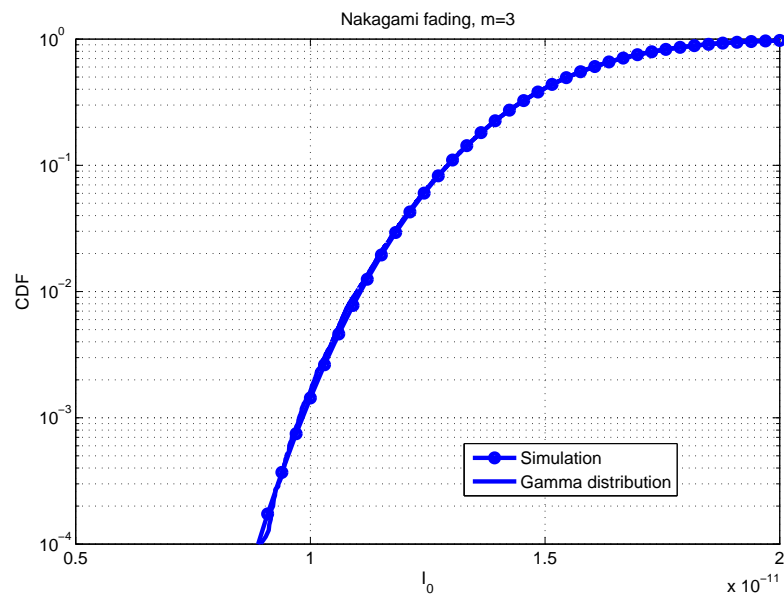
(a) $m = 2$ (b) $m = 3$

Fig. 6.3 CDF of the aggregate interference in Nakagami fading channels with non-cooperative sensing and the beacon transmitter at the PU receiver.

calculated as

$$P_{\text{out}} = \text{E}[\text{Prob}[C_{I_0} \leq C_0 | I_0]] \quad (6.14)$$

where $\text{Prob}[C_{I_0} \leq C_0 | I_0] = \text{Prob}[|\tilde{h}_0|^2 \leq P_r^{-1}(I_0 + \sigma_0^2)]$ and $P_r = P_0(2^{C_0} - 1)^{-1}R_0^{-\alpha}$. Assuming Rayleigh fading channel, $|\tilde{h}_0|^2$ has the exponential distribution with parameter 1 and I_0 has the Gamma distribution represented by its PDF $f_{I_0}(i_0; N_s, P\beta\gamma)$ given by (6.8). As a result,

$$\text{Prob}[|\tilde{h}_0|^2 \leq P_r^{-1}(I_0 + \sigma_0^2)] = 1 - e^{-P_r^{-1}(I_0 + \sigma_0^2)} \quad (6.15)$$

and

$$\begin{aligned} P_{\text{out}} &= 1 - e^{-\frac{\sigma_0^2}{P_r}} \int_0^{+\infty} e^{-\frac{i_0}{P_r}} f_{I_0}(i_0; N_s, P\beta\gamma) di_0 \\ &= 1 - e^{-\frac{\sigma_0^2}{P_r}} \left(1 + \frac{\theta}{P_r}\right)^{-\zeta} = 1 - e^{-\frac{\sigma_0^2}{P_r}} \left(1 + \frac{P\beta\gamma}{P_r}\right)^{-N_s}. \end{aligned} \quad (6.16)$$

For low outage probability, e.g., 3% or less, the above expression can be approximated as

$$P_{\text{out}} = 1 - \left(1 - \frac{\sigma_0^2}{P_r}\right) \left(1 - N_s \frac{P\beta\gamma}{P_r}\right) \approx \frac{\sigma_0^2 + N_s P\beta\gamma}{P_r} = \left(\frac{P_0 R_0^{-\alpha}}{\sigma_0^2 + N_s P\beta\gamma}\right)^{-1} (2^{C_0} - 1). \quad (6.17)$$

In the above expression, $P_0 R_0^{-\alpha}$ is the average power of the received PU signal, whereas $N_s P\beta$ represents the average total transmitted power from SUs. $N_s P\beta\gamma$ can be interpreted as the effective interference, and $\frac{P_0 R_0^{-\alpha}}{\sigma_0^2 + N_s P\beta\gamma}$ represents the average signal-to-SU-interference-and-noise ratio (SINR) at the PU receiver. In other words, the above expression indicates that the capacity-outage probability is approximately proportional to the inverse of the SINR, and exponentially increases with the required PU threshold rate C_0 . The expression is also applicable for the case of no SU by setting N_s , β , or γ to 0. Figure 6.4 illustrates the plots of the capacity-outage probability versus the PU threshold rate C_0 (in b/s/Hz) for different SINR values. The plot confirms the precision of the analytical derivation in (6.16) as it closely matches the simulation results. It also supports the result that the capacity-outage probability is approximately proportional to the inverse of the SINR by comparing different plots for a given C_0 .

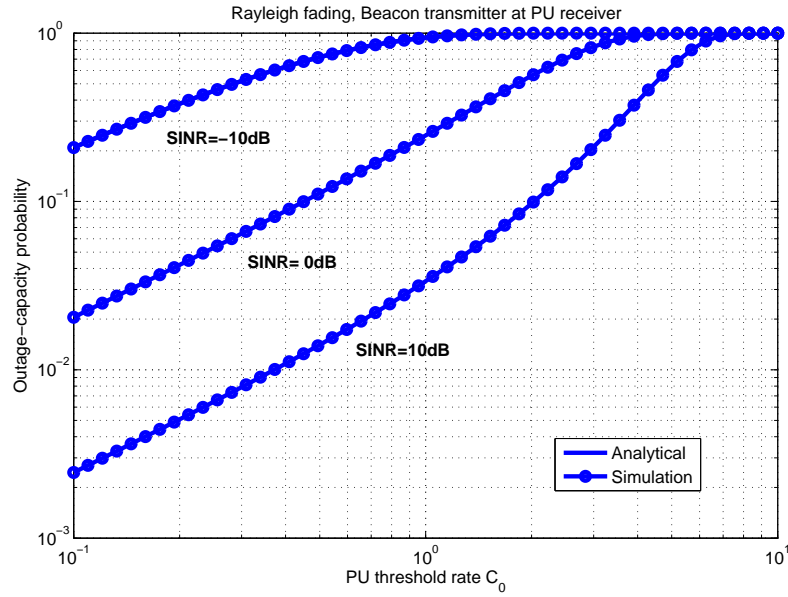


Fig. 6.4 PU capacity-outage probability versus required threshold rate for various SINRs in a Rayleigh fading channel with the beacon transmitter at the PU receiver.

Assuming different activity factors β_k^i for SUs in a specific channel i , the effective interference power (i.e., aggregate interference mean) which limit the capacity-outage probability of PU is $\sum_{k=1}^{N_s} P\beta_k^i\gamma$. Hence, SUs need to keep this effective interference parameter below a certain level (i.e., I_{th}) to guarantee an acceptable capacity-outage probability for the PUs in each channel. Thus,

$$\sum_{k=1}^{N_s} P\beta_k^i\gamma \leq I_{th} \Rightarrow \sum_{k=1}^{N_s} \beta_k^i \leq \beta_{th}. \quad (6.18)$$

where $\beta_{th} = \frac{I_{th}}{P\gamma}$. Since we already had the orthogonal sharing constraints (i.e., $\sum_{k=1}^{N_s} \beta_k^i \leq 1$) in the activity factor allocation problem (3.8), the PU capacity-outage constraints (due to the imperfect sensing) do not affect the developed algorithms in Chapter 3 and Chapter 4.

6.4 Beacon Transmitter at the Primary User Transmitter

6.4.1 Interference Model

Rayleigh fading

When the beacon transmitter is located at the PU transmitter, the distance between the beacon transmitter and the SU transmitter k is $d_{B,k} = \sqrt{r_k^2 + R_0^2 - 2r_k R_0 \cos \theta_k}$. From (6.5) and (6.7), the instantaneous interference from the SU transmitter k to the PU receiver becomes

$$I_k = P\beta\gamma|\tilde{h}_k|^2 \left[1 + \frac{R_0^2}{r_k^2} - 2\frac{R_0}{r_k} \cos \theta_k \right]^{\alpha/2} \quad (6.19)$$

where r_k is a random variable with PDF $f_{r_k}(r_k) = 2r_k(R^2 - \varepsilon^2)^{-1}$, where $\varepsilon \leq r_k \leq R$, and the angle θ_k , which the SU transmitter k makes to the line connecting the PU transmitter and receiver, is uniformly distributed between 0 and 2π . The aggregate interference from SUs is

$$I_0 = \sum_{k=1}^{N_s} P\beta\gamma|\tilde{h}_k|^2 \left[1 + \frac{R_0^2}{r_k^2} - 2\frac{R_0}{r_k} \cos \theta_k \right]^{\alpha/2}. \quad (6.20)$$

To present a statistical model for the interference, the aggregate interference mean is calculated. Since $E[|\tilde{h}_k|^2] = 1$, $E[I_0] = N_s P\beta\gamma E \left[\left[1 + \frac{R_0^2}{r_k^2} - 2\frac{R_0}{r_k} \cos \theta_k \right]^{\alpha/2} \right]$. By approximating $E[I_0]$ with four terms, the mean of aggregate interference becomes

$$E[I_0] \simeq N_s P\beta\gamma \left(1 - \binom{\frac{\alpha}{2}}{1} E \left[2\frac{R_0}{r_k} \cos \theta_k \right] + \binom{\frac{\alpha}{2}}{1} E \left[\frac{R_0^2}{r_k^2} \right] + \binom{\frac{\alpha}{2}}{2} E \left[4\frac{R_0^2}{r_k^2} \cos^2 \theta_k \right] \right). \quad (6.21)$$

Since $E[\cos \theta_k] = 0$, $E[\cos^2 \theta_k] = 0.5$ and $E[r_k^{-2}] = \frac{2(\ln(R) - \ln(\varepsilon))}{(R^2 - \varepsilon^2)}$,

$$E[I_0] \simeq N_s P\beta\gamma \left(1 + 0.5\alpha^2 R_0^2 \left(\frac{\ln(R) - \ln(\varepsilon)}{R^2 - \varepsilon^2} \right) \right). \quad (6.22)$$

Based on the probabilistic properties of θ_k , $|\tilde{h}_k|^2$, and r_k , sample values of I_0 can be generated by simulation to obtain the histogram of its distribution as shown in Figure 6.5. The aggregate

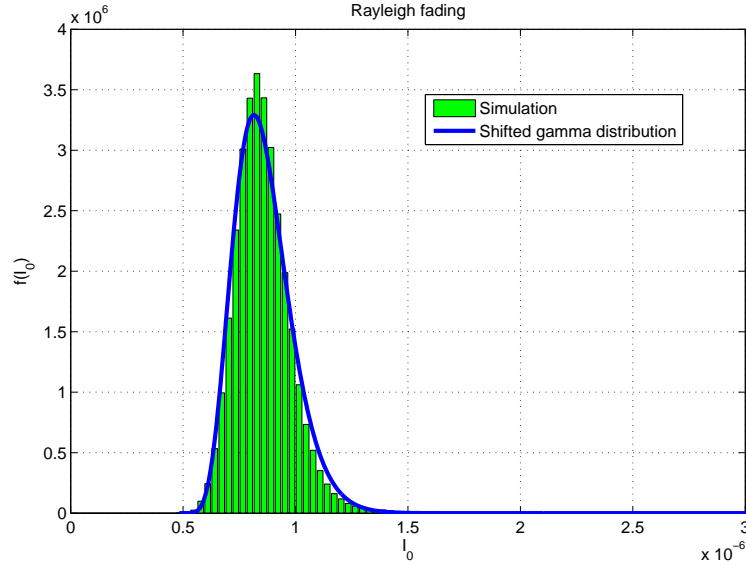


Fig. 6.5 Histogram and PDF of interference I_0 in a Rayleigh fading channel with path-loss exponent $\alpha = 2.1$.

interference from SUs can be approximated as

$$I_0 \approx \sum_{k=1}^{N_s} P\beta\gamma |\tilde{h}_k|^2 + \bar{I}_0. \quad (6.23)$$

In other words, in a Rayleigh channel, the aggregate interference from SUs can be approximated as a shifted-Gamma distributed random variable with the PDF

$$f_{I_0}(i_0; N_s, P\beta\gamma, \bar{I}_0) = \frac{(i_0 - \bar{I}_0)^{N_s-1} e^{-\frac{(i_0 - \bar{I}_0)}{P\beta\gamma}}}{(P\beta\gamma)^{N_s} \Gamma(N_s)}, i > \bar{I}_0 \quad (6.24)$$

where N_s , $P\beta\gamma$ and \bar{I}_0 are, respectively, the shape parameter, the scale parameter and the shift parameter. According to (6.22) and (6.23), $\bar{I}_0 \simeq 0.5N_sP\beta\gamma\alpha^2R_0^2 \left(\frac{\ln(R) - \ln(\varepsilon)}{R^2 - \varepsilon^2} \right)$. The shift parameter empowers us to match the skewness of the distribution, in addition to the scale and shape parameters. If μ , σ^2 and κ are considered as mean, variance, and skewness of the aggregate interference I_0 , then $N_s = 4\kappa^{-2}$, $P\beta\gamma = \frac{\sigma\kappa}{2}$ and $\bar{I}_0 = \mu - 2\sigma\kappa^{-1}$.

The CDF of the aggregate interference plotted in Figure 6.6 shows that the shifted-Gamma approximation closely follows the simulation results and is more accurate than the Gamma approximation.

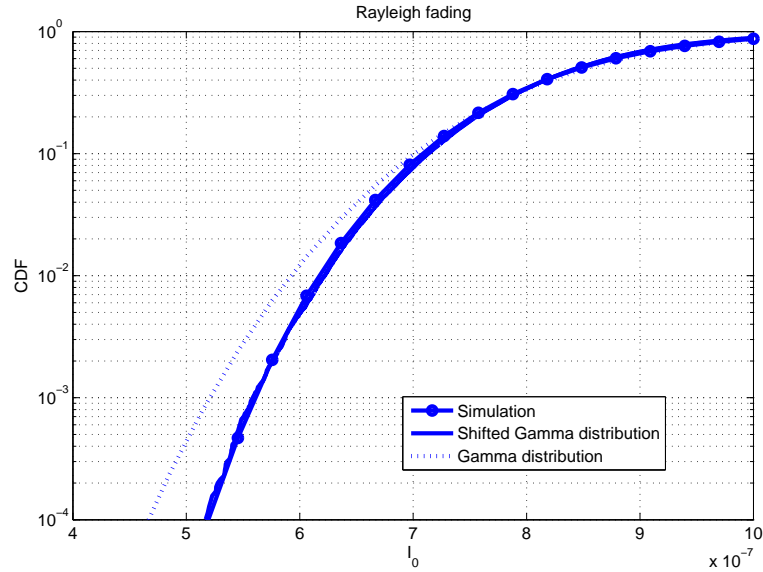


Fig. 6.6 CDF of aggregate interference in a Rayleigh fading channel for the beacon transmitter at the PU transmitter.

6.4.2 Capacity-Outage Probability

A closed-form expression for the outage probability of the PU related to the mean and variance of the interference can be derived to quantify the effect of SUs by using (6.15), where I_0 has the shifted-Gamma distribution represented by its PDF $f_{I_0}(i_0; N_s, P\beta\gamma, \bar{I}_0)$ given by (6.24). As a result,

$$P_{\text{out}} = 1 - e^{-\frac{\sigma_0^2}{P_r}} \int_0^{+\infty} e^{-\frac{i_0}{P_r}} f_{I_0}(i_0; N_s, P\beta\gamma, \bar{I}_0) di_0 = 1 - e^{-\frac{(\sigma_0^2 + \bar{I}_0)}{P_r}} \left(1 + \frac{P\beta\gamma}{P_r}\right)^{-N_s}. \quad (6.25)$$

For low outage probability, e.g., 3% or less, the above expression can be approximated as

$$\begin{aligned} P_{\text{out}} &\approx 1 - \left(1 - \frac{(\sigma_0^2 + \bar{I}_0)}{P_r}\right) \left(1 - N_s \frac{P\beta\gamma}{P_r}\right) \approx \frac{(\sigma_0^2 + \bar{I}_0) + N_s P\beta\gamma}{P_r} \\ &= \left(\frac{P_0 R_0^{-\alpha}}{\sigma_0^2 + \bar{I}_0 + N_s P\beta\gamma}\right)^{-1} (2^{C_0} - 1). \end{aligned} \quad (6.26)$$

The expression in (6.26) is very much similar to (6.17) with the same average power of the received PU signal, as represented by $P_0 R_0^{-\alpha}$, whereas the effective interference becomes $N_s P\beta\gamma + \bar{I}_0$, which is increased by an additional term \bar{I}_0 , as compared to that in the case of beacon trans-

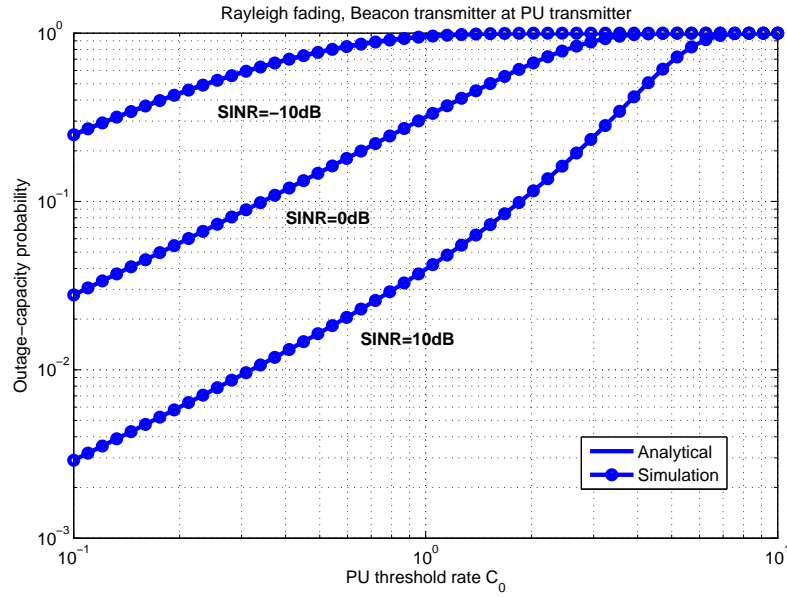


Fig. 6.7 PU capacity-outage probability versus required threshold rate for various SINRs in a Rayleigh fading channel with the beacon transmitter at the PU transmitter.

mitter at the PU receiver.

Figure 6.7 illustrates the plots of the capacity-outage probability versus the PU threshold rate C_0 (in b/s/Hz) for different values of SINR $\triangleq \frac{P_0 R_0^{-\alpha}}{\sigma_0^2 + N_s P \beta \gamma}$. The plots confirm the precision of the analytical derivation in (6.25) as they closely match the simulation results. Furthermore, as compared to results in Figure 6.4, for the same SINR and PU threshold rate C_0 , the beacon transmitter at the PU transmitter yields a higher capacity-outage probability than the beacon transmitter at the PU receiver.

6.4.3 Beacon Transmitter Placement Comparison

In this section, with focus on the general network model in Figure 6.1, we study the effect of beacon transmitter placement on the performance of the network by comparing the aggregate interference mean and the capacity-outage probability of PU for two different scenarios: the beacon transmitter 1) at the PU transmitter or 2) at the PU receiver.

As shown in (6.5), the contribution level of SU k to the aggregate interference depends on the product $P_{m,k} L_k$. The probability of miss-detection $P_{m,k}$ (and also the probability of causing interference) depends on the distance from the SU transmitter k to the beacon transmitter, $d_{B,k}$,

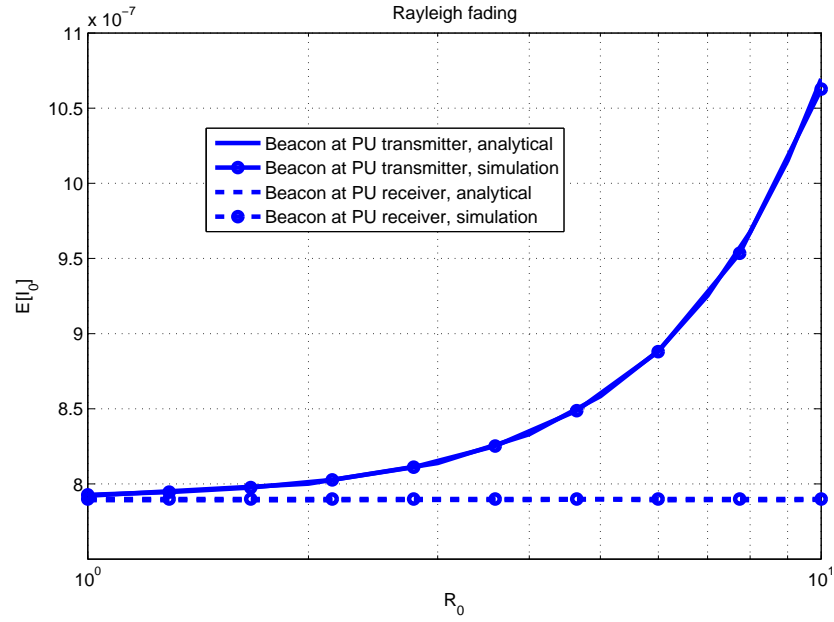


Fig. 6.8 Interference mean $E[I_0]$ versus PU transmitter-receiver distance R_0 .

whereas the interference level L_k depends on the distance from the SU transmitter k to the PU receiver, r_k . This fact makes the location of beacon transmitter (at the PU transmitter or at the PU receiver) influencing the effective aggregate interference differently. In locations of high interference level L_k (i.e., when the SU transmitter is close to the PU receiver), placing the beacon transmitter at the PU transmitter increases the probability of causing interference $P_{m,k}$, whereas placing the beacon transmitter at the PU receiver decreases the probability of causing interference. As a result, placing the beacon transmitter at the PU transmitter causes higher $P_{m,k}L_k$ and hence higher effective aggregate interference in comparison with locating the beacon transmitter at the PU receiver.

As shown in (6.26), as compared to the case with the beacon transmitter at the PU receiver, the use of beacon transmitter at the PU transmitter introduces extra interference, represented by \bar{I}_0 . Consequently, the PU capacity-outage probability is increased. It means that, for the network model considered in Figure 6.1, placing the beacon transmitter at the PU receiver is more beneficial to avoid interference increase although it is more practical to put the beacon transmitter at the PU transmitter.

Figure 6.8 illustrates the plots of aggregate interference mean versus R_0 for two different scenarios, i.e., the beacon transmitter at the PU receiver and the beacon transmitter at the PU

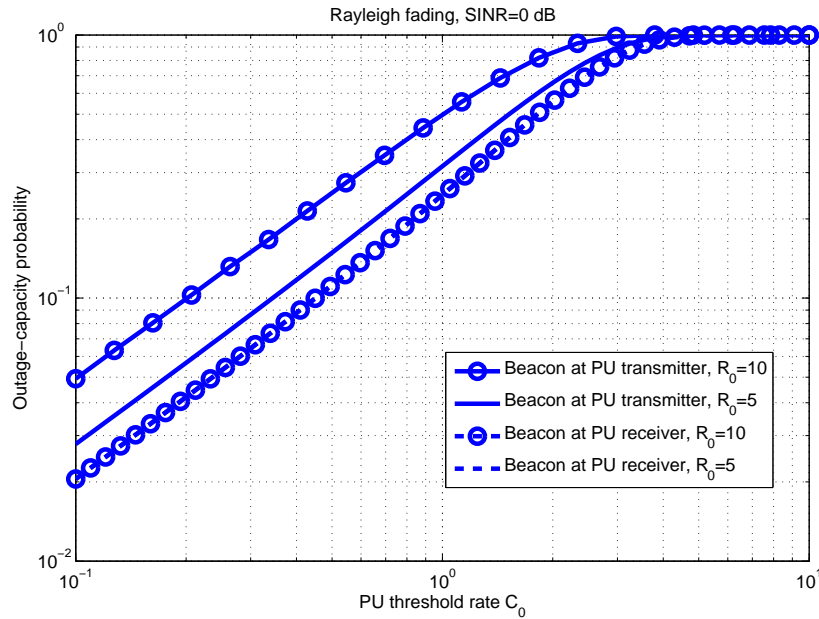


Fig. 6.9 PU capacity-outage probability versus required threshold rate.

transmitter. Both analytical results and simulation results are provided. It can be observed that the analytical results according to $E[I_0] = N_s P \beta \gamma$ for the case with beacon transmitter at primary receiver and (6.22) match closely with the respective simulation results. It is apparent that the mean value (i.e., $E[I_0] = N_s P \beta \gamma$) is independent of R_0 when the beacon transmitter located at the PU receiver. However, when the beacon transmitter is located at the PU transmitter, the mean value according to (6.22) is an increasing function of R_0 . The plots show that the interference increase caused by locating the beacon transmitter at the PU transmitter is larger when the PU transmitter-receiver link is longer.

Figure 6.9 compares the capacity-outage probability of two different beacon transmitter placements, and shows that setting the beacon transmitter at the PU receiver improves the capacity-outage performance of PU by reducing the effective interference. Furthermore, in accordance with the results in Figure 6.8, it confirms that this PU capacity-outage performance improvement increases with larger PU transmitter-receiver distance R_0 .

6.5 Cooperative Sensing

In this section, we provide a study on the effect of cooperative sensing (i.e., OR sensing and ML sensing) on alleviating the aggregate interference in Nakagami fading channels assuming a beacon transmitter at the PU receiver (i.e., $d_{B,k} = r_k$ and $\tilde{g}_k = \tilde{h}_k$). Since our objective is to highlight the impact of SU cooperation on the aggregate interference rather than designing advanced cooperation schemes, we simply consider the following cooperation protocol. Upon detecting a beacon, a SU broadcasts a signal—which can be the preliminary result as 1 bit in OR cooperation or the received beacon signal power in ML cooperation—to its neighbors within its cooperation range. In this simple protocol, SUs broadcast their messages in different time-slots of a control frame on a dedicated control channel.

The probabilistic properties of aggregate interference are investigated for OR and ML cooperative sensing in Nakagami fading channels. The closed-form expressions for capacity-outage probability are derived in Rayleigh fading channels. Comparing the mean of interference and capacity-outage probability, it can be concluded that increasing the cooperation range (i.e., increasing the number of cooperating SUs) offers lower interference and, hence, better capacity-outage probabilities. In addition, it is shown that employing ML cooperative sensing offers lower interference at the cost of requiring more signaling overheads.

6.5.1 OR Detector

Interference Model

In OR cooperative detection, it is assumed that each SU sends its preliminary detection decision as 1 bit via the cooperation channel. The SUs within a certain range (cooperation R_c) can correctly receive the other SUs' preliminary decisions. Each SU will use the OR rule on the preliminary decisions to decide finally if the PU exists. Then, the new beacon miss-detection probability of each SU with OR sensing is the product of the preliminary miss-detection probability of that SU and the probability that all of the SUs in its cooperation range miss-detect the beacon.

According to (6.9), the miss-detection probability can be written as $P_{m,k} = \prod_{j=1}^{N_c} \frac{\Gamma(m, m\gamma r_j^\alpha)}{\Gamma(m)}$ where $N_c = 1 + \lambda_d \pi R_c^2$ is the number of cooperating SUs. Considering $R_c < R$, where R is the outer radius of the network, all r_j in the cooperation range of SU k are assumed equal to r_k to simplify the problem. Therefore, the new beacon miss-detection probability is $P_{m,k} \simeq$

$\left(\frac{\Gamma(m, m\gamma r_k^\alpha)}{\Gamma(m)}\right)^{N_c}$. For small $\gamma \ll 1$, it can be approximated as

$$P_{m,k} \simeq \left(\frac{(m\gamma r_k^\alpha)^m}{m\Gamma(m)}\right)^{N_c}. \quad (6.27)$$

Since $d_{B,k} = r_k$, according to (6.5) and (6.27),

$$I_0 = \sum_{k=1}^{N_s} I_k, \quad I_k = P\beta \frac{(m\gamma)^{N_c m}}{(m\Gamma(m))^{N_c}} |\tilde{h}_k|^2 r_k^{\alpha(N_c m - 1)}. \quad (6.28)$$

Similar to (6.11) and (6.12), the mean and variance of aggregate interference can be derived as

$$E[I_0] = N_s P\beta \frac{(m\gamma)^{N_c m}}{(m\Gamma(m))^{N_c}} \frac{2R^{\alpha(N_c m - 1)}}{\alpha(N_c m - 1) + 2}, \quad (6.29)$$

$$\text{var}[I_0] = N_s \left(P\beta \frac{(m\gamma)^{N_c m}}{(m\Gamma(m))^{N_c}}\right)^2 \frac{R^{\alpha(N_c m - 1)}}{m} \left[\frac{2 - \alpha(m - 1)(mN_c - 1)}{(\alpha(mN_c - 1) + 1)(\alpha(mN_c - 1) + 2)}\right]. \quad (6.30)$$

Similar to the non-cooperative case, by using mean squared-error curve-fitting for different number of SUs, the Gamma distribution matches closely with the simulation results. For a given set of $\{r_k\}$, I_k , $k = 1, \dots, N_s$ are Gamma random variables. As the sum of Gamma random variables, I_0 (conditioned on $\{r_k\}$) is a Gamma random variable with $E[I_0|\{r_k\}] \simeq P\beta \frac{(m\gamma)^{N_c m}}{(m\Gamma(m))^{N_c}} \sum_{k=1}^{N_s} r_k^{\alpha(N_c m - 1)}$ and $\text{var}[I_0|\{r_k\}] = \left(P\beta \frac{(m\gamma)^{N_c m}}{(m\Gamma(m))^{N_c}}\right)^2 \sum_{k=1}^{N_s} \frac{r_k^{2\alpha(N_c m - 1)}}{m}$. For a large number of SUs independently and identically distributed uniformly in the circular area with $\varepsilon \leq r_k \leq R$, I_0 (unconditioned) can be approximated as a Gamma random variable with $E[I_0] \simeq P\beta \frac{(m\gamma)^{N_c m}}{(m\Gamma(m))^{N_c}} E[r_k^{\alpha(N_c m - 1)}]$ and $\text{var}[I_0] = \left(P\beta \frac{(m\gamma)^{N_c m}}{(m\Gamma(m))^{N_c}}\right)^2 \text{var}\left[|\tilde{h}_k|^2 r_k^{\alpha(N_c m - 1)}\right]$ in (6.29) and (6.30). According to (6.29) and (6.30), the shape parameter ζ and the scale parameter θ of Gamma distribution are derived as

$$\begin{aligned} \zeta &= N_s m \frac{4(\alpha(mN_c - 1) + 1)}{(\alpha(mN_c - 1) + 2)(2 - \alpha(m - 1))(mN_c - 1)}, \\ \theta &= P\beta \frac{(m\gamma)^{N_c m}}{(m\Gamma(m))^{N_c}} \frac{R^{\alpha(N_c m - 1)}}{m} \frac{2 - \alpha(m - 1)(mN_c - 1)}{2(\alpha(mN_c - 1) + 1)}. \end{aligned} \quad (6.31)$$

Figure 6.10 shows the CDF of the aggregate interference for $R_c = 10$ in Nakagami fading channel with $m = 1$ and $m = 2$. It shows that the Gamma distribution provides a close fit for the

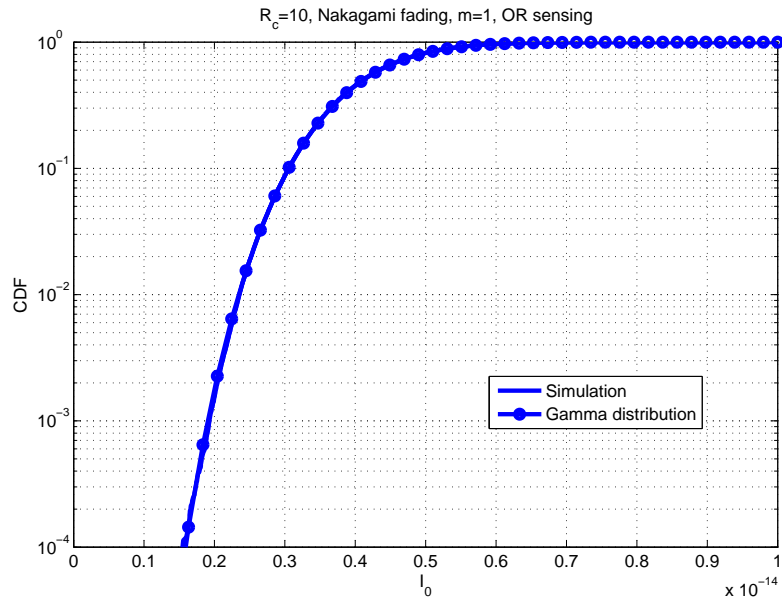
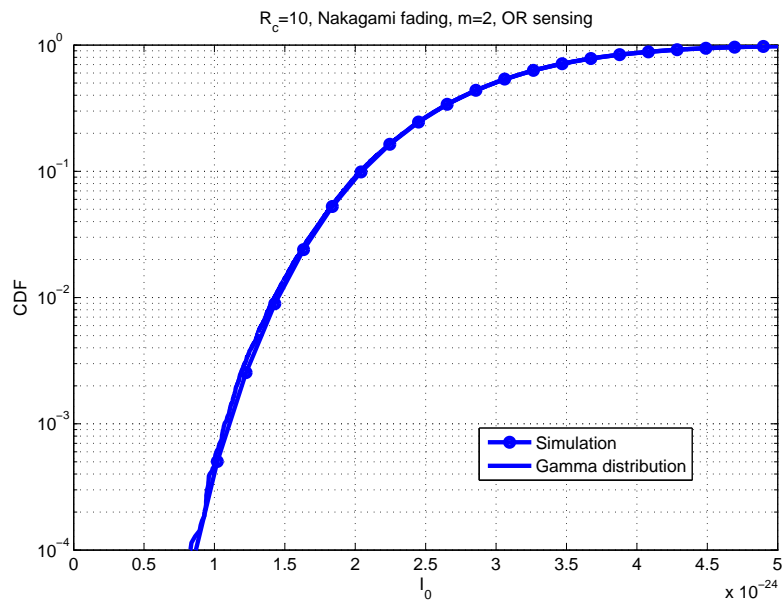
(a) $m = 1$ (b) $m = 2$

Fig. 6.10 CDF of aggregate interference in Nakagami fading channels with OR sensing ($R_c = 10$).

aggregate interference.

Capacity-outage probability

In this section, we derive the capacity-outage probability of PU in the Rayleigh fading channel. Since the aggregate interference is approximated as a Gamma random variable with the calculated parameters in (6.31), similar to (6.16), the capacity-outage probability becomes

$$\begin{aligned} P_{\text{out}} &= 1 - e^{-\frac{\sigma_0^2}{P_r}} \left(1 + \frac{\theta}{P_r}\right)^{-\zeta} \\ &= 1 - e^{-\frac{\sigma_0^2}{P_r}} \left(1 + \frac{P\beta\gamma^{N_c} R^{\alpha(N_c-1)} / (\alpha(N_c-1) + 1)}{P_r}\right)^{\frac{2N_s(\alpha(N_c-1)+1)}{(\alpha(N_c-1)+2)}}. \end{aligned} \quad (6.32)$$

For low outage probability, e.g., 3% or less, the expression in (6.32) can be approximated as

$$\begin{aligned} P_{\text{out}} &\approx 1 - \left(1 - \frac{\sigma_0^2}{P_r}\right) \left(1 - \frac{2N_s}{(\alpha(N_c-1) + 2)} \frac{P\beta\gamma^{N_c} R^{\alpha(N_c-1)}}{P_r}\right) \\ &\approx \frac{\sigma_0^2 + \frac{2N_s P\beta\gamma^{N_c} R^{\alpha(N_c-1)}}{(\alpha(N_c-1)+2)}}{P_r} = \left(\frac{P_0 R_0^{-\alpha}}{\sigma_0^2 + \frac{2N_s P\beta\gamma^{N_c} R^{\alpha(N_c-1)}}{(\alpha(N_c-1)+2)}}\right)^{-1} (2^{C_0} - 1). \end{aligned} \quad (6.33)$$

In the above expression, $\frac{2N_s P\beta\gamma^{N_c} R^{\alpha(N_c-1)}}{\alpha(N_c-1)+2}$ represents the average total transmitted power from SUs applying OR cooperative sensing, which can be interpreted as the effective interference, and $\frac{P_0 R_0^{-\alpha}}{\sigma_0^2 + \frac{2N_s P\beta\gamma^{N_c} R^{\alpha(N_c-1)}}{\alpha(N_c-1)+2}}$ represents the average signal-to-SU-interference-and-noise (SINR) at the PU receiver. In other words, the above expression indicates that the capacity-outage probability is approximately proportional to the inverse of the SINR, and exponentially increases with the required PU threshold rate C_0 similar to (6.17) and (6.26). The result is also applicable for the non-cooperative sensing schemes when $N_c = 1$. It is because SINR turns to $\frac{P_0 R_0^{-\alpha}}{\sigma_0^2 + N_s P\beta\gamma}$ in this case.

Figure 6.11 illustrates the plots of the capacity-outage probabilities versus the PU threshold rate C_0 (in b/s/Hz) for $R_c = 10$ for different values of SINR $\triangleq \frac{P_0 R_0^{-\alpha}}{\sigma_0^2 + N_s P\beta\gamma}$.

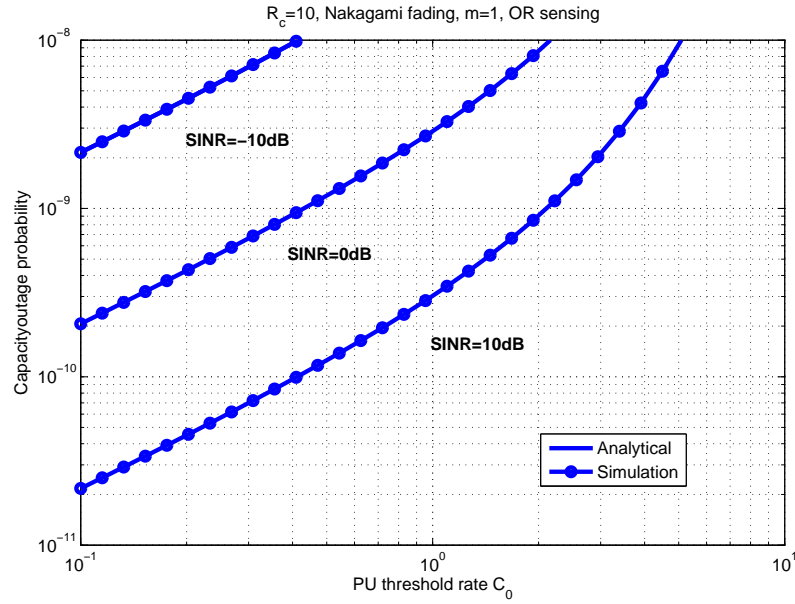


Fig. 6.11 PU capacity-outage probability versus required threshold rate for various SINRs with OR sensing in a Rayleigh fading channel.

6.5.2 Maximum Likelihood Detector

Interference Model

In ML cooperative detection, each SU sends the received beacon signal power to the other SUs in its cooperation range. Thus, at each SU, a final detection decision will be made based on the total sum of received beacon powers, including directly from the beacon transmitter and the nearby SUs. Then, according to (6.1), the new beacon miss-detection probability of each SU with ML sensing will be $P_{m,k} = \text{Prob}[\eta_{k-\text{Tot}} < \eta_0]$ where $\eta_{k-\text{Tot}}$ denotes total received beacon SNR at the SU k . $\eta_{k-\text{Tot}}$ can be presented as $\eta_{k-\text{Tot}} = \eta_k + \sum_{j=1, j \neq k}^{N_c} \hat{\eta}_j$ where η_k is the beacon SNR which is received at the SU k directly from the beacon transmitter and $\hat{\eta}_j$ is the received beacon SNR relayed from SU j . Due to double AWGN at relay and at destination SU, $\hat{\eta}_j = \frac{1}{2}\eta_j$ where η_j represents the directly received beacon SNR from beacon transmitter at SU j . Hence,

$$\eta_{k-\text{Tot}} = \eta_k + \frac{1}{2} \sum_{j=1, j \neq k}^{N_c} \eta_j = \frac{P_b \left[\frac{1}{2} \sum_{j=1, j \neq k}^{N_c} |h_j|^2 r_j^{-\alpha} + |h_k|^2 r_k^{-\alpha} \right]}{\sigma_B^2}.$$

Considering $R_c < R$, all r_j in the cooperation range of SU k are considered equal to r_k . Then,

$\eta_{k-Tot} = \frac{P_b r_k^{-\alpha}}{\sigma_B^2} \left[\frac{1}{2} \sum_{j=1, j \neq k}^{N_c} |\tilde{h}_j|^2 + |\tilde{h}_k|^2 \right]$. Hence, the miss-detection probability becomes

$$P_{m,k} = \text{Prob}[\eta_{k-Tot} < \eta_0] = \text{Prob} \left[\frac{1}{2} \sum_{j=1, j \neq k}^{N_c} |\tilde{h}_j|^2 + |\tilde{h}_k|^2 < \gamma r_k^\alpha \right] \leq \text{Prob} \left[\sum_{j=1}^{N_c} |\tilde{h}_j|^2 < 2\gamma r_k^\alpha \right]. \quad (6.34)$$

To find a closed-form expression, the miss-detection probability of ML cooperative sensing is approximated with a tight upper-bound for $N_c \gg 1$. Considering Nakagami fading with m and $P_r = 1$, $\sum_{j=1}^{N_c} |\tilde{h}_j|^2$ has a Gamma distribution with $\zeta = N_c m$ and $\theta = \frac{1}{m}$. According to the CDF of Gamma distribution, the miss-detection is derived as

$$P_{m,k} \simeq \frac{\Gamma(\zeta, 2\gamma r_k^\alpha / \theta)}{\Gamma(\zeta)} \simeq \frac{\Gamma(N_c m, 2m\gamma r_k^\alpha)}{\Gamma(N_c m)}. \quad (6.35)$$

For small γ , the lower incomplete Gamma function can be approximated as $\Gamma(N_c m, m\gamma r_k^\alpha) \approx \frac{(2m\gamma r_k^\alpha)^{N_c m}}{N_c m}$. Therefore, according to (6.5) and (6.35), the aggregate interference becomes

$$I_0 = \sum_{k=1}^{N_s} I_k, \quad I_k \simeq P\beta \frac{(2m\gamma)^{N_c m}}{N_c m \Gamma(N_c m)} |\tilde{h}_k|^2 r_k^{\alpha(N_c m - 1)}. \quad (6.36)$$

Similar to (6.11) and (6.12), the mean and variance of aggregate interference are computed as

$$\mathbb{E}[I_0] = N_s P\beta \frac{(2m\gamma)^{N_c m}}{N_c m \Gamma(N_c m)} \frac{2R^{\alpha(N_c m - 1)}}{\alpha(N_c m - 1) + 2}, \quad (6.37)$$

$$\text{var}[I_0] = N_s \left(P\beta \frac{(2m\gamma)^{N_c m}}{N_c m \Gamma(N_c m)} \right)^2 \frac{2R^{\alpha(N_c m - 1)}}{m} \left[\frac{2 - \alpha(m - 1)(mN_c - 1)}{(\alpha(mN_c - 1))(\alpha(mN_c - 1) + 2)} \right]. \quad (6.38)$$

Similar to non-cooperative sensing and OR sensing, the Gamma distribution also matches closely with the simulation results in ML sensing with the following scale and shape parameters:

$$\begin{aligned} \zeta &= N_s m \frac{4(\alpha(mN_c - 1) + 1)}{(\alpha(mN_c - 1) + 2)(2 - \alpha(m - 1)(mN_c - 1))}, \\ \theta &= \frac{P\beta(2m\gamma)^{N_c m} R^{\alpha(N_c m - 1)}}{N_c m \Gamma(N_c m)} \frac{2 - \alpha(m - 1)(mN_c - 1)}{m \cdot 2(\alpha(mN_c - 1) + 1)}. \end{aligned} \quad (6.39)$$

Figures 6.12 shows the CDF of the aggregate interference for $R_c = 10$ in Nakagami fading channels with $m = 1$ and $m = 2$. It shows that the Gamma distribution provides a close estimate of the interference CDF.

In Figures 6.13, the mean of interference is plotted as a function of cooperation range based on simulation results and analytical results according to (6.29) and (6.37). Figure 6.13 confirms the accuracy of the analytical derivations in (6.29) and (6.37) since they closely match the simulation results. It is also shown that the mean of interference is a decreasing function of R_c , since increasing the number of cooperating users (i.e., increasing R_c) is beneficial to reduce the miss-detection probability. When R_c is equal to R (e.g. $R_c = R = 50$), it represents the scenario where all SUs cooperate for spectrum sensing. It illustrates that the cooperation of all SUs will be beneficial to cause the least interference mean. In addition, the results show that ML sensing offers lower interference due to further detection improvement based on more signaling information as compared to the OR detector.

Capacity-outage probability

In this section, we study the capacity-outage probability of PU for ML cooperative sensing. According to (6.16) and (6.39), the outage probability is

$$P_{\text{out}} = 1 - e^{-\frac{\sigma_0^2}{P_r}} \left(1 + \frac{\theta}{P_r}\right)^{-\zeta} = 1 - e^{-\frac{\sigma_0^2}{P_r}} \left(1 + \frac{P\beta(2\gamma)^{N_c} R^{\alpha(N_c-1)}}{N_c\Gamma(N_c)(\alpha(N_c-1)+1)P_r}\right)^{-\frac{2N_s(\alpha(N_c-1)+1)}{(\alpha(N_c-1)+2)}}. \quad (6.40)$$

For low outage probability, e.g., 3% or less, (6.40) can be approximated as

$$P_{\text{out}} \approx 1 - \left(1 - \frac{\sigma_0^2}{P_r}\right) \left(1 - \frac{2N_s}{(\alpha(N_c-1)+2)} \frac{P\beta(2\gamma)^{N_c} R^{\alpha(N_c-1)}}{P_r}\right) \\ \approx \frac{\sigma_0^2 + \frac{2N_s P\beta(2\gamma)^{N_c} R^{\alpha(N_c-1)}}{N_c\Gamma(N_c)(\alpha(N_c-1)+2)}}{P_r} = \left(\frac{P_0 R_0^{-\alpha}}{\sigma_0^2 + \frac{2N_s P\beta(2\gamma)^{N_c} R^{\alpha(N_c-1)}}{N_c\Gamma(N_c)(\alpha(N_c-1)+2)}}\right)^{-1} (2^{C_0} - 1), N_c \gg 1. \quad (6.41)$$

Comparing to the capacity-outage probability for OR sensing, it is obvious that the capacity-outage probability is smaller with cooperative ML sensing because of lower effective interference $\frac{2N_s P\beta(2\gamma)^{N_c} R^{\alpha(N_c-1)}}{N_c\Gamma(N_c)(\alpha(N_c-1)+2)}$ for $N_c \gg 1$. Figures 6.14 illustrates the capacity-outage probability versus the PU threshold rate C_0 (in b/s/Hz) for $R_c = 10$ for different values of SINR $\triangleq \frac{P_0 R_0^{-\alpha}}{\sigma_0^2 + N_s P\beta\gamma}$.

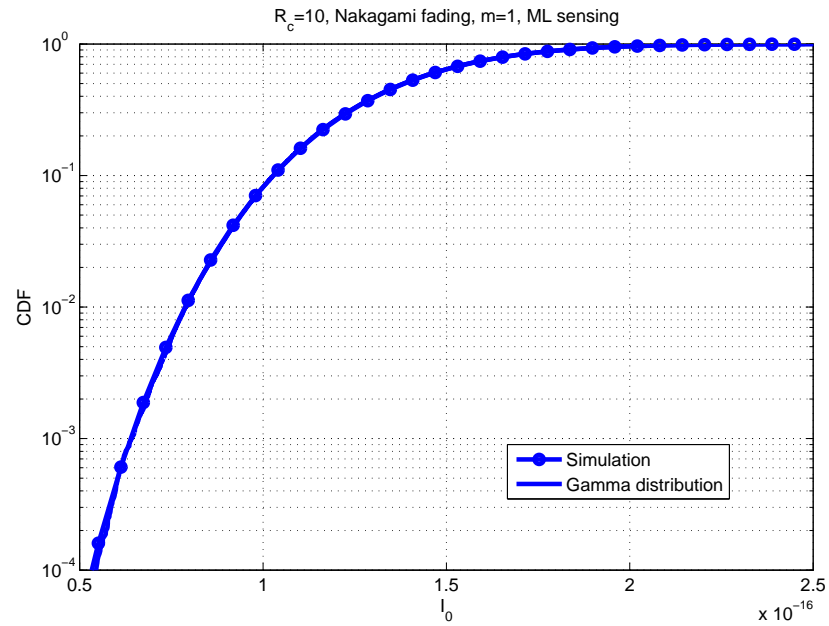
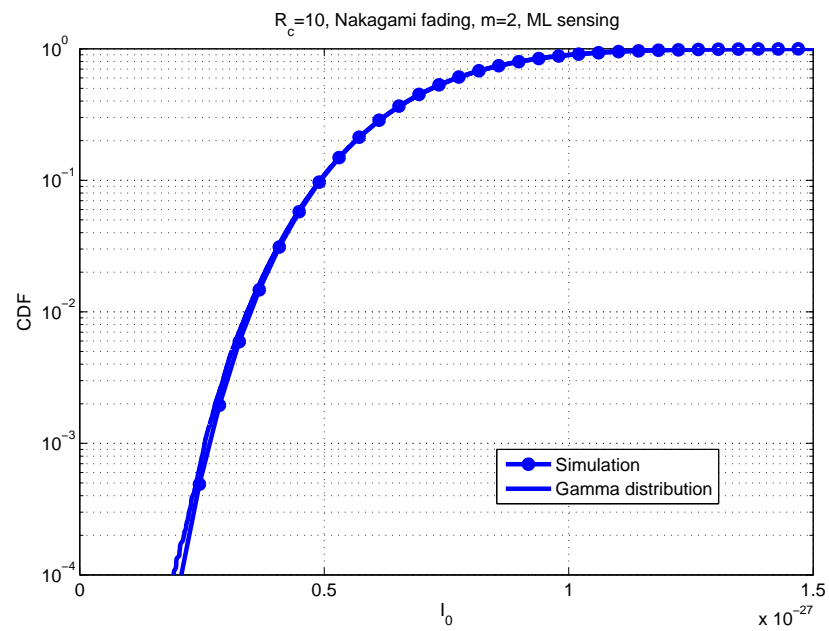
(a) $m = 1$ (b) $m = 2$

Fig. 6.12 CDF of aggregate interference in Nakagami fading channels with ML sensing ($R_c = 10$).

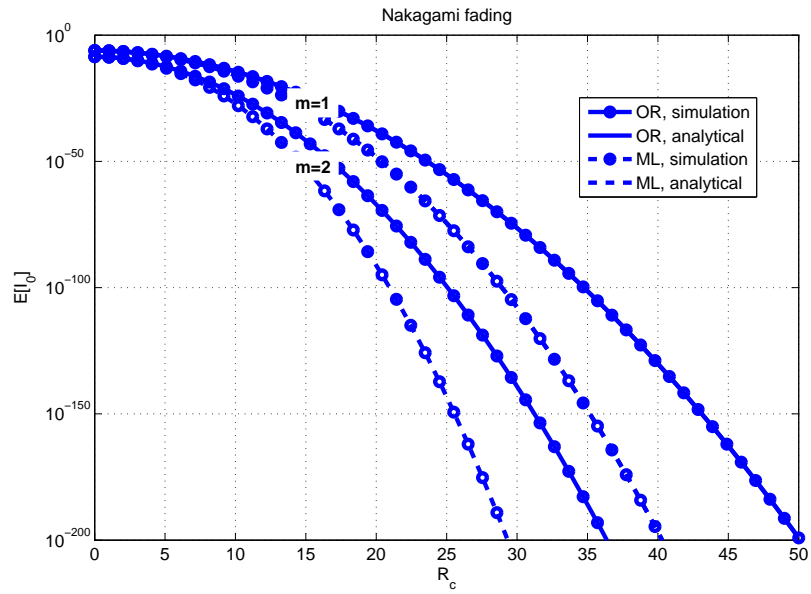


Fig. 6.13 Interference mean $E[I_0]$ versus cooperation range R_c in Nakagami fading channels.

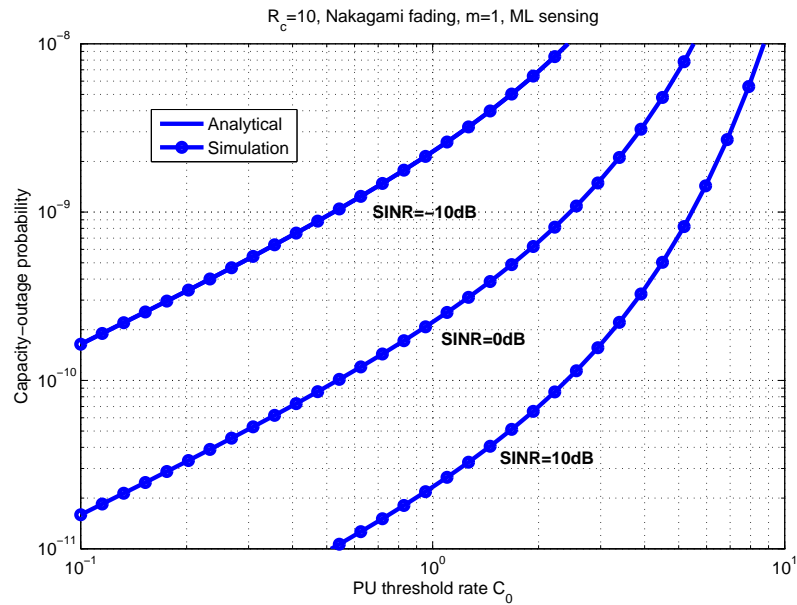


Fig. 6.14 PU capacity-outage probability versus required threshold rate for various SINRs with ML sensing in a Rayleigh fading channel.

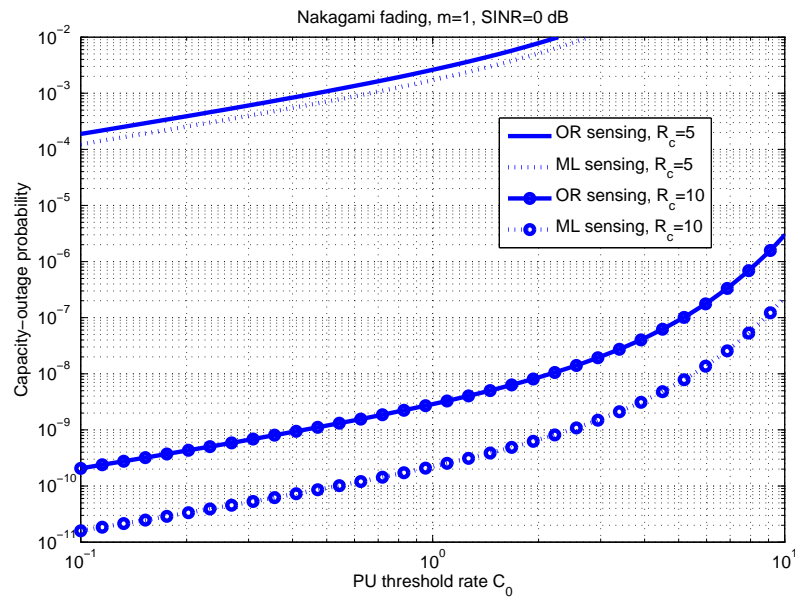


Fig. 6.15 PU capacity-outage probability versus required threshold rate for ML and OR sensing in a Rayleigh fading channel.

Figure 6.15 compares the capacity-outage probabilities for ML and OR sensing in a certain SINR for small and large N_c . It is shown that the larger number of cooperating SUs offers larger performance gains for ML sensing in comparison with OR sensing. Moreover, it is shown how cooperative sensing with larger number of cooperating SUs improves the capacity-outage probability by offering lower interference. For example, increasing the cooperation range from $R_c = 5$ to 10 approximately reduces capacity-outage probability of the PU by six orders of magnitude for OR cooperation and seven orders of magnitude for ML cooperation.

6.6 Concluding Remarks

In this chapter, we have studied the aggregate interference model and its probability distribution in a cognitive radio network—which consists of multiple SUs and a single PU—with beacon signaling. The capacity-outage probability of the PU has also been discussed to investigate the effects of aggregate interference on the PU performance.

First, we have derived closed-form expressions representing the aggregate interference imposed by SUs to the PU receiver and PU capacity-outage probability for both cases: beacon transmitter at PU transmitter and receiver. These results can be used to establish cognitive ra-

dio network parameters and/or to estimate its performance. We have provided simulation and numerical results to verify the derived closed-form results. It is shown that locating the beacon transmitter at the PU receiver could be beneficial to enhance the performance by comparing the mean value of aggregate interference and the capacity-outage probability of PU.

Then, we have derived closed-form expressions for interference and capacity-outage probability for OR and ML cooperative sensing. Simulation and analytical results indicate that cooperation can be used to maintain the capacity-outage probability of the PU at the desired level when it is not practical to enhance the sensitivity of the individual detectors. Comparing the capacity-outage probabilities and interference means, it is shown that ML cooperative sensing offers lower interference in comparison with OR cooperative sensing.

Chapter 7

Conclusions

7.1 Summary

Opportunistic spectrum access and the adopting technology, i.e., cognitive radio, are expected to lead the key evolutions in the next-generation wireless communications, aiming to improve the spectral efficiency and enhance the performance of wireless systems. Nevertheless, standardization and development of OSA have to deal with several technical considerations and regulatory requirements. Due to the time-varying and dynamic nature of spectrum resources in a cognitive radio network, OSA design necessitates adaptive decision making and learning techniques that enable efficient spectrum utilization. In addition, there is a crucial requirement to prevent the performance degradation for the licensed users. In this work, we have addressed the modeling, development and analysis of OSA schemes from both SU and PU viewpoints, aiming to optimize the opportunistic secondary access and ensure an acceptable level of protection for the legacy users.

In Chapter 3, we have proposed an adaptive hopping transmission strategy for SUs and developed an optimal access algorithm with the objective of reducing PU-SU conflicts due to the random PU returns. To realize distributed implementation in the absence of coordination and synchronization among SUs, a random access (i.e., adaptive CSMA) scheme has been proposed which efficiently shares the opportunities among SUs based on their activity factors. Using the feedbacks from the proposed CSMA scheme, a learning-based distributed algorithm has been developed which requires no additional control message exchange among SUs to reach the globally optimal solution.

In Chapter 4, we have considered game-theoretic approaches in the OSA design, aiming to

accelerate the convergence process of the distributed OSA schemes for SUs. Via the potential game framework, the existence, feasibility and optimality of a stable pure-strategy NE have been established by presenting sufficient conditions. Aiming to achieve an equilibrium point, learning algorithms have been developed and their convergence properties have been studied. Furthermore, with a different design objective, the effects of intrinsic collisions among SUs—using the proposed adaptive CSMA scheme for spectrum sharing—have been addressed in the activity factor allocation problem.

In Chapter 5, we have addressed the throughput analysis of the proposed adaptive CSMA scheme in the presence of inevitable collisions among SUs. While throughput represents the ratio of successfully transmitted opportunities without facing any collisions, it has been established that the adaptive CSMA plays an important role to reduce the contention among SUs. Through analysis and simulation, it has been confirmed that the proposed adaptive CSMA scheme offers performance gains, such as high throughput and long-term fairness, in comparison with the conventional CSMA scheme.

In Chapter 6, we have considered the PU performance analysis in the presence of interference from SUs. Recognizing that spectrum sensing suffers from errors due to noise and fading, the statistical characteristics of the aggregate interference have been investigated. Based on the developed model, we have introduced and derived the capacity-outage probability of PU as a metric to protect the primary performance in the OSA design. For spectrum sensing using beacons, it has been shown that placing the beacon transmitter at the PU receiver reduces the mean-value of the aggregate interference, and hence improves the capacity-outage probability of the PU.

7.2 Potential Future Studies

The main focus of this Ph.D. thesis has been on improving the spectral efficiency of a cognitive radio network via adaptive resource allocation. Although we have proposed some mechanisms to support a fair spectrum allocation among different SUs, there is no QoS guarantee for individual SUs in the proposed OSA schemes. Considering that several emerging applications for cognitive radios (such as multimedia streaming) are delay-sensitive, supporting the delay QoS in such applications is indispensable. However, there is only a limited number of studies (e.g., [119–121]) that address resource allocation design for delay-sensitive applications in hierarchical cognitive radio networks. Therefore, further research is needed to study a multi-user resource allocation method in which SUs need to optimally adjust their transmission strategies according to the avail-

able resources, while fulfilling the necessary latency requirements, specifically in a distributed manner. Due to the stochastic nature of the spectrum opportunities, satisfying the delay requirements for SUs is a major challenge in a cognitive radio network. Such uncertainty in the resource availability and the competition among multiple SUs significantly influences the queuing delay of SUs. In such a situation, a promising research direction is to apply a stochastic game framework [122] in which the uncertainties can be modeled in the decision making process of multiple SUs.

Moreover, in this work, the orthogonal time sharing has been considered in the OSA design to manage the spectrum sharing among different SUs, either with the assistance of a central coordinator or through the proposed adaptive CSMA scheme. Aiming to improve the spectrum utilization of SUs based on the spatial diversity, it would be interesting to study an overlapping sharing scheme in which SUs are allowed to simultaneously access an idle channel. Overlapping sharing takes advantage of the multi-user and spatial diversities and enables concurrent transmissions of SUs to enhance spectral efficiency. Nevertheless, as there is a mutual interference among the SUs, it is required to guarantee a minimum QoS for SUs. Interference management among SUs in the overlapping sharing makes the problem generally non-convex and thus, challenging to solve.

Furthermore, throughout this study, we have assumed a full knowledge of the availability of all channels for each SU. However, the assumption of continuous full-spectrum sensing is energy inefficient and hardware demanding. Addressing the case of partial sensing, [22] considers that each SU can choose a subset of channels to sense and decide to access based on its sensing observations. Subsequently, a joint design of sensing and access strategies is studied under the framework of finite-horizon POMDP. However, it is assumed that both PUs and SUs have the same transmission time-slot structure. Thus, another potential research direction is thus a cross-layer design of sensing and access strategies, while taking into account the effect of random PU returns.

Appendix A

Appendix to Chapter 3

A.1 Proof of Proposition 1

From (3.22),

$$\begin{aligned} |\mu_i^{n+1} - \mu_i^*|^2 &= |\mu_i^n - \mu_i^* + \gamma_n (-\nabla g(\mu_i^n) + w_n)|^2 \\ &= |\mu_i^n - \mu_i^*|^2 + 2\gamma_n (-\nabla g(\mu_i^n) + w_n) (\mu_i^n - \mu_i^*) + \gamma_n^2 |-\nabla g(\mu_i^n) + w_n|^2. \end{aligned} \quad (\text{A.1})$$

Since the dual objective function $g(\mu_i^n)$ is convex, $\nabla g(\mu_i^n) (\mu_i^n - \mu_i^*) \geq g(\mu_i^n) - g(\mu_i^*)$. Then,

$$\begin{aligned} |\mu_i^{n+1} - \mu_i^*|^2 &\leq |\mu_i^n - \mu_i^*|^2 - 2\gamma_n (g(\mu_i^n) - g(\mu_i^*)) + 2\gamma_n w_n (\mu_i^n - \mu_i^*) \\ &\quad + \gamma_n^2 |-\nabla g(\mu_i^n) + w_n|^2. \end{aligned} \quad (\text{A.2})$$

By adding and subtracting $\nabla g(\mu_i^*)$ in the last term of (A.2), since $|r + s|^2 \leq 2|r|^2 + 2|s|^2$ for any $r, s \in \mathbb{R}$,

$$\begin{aligned} |\mu_i^{n+1} - \mu_i^*|^2 &\leq |\mu_i^n - \mu_i^*|^2 - 2\gamma_n (g(\mu_i^n) - g(\mu_i^*)) + 2\gamma_n w_n (\mu_i^n - \mu_i^*) \\ &\quad + 2\gamma_n^2 |\nabla g(\mu_i^n) - \nabla g(\mu_i^*)|^2 + 2\gamma_n^2 |\nabla g(\mu_i^*) - w_n|^2. \end{aligned} \quad (\text{A.3})$$

According to Remark 2 in Chapter 3, due to Lipschitz continuity of ∇g , we have

$$\begin{aligned} |\mu_i^{n+1} - \mu_i^*|^2 &\leq (1 + 2D_0^2\gamma_n^2) |\mu_i^n - \mu_i^*|^2 - 2\gamma_n (g(\mu_i^n) - g(\mu_i^*)) + 2\gamma_n w_n (\mu_i^n - \mu_i^*) \\ &\quad + 2\gamma_n^2 |\nabla g(\mu_i^*) - w_n|^2. \end{aligned} \quad (\text{A.4})$$

By taking the conditional expectation given $\mathcal{F}_n = \{\mu_i^0, \dots, \mu_i^n\}$, we obtain

$$\begin{aligned} \mathbb{E} \left[|\mu_i^{n+1} - \mu_i^*|^2 \mid \mathcal{F}_n \right] &\leq (1 + 2D_0^2\gamma_n^2) |\mu_i^n - \mu_i^*|^2 - 2\gamma_n [g(\mu_i^n) - g(\mu_i^*) - \mathbb{E}[w_n](\mu_i^n - \mu_i^*)] \\ &\quad + 4\gamma_n^2 [|\nabla g(\mu_i^*)|^2 + \mathbb{E}[|w_n|^2]]. \end{aligned} \quad (\text{A.5})$$

Based on Remark 1 in Chapter 3 and the fact that $\nabla g(\mu_i)$ is bounded, it is clear that $[|\nabla g(\mu_i^*)|^2 + \mathbb{E}[|w_n|^2]]$ is bounded, and hence, $\sum_{n=0}^{\infty} \gamma_n^2 [|\nabla g(\mu_i^*)|^2 + \mathbb{E}[|w_n|^2]] < \infty$ considering Assumption 1. Using Robbins-Siegmund Lemma in [82, page 50], since (A.5) holds for all n , $\sum_{n=0}^{\infty} \gamma_n^2 < \infty$ and $\sum_{n=0}^{\infty} \gamma_n^2 [|\nabla g(\mu_i^*)|^2 + \mathbb{E}[|w_n|^2]] < \infty$, it can be concluded that the sequence $\{|\mu_i^n - \mu_i^*|^2\}$ is convergent and $\sum_{n=0}^{\infty} \gamma_n [g(\mu_i^n) - g(\mu_i^*) - \mathbb{E}[w_n](\mu_i^n - \mu_i^*)] < \infty$ with probability of 1. Since $\sum_{n=0}^{\infty} \gamma_n = \infty$ and $\lim_{n \rightarrow \infty} \mathbb{E}[w_n] = 0$ according to Remark 1 in Chapter 3, the later relation implies $\lim_{n \rightarrow \infty} g(\mu_i^n) = g(\mu_i^*)$ (i.e., $\lim_{n \rightarrow \infty} \nabla g(\mu_i^n) = 0$) with probability of 1. Therefore, $\{\mu_i^n\}$ converges to the μ_i^* with probability of 1. ■

A.2 Proof of Proposition 2

By definition,

$$\mu_i^{n+1} - \mu_i^* = [\mu_i^n - \mu_i^* - \gamma_n \nabla g(\mu_i^n)] + \gamma_n w_n. \quad (\text{A.6})$$

Squaring both sides of (A.6), taking the expected value and using $\gamma_n = an^{-c}$, we have

$$\begin{aligned} \mathbb{E} \left[|\mu_i^{n+1} - \mu_i^*|^2 \right] &= \mathbb{E} [|\mu_i^n - \mu_i^* - an^{-c} \nabla g(\mu_i^n)|^2] + a^2 n^{-2c} \mathbb{E}[|w_n|^2] \\ &\quad + 2an^{-c} \mathbb{E} [w_n (\mu_i^n - \mu_i^* - an^{-c} \nabla g(\mu_i^n))]. \end{aligned} \quad (\text{A.7})$$

Using the inequality $xy \leq \frac{1}{2}(x^2 + y^2)$, the third term of (A.7) becomes

$$\begin{aligned} \mathbb{E} [w_n (\mu_i^n - \mu_i^* - an^{-c} \nabla g(\mu_i^n))] &= \mathbb{E}[w_n] \mathbb{E}[\mu_i^n - \mu_i^* - an^{-c} \nabla g(\mu_i^n)] \\ &\leq \frac{1}{2} (\mathbb{E}^2[w_n] + \mathbb{E}^2[\mu_i^n - \mu_i^* - an^{-c} \nabla g(\mu_i^n)]) \\ &\leq \frac{1}{2} (D_3 K_e^2 n^{-2b} + \frac{1}{D_3} \mathbb{E} [|\mu_i^n - \mu_i^* - an^{-c} \nabla g(\mu_i^n)|^2]) \end{aligned} \quad (\text{A.8})$$

where D_3 is a positive real constant. According to Remark 1 in Chapter 3,

$$\mathbb{E}[|w_n|^2] = \text{var}[w_n] + \mathbb{E}^2[w_n] \leq K_\nu n^{-b} + K_e^2 n^{-2b}. \quad (\text{A.9})$$

From (A.8) and (A.9), (A.7) can be written as

$$\begin{aligned} \mathbb{E} \left[|\mu_i^{n+1} - \mu_i^*|^2 \right] &\leq \left(1 + \frac{a}{D_3} n^{-c}\right) \mathbb{E} \left[|\mu_i^n - \mu_i^* - an^{-c} \nabla g(\mu_i^n)|^2 \right] + a^2 K_\nu n^{-2c-b} \\ &\quad + a^2 K_e^2 n^{-2c-2b} + a D_3 K_e^2 n^{-c-2b}. \end{aligned} \quad (\text{A.10})$$

Considering Remark 4 in Chapter 3,

$$\mathbb{E} \left[|\mu_i^n - \mu_i^* - an^{-c} \nabla g(\mu_i^n)|^2 \right] \leq (1 - 2D_1 a n^{-c} + a^2 D_2^2 n^{-2c}) \mathbb{E} \left[|\mu_i^n - \mu_i^*|^2 \right]. \quad (\text{A.11})$$

Then, we have

$$\begin{aligned} \left(1 + \frac{a}{D_3} n^{-c}\right) \mathbb{E} \left[|\mu_i^n - \mu_i^* - an^{-c} \nabla g(\mu_i^n)|^2 \right] &\leq \\ \left(1 - 2D_1 a n^{-c} + \frac{a}{D_3} n^{-c} + \mathcal{O}(n^{-c})\right) \mathbb{E} \left[|\mu_i^n - \mu_i^*|^2 \right]. \end{aligned} \quad (\text{A.12})$$

For n sufficiently large (e.g., $n > N_0$) and D_3 properly selected in (A.8), there exists $q > D_1 a$ such that

$$\left(1 + \frac{a}{D_3} n^{-c}\right) \mathbb{E} \left[|\mu_i^n - \mu_i^* - an^{-c} \nabla g(\mu_i^n)|^2 \right] \leq (1 - qn^{-c}) \mathbb{E} \left[|\mu_i^n - \mu_i^*|^2 \right]. \quad (\text{A.13})$$

Considering (A.13), (A.10) becomes

$$\begin{aligned} \mathbb{E} \left[|\mu_i^{n+1} - \mu_i^*|^2 \right] &\leq (1 - qn^{-c}) \mathbb{E} \left[|\mu_i^n - \mu_i^*|^2 \right] + a^2 K_\nu n^{-2c-b} \\ &\quad + a^2 K_e^2 n^{-2c-2b} + a D_3 K_e^2 n^{-c-2b}. \end{aligned} \quad (\text{A.14})$$

Notice that there is a positive real constant (i.e., D_4) such that for $n > N_0$, $a^2 K_\nu n^{-2c-b} + a^2 K_e^2 n^{-2c-2b} \leq D_4 n^{-2c-b}$. For $n > N_0$, iteration of (A.14) results in

$$\begin{aligned} \mathbb{E} \left[\left| \mu_i^{n+1} - \mu_i^* \right|^2 \right] &\leq A_{N_0, n} \mathbb{E} \left[\left| \mu_i^{N_0+1} - \mu_i^* \right|^2 \right] + a D_3 K_e^2 \sum_{m=N_0+1}^n A_{mn} m^{-c-2b} \\ &\quad + D_4 \sum_{m=N_0+1}^n A_{mn} m^{-2c-b} \end{aligned} \quad (\text{A.15})$$

where $A_{mn} = \begin{cases} \prod_{h=m+1}^n (1 - qh^{-c}), & 0 \leq m < n \\ 1, & m = n \end{cases}$. The rest of the proof is divided into two steps. First, we assume that $0.5 < c < 1$. Then, we consider the case in which $c = 1$.

A.2.1 Step 1 ($0.5 < c < 1$)

It is well-known that

$$\begin{aligned} |A_{mn}| &\leq e^{-q \sum_{h=m+1}^n h^{-c}} \\ &\leq e^{qm^{-c} - q \int_m^n x^{-c} dx} = e^{qm^{-c} - \frac{q(n^{1-c} - m^{1-c})}{1-c}}. \end{aligned} \quad (\text{A.16})$$

Therefore, the first term of (A.15) is of $\mathcal{O}(e^{-n^{1-c}})$. The second term of (A.15) can be written as

$$\sum_{m=N_0+1}^n A_{mn} m^{-c-2b} = n^{-2b} \sum_{m=N_0+1}^n A_{mn} m^{-c} + \sum_{m=N_0+1}^{n-1} (m^{-2b} - (m+1)^{-2b}) \sum_{r=N_0+1}^m A_{rn} r^{-c}. \quad (\text{A.17})$$

Since $A_{mn} m^{-c} = q^{-1} (A_{mn} - A_{m-1, n})$, (A.17) becomes

$$\sum_{m=N_0+1}^n A_{mn} m^{-c-2b} = q^{-1} n^{-2b} (1 - A_{N_0 n}) + q^{-1} \sum_{m=N_0+1}^{n-1} (m^{-2b} - (m+1)^{-2b}) (A_{mn} - A_{N_0 n}). \quad (\text{A.18})$$

Taking into consideration that $A_{N_0n} = \mathcal{O}(e^{-n^{1-c}})$ and $b > 1 - c$, then $e^{-n^{1-c}} = \mathcal{O}(n^{-2b-1})$. Also,

$$\begin{aligned} \sum_{m=N_0+1}^{n-1} (m^{-2b} - (m+1)^{-2b})A_{mn} &= \sum_{m=N_0+1}^{n-1} (2bm^{-2b-1} + \mathcal{O}(m^{-2b-2}))A_{mn} \\ &\leq \sum_{m=N_0+1}^n D_5 m^{-c-2b} A_{mn} + \mathcal{O}(m^{-2b-1}). \end{aligned} \quad (\text{A.19})$$

where D_5 is a positive real constant. Subsequently, (A.18) becomes

$$\sum_{m=N_0+1}^n A_{mn} m^{-c-2b} \leq q^{-1} n^{-2b} + D_5 q^{-1} \sum_{m=N_0+1}^n A_{mn} m^{-c-2b} + \mathcal{O}(n^{-2b-1}). \quad (\text{A.20})$$

Consequently, we have

$$\sum_{m=N_0+1}^n A_{mn} m^{-c-2b} \leq \frac{q^{-1}}{1 - D_5 q^{-1}} n^{-2b} + \mathcal{O}(n^{-2b-1}). \quad (\text{A.21})$$

Similarly,

$$\sum_{m=N_0+1}^n A_{mn} m^{-2c-b} \leq \frac{q^{-1}}{1 - D_5 q^{-1}} n^{-b-c} + \mathcal{O}(n^{-b-c-1}). \quad (\text{A.22})$$

As a result,

$$\mathbb{E} \left[\left| \mu_i^{n+1} - \mu_i^* \right|^2 \right] \leq \frac{aD_3 K_e^2 q^{-1}}{1 - D_5 q^{-1}} n^{-2b} + \frac{D_4 q^{-1}}{1 - D_5 q^{-1}} n^{-b-c} + \mathcal{O}(n^{-2b-1} + n^{-b-c-1}). \quad (\text{A.23})$$

which concludes the proof for this case. ■

A.2.2 Step 2 (c = 1)

In this case,

$$\begin{aligned} |A_{mn}| &\leq e^{-q \sum_{h=m+1}^n h^{-1}} h^{-1} \leq e^{qm^{-1} - q \int_m^n x^{-1} dx} \\ &= e^{qm^{-1}} m^q n^{-q}. \end{aligned} \quad (\text{A.24})$$

Therefore, $A_{N_0n} = \mathcal{O}(n^{-q})$, and hence, the first term of (A.15) is of $\mathcal{O}(n^{-q})$. The second term of (A.15) becomes

$$\sum_{m=N_0+1}^n A_{mn} m^{-1-2b} \leq n^{-q} e^{qm_0^{-1}} \int_{N_0}^n x^{-1-2b+q} dx \leq D_6 n^{-2b}. \quad (\text{A.25})$$

where D_6 is a positive real constant. Similarly,

$$\sum_{m=N_0+1}^n A_{mn} m^{-2-b} \leq D_7 n^{-b-1}. \quad (\text{A.26})$$

where D_7 is a positive real constant. As a consequence, considering that D_8 is a positive real constant,

$$\begin{aligned} \mathbb{E} \left[\left| \mu_i^{n+1} - \mu_i^* \right|^2 \right] &\leq D_8 n^{-q} + D_6 n^{-2b} + D_7 n^{-b-1} \\ &\leq D_8 n^{-D_1 a} + D_6 n^{-2b} + D_7 n^{-b-1}. \end{aligned} \quad (\text{A.27})$$

which concludes the proof. ■

Appendix B

Appendix to Chapter 4

B.1 Proof of Theorem 3

Suppose that $\beta = \{\beta_k\}_{k=1}^{N_s}$, where $\beta_k \in \mathcal{B}_k$, is a pure-strategy NE of game \mathcal{G} , but it is not feasible, i.e., it violates at least one of the constraints in (3.8b). Further, suppose that m is the index of channel which has the most severe violation, i.e., $m = \arg \max_{i \in \mathcal{N}_a} \left(\sum_{j=1}^{N_s} \beta_j^i - 1 \right)$. Thus, $\sum_{j=1}^{N_s} \beta_j^m > 1$. Considering $k \in \mathcal{N}_s$ such that $\beta_k^m > 0$, from (4.1), we have

$$u_k(\beta_k, \beta_{-k}) = \sum_{i=1}^{N_a} \beta_k^i C_k^i (1 - \beta_k^i \alpha_i) - \mu_m \left(\sum_{j=1}^{N_s} \beta_j^m - 1 \right) - \sum_{i=1, i \neq m}^{N_a} \mu_i \Theta \left(\sum_{j=1}^{N_s} \beta_j^i - 1 \right). \quad (\text{B.1})$$

Assuming that $\sum_{j=1}^{N_s} \beta_j^m = 1 + \epsilon$ where ϵ is a positive discrete value (i.e., $\epsilon \geq \frac{1}{S}$), there exists a channel n such that $\sum_{j=1}^{N_s} \beta_j^n \leq 1 - \xi$ where $\frac{1}{S} \leq \xi < \min(1, \epsilon)$ since $N_a \geq N_s$. Then, an alternative admissible strategy $\tilde{\beta}_k = \left[\tilde{\beta}_k^i \right]_{i \in \mathcal{N}_a} \in \mathcal{B}_k$ can be constructed such that $\tilde{\beta}_k^i =$

$$\begin{cases} \beta_k^i, & i \neq m, n \\ \beta_k^i - \delta, & i = m \\ \beta_k^i + \delta, & i = n \end{cases} \quad \text{where } \delta \text{ is a positive discrete value (i.e., } \delta \in \{\frac{1}{S}, \frac{2}{S}, \dots, 1\}) \text{ satisfying}$$

$\delta \leq \xi, 0 \leq \beta_k^m - \delta \leq 1$ and $0 \leq \beta_k^n + \delta \leq 1$. Note that $\sum_{j=1}^{N_s} \tilde{\beta}_j^n - 1 = \delta - \xi \leq 0$ since $\delta \leq \xi$,

and hence, $\Theta \left(\sum_{j=1}^{N_s} \tilde{\beta}_j^n - 1 \right) = \Theta \left(\sum_{j=1}^{N_s} \beta_j^n - 1 \right) = 0$. Then, $u_k \left(\tilde{\boldsymbol{\beta}}_k, \boldsymbol{\beta}_{-k} \right)$ can be obtained as

$$\begin{aligned} u_k(\tilde{\boldsymbol{\beta}}_k, \boldsymbol{\beta}_{-k}) &= \sum_{i=1}^{N_a} \tilde{\beta}_k^i C_k^i (1 - \tilde{\beta}_k^i \alpha_i) - \sum_{i=1}^{N_a} \mu_i \Theta \left(\sum_{j=1}^{N_s} \tilde{\beta}_j^i - 1 \right) \\ &= \sum_{i=1}^{N_a} \tilde{\beta}_k^i C_k^i (1 - \tilde{\beta}_k^i \alpha_i) - \mu_m \Theta \left(\sum_{j=1}^{N_s} \beta_j^m - 1 - \delta \right) - \sum_{i=1, i \neq m}^{N_a} \mu_i \Theta \left(\sum_{j=1}^{N_s} \beta_j^i - 1 \right). \end{aligned} \quad (\text{B.2})$$

Thus, from (B.1) and (B.2),

$$\begin{aligned} u_k(\boldsymbol{\beta}_k, \boldsymbol{\beta}_{-k}) - u_k(\tilde{\boldsymbol{\beta}}_k, \boldsymbol{\beta}_{-k}) &= \sum_{i=1}^{N_a} \beta_k^i C_k^i (1 - \beta_k^i \alpha_i) - \sum_{i=1}^{N_a} \tilde{\beta}_k^i C_k^i (1 - \tilde{\beta}_k^i \alpha_i) \\ &\quad - \mu_m \left(\sum_{j=1}^{N_s} \beta_j^m - 1 \right) + \mu_m \Theta \left(\sum_{j=1}^{N_s} \beta_j^m - 1 - \delta \right). \end{aligned} \quad (\text{B.3})$$

Since $\delta \leq \epsilon$, we have

$$\mu_m \Theta \left(\sum_{j=1}^{N_s} \beta_j^m - 1 - \delta \right) - \mu_m \left(\sum_{j=1}^{N_s} \beta_j^m - 1 \right) = \mu_m \Theta(\epsilon - \delta) - \mu_m \epsilon \leq -\mu_m \delta. \quad (\text{B.4})$$

Subsequently, from (B.3) and (B.4),

$$u_k(\boldsymbol{\beta}_k, \boldsymbol{\beta}_{-k}) - u_k(\tilde{\boldsymbol{\beta}}_k, \boldsymbol{\beta}_{-k}) \leq \sum_{i=1}^{N_a} \beta_k^i C_k^i (1 - \beta_k^i \alpha_i) - \sum_{i=1}^{N_a} \tilde{\beta}_k^i C_k^i (1 - \tilde{\beta}_k^i \alpha_i) - \mu_m \delta. \quad (\text{B.5})$$

Under the assumption of $\mu_i > \mu_{th}, \forall i \in \mathcal{N}_a$, from (4.8), we have

$$\mu_m > S \sum_{i=1}^{N_a} \beta_k^i C_k^i (1 - \beta_k^i \alpha_i). \quad (\text{B.6})$$

Since $\delta \geq \frac{1}{S}$, from (B.6), it can be concluded that

$$\sum_{i=1}^{N_a} \beta_k^i C_k^i (1 - \beta_k^i \alpha_i) - \mu_m \delta < 0. \quad (\text{B.7})$$

Thus, based on (B.5) and (B.7),

$$u_k(\beta_k, \beta_{-k}) - u_k(\tilde{\beta}_k, \beta_{-k}) \leq 0. \quad (\text{B.8})$$

Note that this contradicts the assumption that $\beta = \{\beta_k\}_{k=1}^{N_s}$ is a pure-strategy NE of game \mathcal{G} according to the definition of NE in (4.6). Thus, β is not a pure-strategy NE of \mathcal{G} . Hence, it can be concluded that all pure-strategy NE must be feasible if $\mu_i > \mu_{th}, \forall i \in \mathcal{N}_a$. ■

B.2 Proof of Theorem 4

Assume that $\beta = \{\beta_k\}_{k=1}^{N_s}$ is the optimal solution of (3.8). Assuming $\mu_i > \mu_{th}, \forall i \in \mathcal{N}_a$, β is the maximizer of the potential function Φ . Based on Theorem 2 in [89], the maximizer of the potential function is the NE of the potential game. Hence, β is the NE of the game \mathcal{G} .

Subsequently, we need to establish that β is the Pareto-optimal NE. Assume that β is not Pareto-optimal. Then, there exists an arbitrary strategy profile $\beta' = \{\beta'_k\}_{k=1}^{N_s}$ such that

$$u_k(\beta'_k, \beta'_{-k}) \geq u_k(\beta_k, \beta_{-k}), \forall k \in \mathcal{N}_s, k \neq j \quad (\text{B.9})$$

and, for some j ,

$$u_j(\beta'_j, \beta'_{-j}) > u_j(\beta_j, \beta_{-j}). \quad (\text{B.10})$$

As a result,

$$\sum_{k=1}^{N_s} u_k(\beta') > \sum_{k=1}^{N_s} u_k(\beta). \quad (\text{B.11})$$

Since β is a NE of the game \mathcal{G} , it is feasible based on Theorem 3 (i.e., $\sum_{i=1}^{N_a} \mu_i \Theta \left(\sum_{j=1}^{N_s} \beta_j^i - 1 \right) = 0$). Then, we have

$$\Phi(\beta) = \sum_{k=1}^{N_s} u_k(\beta). \quad (\text{B.12})$$

Furthermore, considering that $\mu_i, \forall i \in \mathcal{N}_a$ are positive scalars, from (4.1) and (4.4), for an

arbitrary β' , we have

$$\Phi(\beta') \geq \sum_{k=1}^{N_s} u_k(\beta'). \quad (\text{B.13})$$

Consequently, based on (A.11), (A.12) and (A.13),

$$\Phi(\beta') > \Phi(\beta). \quad (\text{B.14})$$

This contradicts the fact that β is the maximizer of the potential function Φ . Thus, the optimal solution of (3.8) is the Pareto-optimal pure-strategy NE of the game \mathcal{G} . ■

References

- [1] FCC Spectrum Policy Task Force, “Report of the spectrum efficiency working group,” Federal Communications Commission, Tech. Rep. ET Docket No. 02-135, Nov. 2002.
- [2] M. H. Islam, C. L. Koh, S. W. Oh, X. Qing, Y. Y. Lai, C. Wang, Y.-C. Liang, B. E. Toh, F. Chin, G. L. Tan, and W. Toh, “Spectrum survey in Singapore: Occupancy measurements and analyses,” in *Proc. IEEE Intl. Conf. on Cognitive Radio Oriented Wireless Networks and Commun. (CROWNCOM)*, Singapore, May 2008.
- [3] K. Harrison, S. M. Mishra, and A. Sahai, “How much white-space capacity is there?” in *Proc. IEEE Intl. Symp. New Frontiers in Dynamic Spectrum Access Networks (DySPAN)*, Singapore, Apr. 2010.
- [4] J. V. D. Beek, J. Riihijarvi, A. Achtzehn, and P. Mahonen, “TV white space in Europe,” *IEEE Trans. Mobile Comput.*, vol. 11, no. 2, pp. 178–188, Feb. 2012.
- [5] J. Mitola, “Cognitive radio for flexible mobile multimedia communications,” in *Proc. IEEE Intl. Workshop on Mobile Multimedia Commun. (MOMUC)*, San Diego, CA, USA, Nov. 1999.
- [6] I. F. Akyildiz, W. Y. Lee, M. C. Vuran, and S. Mohanty, “NeXt generation/dynamic spectrum access/cognitive radio wireless networks: A survey,” *Computer Networks (Elsevier)*, vol. 50, no. 13, pp. 2127–2159, Sep. 2006.
- [7] Q. Zhao and B. M. Sadler, “A survey of dynamic spectrum access: Processing, networking, and regulatory policy,” *IEEE Signal Process. Mag.*, vol. 24, no. 3, pp. 79–89, May 2007.
- [8] I. F. Akyildiz, W. Y. Lee, M. C. Vuran, and S. Mohanty, “A survey on spectrum management in cognitive radio networks,” *IEEE Commun. Mag.*, vol. 46, no. 4, pp. 40–48, Apr. 2008.
- [9] B. Jabbari, R. Pickholtz, and M. Norton, “Dynamic spectrum access and management,” *IEEE Wireless Commun. Mag.*, vol. 17, no. 4, pp. 6–15, Aug. 2010.
- [10] J. Mitola, *Software Radios: Wireless Architecture for the 21st Century*. New York: Wiley, 2000.

- [11] S. Haykin, "Cognitive radio: Brain-empowered wireless communications," *IEEE J. Sel. Areas Commun.*, vol. 23, no. 2, pp. 201–220, Feb. 2005.
- [12] A. Goldsmith, S. A. Jafar, I. Maric, and S. Srinivasa, "Breaking spectrum gridlock with cognitive radios: An information theoretic perspective," *Proc. IEEE*, vol. 97, no. 5, pp. 894–914, May 2009.
- [13] FCC, "Notice of proposed rulemaking," ET Docket No. 04-113, May 2004.
- [14] —, "Second report and order and memorandum opinion and order," ET Docket No. 08-260, Nov. 2008.
- [15] —, "Unlicensed operations in the TV broadcast bands," Second Memorandum Opinion and Order, ET Docket No. 10-174, Sep. 2010.
- [16] IEEE Std. 802.22, "Information Technology–Telecommunications and Information Exchange between Systems–Wireless Regional Area Networks (WRAN)–Specific Requirements–Part 22: Cognitive Wireless RAN Medium Access Control (MAC) and Physical Layer (PHY) Specifications: Policies and Procedures for Operation in the TV Bands," pp. 1–680, <http://www.ieee802.org/22/>, Jul. 2011.
- [17] C. Stevenson, G. Chouinard, L. Zhongding, H. Wendong, S. J. Shellhammer, and W. Caldwell., "IEEE 802.22: The first cognitive radio wireless regional area network standard," *IEEE Commun. Mag.*, vol. 47, no. 1, pp. 130–138, Jan. 2009.
- [18] R. Kennedy and P. Ecclesine, "IEEE P802.11af tutorial," IEEE 802.11-10/0742r0, <https://mentor.ieee.org/802.11/dcn/10/11-10-0742-00-0000-p802-11af-tutorial.ppt>, Jul. 2010.
- [19] K. G. Shin, H. Kim, A. W. Min, and A. Kumar, "Cognitive radios for dynamic spectrum access: From concept to reality," *IEEE Trans. Wireless Commun.*, vol. 17, no. 6, pp. 64–74, Dec. 2010.
- [20] L. Berlemann and S. Mangold, *Cognitive Radio and Dynamic Spectrum Access*. Wiley, 2009.
- [21] C. Ghosh, S. Roy, and D. Cavalcanti, "Coexistence challenges for heterogeneous cognitive wireless networks in TV white spaces," *IEEE Wireless Commun. Mag.*, vol. 18, no. 4, pp. 22–31, Aug. 2011.
- [22] Q. Zhao, L. Tong, A. Swami, and Y. Chen, "Decentralized cognitive MAC for opportunistic spectrum access in ad hoc networks: A POMDP framework," *IEEE J. Sel. Areas Commun.*, vol. 25, no. 3, pp. 589–600, Apr. 2007.

- [23] Y. Chen, Q. Zhao, and A. Swami, "Joint design and separation principle for opportunistic spectrum access in the presence of sensing errors," *IEEE Trans. Inf. Theory*, vol. 54, no. 5, pp. 2053–2071, May 2008.
- [24] Q. Zhao, B. Krishnamachari, and K. Liu, "On myopic sensing for multichannel opportunistic access: Structure, optimality, and performance," *IEEE Trans. Wireless Commun.*, vol. 7, no. 12, pp. 5431–5440, Dec. 2008.
- [25] L. Lai, H. E. Gamal, H. Jiang, and H. Poor, "Cognitive medium access: Exploration, exploitation and competition," *IEEE Trans. Mobile Comput.*, vol. 10, no. 2, pp. 239–253, Feb. 2011.
- [26] K. Liu, Q. Zhao, and B. Krishnamachari, "Dynamic multichannel access with imperfect channel state detection," *IEEE Trans. Signal Process.*, vol. 58, no. 5, pp. 2795–2808, May 2010.
- [27] K. W. Sung, S. L. Kim, and J. Zander, "Temporal spectrum sharing based on primary user activity prediction," *IEEE Trans. Wireless Commun.*, vol. 9, no. 12, pp. 3848–3855, Dec. 2010.
- [28] K. W. Choi and E. Hossain, "Opportunistic access to spectrum holes between packet bursts: A learning-based approach," *IEEE Trans. Wireless Commun.*, vol. 10, no. 8, pp. 2497–2509, Aug. 2011.
- [29] Q. Zhao, S. Geirhofer, L. Tong, and B. M. Sadler, "Opportunistic spectrum access via periodic channel sensing," *IEEE Trans. Signal Process.*, vol. 56, no. 2, pp. 785–796, Feb. 2008.
- [30] X. Liu, B. Krishnamachari, and H. Liu, "Channel selection in multi-channel opportunistic spectrum access networks with perfect sensing," in *Proc. IEEE Intl. Symp. New Frontiers in Dynamic Spectrum Access Networks (DySPAN)*, Singapore, Apr. 2010.
- [31] R. Smallwood and E. Sondik, "The optimal control of partially observable Markov processes over a finite horizon," *Operations Research*, vol. 21, no. 5, pp. 1071–1088, 1973.
- [32] D. A. Berry and B. Fristedt, *Bandit Problems: Sequential Allocation of Experiments*. London: Chapman and Hall, 1985.
- [33] E. Hossain, D. Niyato, and Z. Han, *Dynamic Spectrum Access and Management in Cognitive Radio Networks*. Cambridge, 2009.
- [34] H. Zheng and C. Peng, "Collaboration and fairness in opportunistic spectrum access," in *Proc. IEEE Intl. Conf. Commun. (ICC)*, Seoul, Korea, May 2005.

- [35] C. Cormio and K. R. Chowdhury, "A survey on MAC protocols for cognitive radio networks," *Ad Hoc Networks*, vol. 7, no. 7, pp. 1315–1329, Sep. 2009.
- [36] K. Liu and Q. Zhao, "Cooperative game in dynamic spectrum access with unknown model and imperfect sensing," *IEEE Trans. Wireless Commun.*, vol. 11, no. 4, pp. 1596–1604, 2012.
- [37] D. Niyato and E. Hossain, "Competitive spectrum sharing in cognitive radio networks: A dynamic game approach," *IEEE Trans. Wireless Commun.*, vol. 7, no. 7, pp. 2651–2660, Jul. 2008.
- [38] M. Maskery, V. Krishnamurthy, and Q. Zhao, "Decentralized dynamic spectrum access for cognitive radios: Cooperative design of a non-cooperative game," *IEEE Trans. Wireless Commun.*, vol. 57, no. 2, pp. 459–469, Feb. 2009.
- [39] H. Su and X. Zhang, "Cross-layer based opportunistic MAC protocols for QoS provisionings over cognitive radio wireless networks," *IEEE J. Sel. Areas Commun.*, vol. 26, no. 1, pp. 118–129, Jan. 2008.
- [40] J. Jia, Q. Zhang, and X. Shen, "HC-MAC: A hardware-constrained cognitive MAC for efficient spectrum management," *IEEE J. Sel. Areas Commun.*, vol. 26, no. 1, pp. 106–117, Jan. 2008.
- [41] A. C. C. Hsu, D. S. L. Wei, and C.-C. J. Kuo, "A cognitive MAC protocol using statistical channel allocation for wireless ad-hoc networks," in *Proc. IEEE Wireless Commun. Netw. Conf. (WCNC)*, Kowloon, Hong Kong, Mar. 2007.
- [42] H. Su and X. Zhang, "Channel-hopping based single transceiver MAC for cognitive radio networks," in *Proc. IEEE Conf. on Inf. Sciences and Systems (CISS)*, Princeton, NJ, USA, Mar. 2008.
- [43] B. Hamdaoui and K. G. Shin, "OS-MAC: An efficient MAC protocol for spectrum-agile wireless networks," *IEEE Trans. Mobile Comput.*, vol. 7, no. 8, pp. 915–930, Aug. 2008.
- [44] C. Cordeiro and K. Challapali, "C-MAC: A cognitive MAC protocol for multichannel wireless networks," in *Proc. IEEE Intl. Symp. New Frontiers in Dynamic Spectrum Access Networks (DySPAN)*, Dublin, Ireland, Apr. 2007.
- [45] L. Le and E. Hossain, "A MAC protocol for opportunistic spectrum access in cognitive radio networks," in *Proc. IEEE Wireless Commun. Netw. Conf. (WCNC)*, Las Vegas, NV, USA, Mar.–Apr. 2008.
- [46] S. Huang, X. Liu, and Z. Ding, "Opportunistic spectrum access in cognitive radio networks," in *Proc. IEEE Intl. Conf. on Computer Commun. (INFOCOM)*, Phoenix, AZ, USA, Apr. 2008.

- [47] E. Hossain, L. Le, N. Devroye, and M. Vu, "Cognitive radio: From theory to practical network engineering," in *New Directions in Wireless Communications Research*. Springer, 2009, pp. 251–289.
- [48] I. Tinnirello and S. Choi, "Efficiency analysis of burst transmissions with block ACK in contention-based 802.11e WLANs," in *Proc. IEEE Intl. Conf. Commun. (ICC)*, Seoul, Korea, May 2005.
- [49] D. Skordoulis, Q. Ni, H. Chen, A. Stephens, C. Liu, and A. Jamalipour, "IEEE 802.11n MAC frame aggregation mechanisms for next-generation high-throughput WLANs," *IEEE Wireless Commun. Mag.*, vol. 15, no. 1, pp. 40–47, Feb. 2008.
- [50] Y. Lin and V. W. Wong, "WSN01-1: Frame aggregation and optimal frame size adaptation for IEEE 802.11 n WLANs," in *Proc. IEEE Global Commun. Conf. (GLOBECOM)*, San Francisco, CA, USA, Nov. 2006.
- [51] Y. Kim, S. Choi, K. Jang, and H. Hwang, "Throughput enhancement of IEEE 802.11 WLAN via frame aggregation," in *Proc. IEEE Veh. Tech. Conf. (VTC)*, Los Angeles, CA, USA, Sep. 2004.
- [52] F. Cali, M. Conti, and E. Gregori, "Dynamic tuning of the IEEE 802.11 protocol to achieve a theoretical throughput limit," *IEEE/ACM Trans. Netw.*, vol. 8, no. 6, pp. 785–799, Dec. 2000.
- [53] ———, "IEEE 802.11 protocol: Design and performance evaluation of an adaptive backoff mechanism," *IEEE J. Sel. Areas Commun.*, vol. 18, no. 9, pp. 1774–1786, Sep. 2000.
- [54] Y. C. Tay, K. Jamieson, and H. Balakrishnan, "Collision-minimizing CSMA and its applications to wireless sensor networks," *IEEE J. Sel. Areas Commun.*, vol. 22, no. 6, pp. 1048–1057, Aug. 2004.
- [55] C. S. Hwang and J. M. Cioffi, "Opportunistic CSMA/CA for achieving multi-user diversity in wireless LAN," *IEEE Trans. Wireless Commun.*, vol. 8, no. 6, pp. 2972–2982, Jun. 2009.
- [56] H. Kwon, S. Kim, and B. Lee, "Opportunistic multi-channel CSMA protocol for OFDMA systems," *IEEE Trans. Wireless Commun.*, vol. 9, no. 5, pp. 1552–1557, May 2010.
- [57] X. Hong, C. X. Wang, and J. Thompson, "Interference modeling of cognitive radio networks," in *Proc. IEEE Veh. Tech. Conf. (VTC)*, Marina Bay, Singapore, May 2008.
- [58] M. F. Hanif, M. Shafi, P. J. Smith, and P. Dmochowski, "Interference and deployment issues for cognitive radio systems in shadowing environments," in *Proc. IEEE Intl. Conf. Commun. (ICC)*, Dresden, Germany, Jun. 2009.

- [59] Z. Chen, C. Wang, X. Hong, J. Thompson, S. Vorobyov, X. Ge, and P. Dmochowski, "Interference modeling for cognitive radio networks with power or contention control," in *Proc. IEEE Wireless Commun. Netw. Conf. (WCNC)*, Sydney, Australia, Apr. 2009.
- [60] A. Babaei and B. Jabbari, "Interference modeling and avoidance in spectrum underlay cognitive wireless networks," in *Proc. IEEE Intl. Conf. Commun. (ICC)*, Cape Town, South Africa, May 2010.
- [61] M. Aljuaid and H. Yanikomeroglu, "A cumulant-based characterization of the aggregate interference power in wireless networks," in *Proc. IEEE Veh. Tech. Conf. (VTC)*, Taipei, Taiwan, May 2010.
- [62] R. Zhang, "On peak versus average interference power constraints for protecting primary users in cognitive radio networks," *IEEE Trans. Wireless Commun.*, vol. 8, no. 4, pp. 2112–2120, Apr. 2009.
- [63] N. Hoven and A. Sahai, "Power scaling for cognitive radio," in *Proc. Int. Conf. Wireless Networks, Communications and Mobile Computing*, Maui, HI, USA, Jun. 2005.
- [64] A. Ghasemi and E. Sousa, "Interference aggregation in spectrum-sensing cognitive wireless networks," *IEEE J. Sel. Topics Signal Process.*, vol. 2, no. 1, pp. 41–56, Feb. 2008.
- [65] M. Vu, S. S. Ghassemzadeh, and V. Tarokh, "Interference in a cognitive network with beacon," in *Proc. IEEE Wireless Commun. Netw. Conf. (WCNC)*, Las Vegas, NV, USA, Mar. 2008.
- [66] M. Timmers, S. Pollin, A. Dejonghe, A. Bahai, L. V. der Perre, and F. Catthoor, "Accumulative interference modeling for cognitive radios with distributed channel access," in *Proc. IEEE Intl. Conf. on Cognitive Radio Oriented Wireless Networks and Commun. (CROWNCOM)*, Singapore, May 2008.
- [67] A. Rabbachin, T. Quek, H. Shin, and M. Win, "Cognitive network interference," *IEEE J. Sel. Areas Commun.*, vol. 29, no. 2, pp. 480–493, Feb. 2011.
- [68] M. Derakhshani and T. Le-Ngoc, "Adaptive hopping transmission strategy for opportunistic spectrum access," in *Proc. IEEE Global Commun. Conf. (GLOBECOM)*, Houston, TX, USA, Dec. 2011.
- [69] —, "Learning-based opportunistic spectrum access with hopping transmission strategy," in *Proc. IEEE Wireless Commun. Netw. Conf. (WCNC)*, Paris, France, Apr. 2012.
- [70] —, "Learning-based opportunistic spectrum access with adaptive hopping transmission strategy," *IEEE Trans. Wireless Commun.*, vol. 11, no. 11, pp. 3957–3967, Nov. 2012.

- [71] S. Geirhofer, L. Tong, and B. M. Sadler, "Dynamic spectrum access in WLAN channels: Empirical model and its stochastic analysis," in *Proc. Int. Workshop on Technology and Policy for Accessing Spectrum (TAPAS)*, New York, NY, USA, Aug. 2006.
- [72] Y. C. Liang, Y. Zeng, E. Peh, and A. T. Hoang, "Sensing-throughput tradeoff for cognitive radio networks," *IEEE Trans. Wireless Commun.*, vol. 7, no. 4, pp. 1326–1337, Apr. 2008.
- [73] Y. Xu, Y. Sun, Y. Li, Y. Zhao, and H. Zou, "Joint sensing period and transmission time optimization for energy-constrained cognitive radios," *EURASIP J. Wireless Commun. Netw.*, vol. 2010, no. 92, pp. 1–16, Apr. 2010.
- [74] P. Tehrani, K. Liu, and Q. Zhao, "Opportunistic spectrum access in unslotted primary systems," *Journal of the Franklin Institute (Elsevier)*, vol. 349, no. 3, pp. 985–1010, 2012.
- [75] S. Shetty, M. Song, C. Xin, and E. K. Park, "A learning-based multiuser opportunistic spectrum access approach in unslotted primary networks," in *Proc. IEEE Intl. Conf. on Computer Commun. (INFOCOM)*, Rio de Janeiro, Brazil, Apr. 2009.
- [76] D. Palomar and M. Chiang, "A tutorial on decomposition methods for network utility maximization," *IEEE J. Sel. Areas Commun.*, vol. 24, no. 8, pp. 1439–1451, Aug. 2006.
- [77] P. W. Glynn and P. Heidelberger, "Bias properties of budget constrained simulations," *Operations Research*, vol. 38, no. 5, pp. 801–814, Oct. 1990.
- [78] H. Kushner and G. Yin, *Stochastic Approximation and Recursive Algorithms and Applications*. New York: Springer, 2003.
- [79] J. C. Spall, *Introduction to Stochastic Search and Optimization*. Willey, 2003.
- [80] D. P. Bertsekas and J. N. Tsitsiklis, "Gradient convergence in gradient methods with errors," *SIAM Journal on Optimization*, vol. 10, no. 3, pp. 627–642, Feb. 2000.
- [81] V. B. Tadić, "Convergence and convergence rate of stochastic gradient search in the case of multiple and non-isolated extrema," in *Proc. IEEE Conf. Decision and Control (CDC)*, Atlanta, GA, USA, Dec. 2010.
- [82] B. Polyak, *Introduction to Optimization*. New York: Optimization Software, Inc., 1987.
- [83] J. Sacks, "Asymptotic distribution of stochastic approximation procedures," *The Annals of Mathematical Statistics*, vol. 29, no. 2, pp. 373–405, Jun. 1958.
- [84] M. Derakhshani and T. Le-Ngoc, "Opportunistic spectrum access with hopping transmission strategy: A game theoretic approach," in *Proc. IEEE Veh. Tech. Conf. (VTC)*, Quebec City, QC, Canada, Sep. 2012.

- [85] ———, “Intelligent CSMA-based opportunistic spectrum access: Competition and cooperation,” in *Proc. IEEE Global Commun. Conf. (GLOBECOM)*, Anaheim, CA, USA, Dec. 2012.
- [86] ———, “Distributed learning-based spectrum allocation with noisy observations in cognitive radio networks,” *IEEE Trans. Veh. Technol.*, submitted May 2013.
- [87] C. Alos-Ferrer and N. Netzer, “The logit-response dynamics,” *Games and Economic Behavior*, vol. 68, no. 2, pp. 413–427, Mar. 2010.
- [88] J. Marden and J. Shamma, “Revisiting log-linear learning: Asynchrony, completeness and a payoff-based implementation,” *Games and Economic Behavior*, vol. 75, no. 2, pp. 788–808, Jul. 2010.
- [89] D. Monderer and L. Shapley, “Potential games,” *Games and Economic Behavior*, vol. 14, no. 1, pp. 124–143, 1996.
- [90] A. B. MacKenzie, L. Dasilva, and W. Tranter, *Game Theory for Wireless Engineers*. Morgan and Claypool Publishers, 2006.
- [91] G. Scutari, S. Barbarossa, and D. P. Palomar, “Potential games: A framework for vector power control problems with coupled constraints,” in *Proc. IEEE Int. Conf. on Acoust., Speech and Signal Process. (ICASSP)*, Toulouse, France, May 2006.
- [92] D. Fudenberg and D. K. Levine, *The Theory of Learning in Games*. MIT press, 1998, vol. 2.
- [93] D. Okada and O. Tercieux, “Log-linear dynamics and local potential,” *Journal of Economic Theory*, vol. 147, no. 3, pp. 1140–1164, May 2012.
- [94] S. Lasaulce and H. Tembine, *Game Theory and Learning for Wireless Networks: Fundamentals and Applications*. Academic Press, 2011.
- [95] R. Menon, A. B. MacKenzie, J. Hicks, R. M. Buehrer, and J. H. Reed, “A game-theoretic framework for interference avoidance,” *IEEE Trans. Commun.*, vol. 57, no. 4, pp. 1087–1098, Apr. 2009.
- [96] J. B. Rosen, “Existence and uniqueness of equilibrium points for concave n-person games,” *Econometrica: Journal of the Econometric Society*, vol. 33, no. 3, pp. 520–534, Jul. 1965.
- [97] C. Saraydar, N. B. Mandayam, and D. J. Goodman, “Efficient power control via pricing in wireless data networks,” *IEEE Trans. Commun.*, vol. 50, no. 2, pp. 291–303, Feb. 2002.
- [98] M. Derakhshani and T. Le-Ngoc, “Adaptive access control of CSMA/CA in wireless LANs for throughput improvement,” *submitted to IEEE Global Commun. Conf. (GLOBECOM)*, Dec. 2013.

- [99] —, “Adaptive access control of CSMA/CA in wireless LANs: Design and throughput analysis,” *IEEE Trans. Wireless Commun.*, submitted Jun. 2013.
- [100] G. Bianchi, “Performance analysis of the IEEE 802.11 distributed coordination function,” *IEEE J. Sel. Areas Commun.*, vol. 18, no. 3, pp. 535–547, Mar. 2000.
- [101] IEEE 802.11g WG, “Wireless LAN medium access control (MAC) and physical layer (PHY) specifications: Further higher data rate extension in the 2.4 GHz band,” Jan. 2003.
- [102] M. Derakhshani, T. Le-Ngoc, and M. Vu, “Interference and outage analysis in a cognitive radio network with beacon,” in *Proc. IEEE Queen’s Biennial Symp. on Commun. (QBSC)*, Kingston, ON, Canada, May 2010.
- [103] M. Derakhshani and T. Le-Ngoc, “Beacon transmitter placement effect on aggregate interference and capacity-outage performance in a cognitive radio network,” in *Proc. IEEE Veh. Tech. Conf. (VTC)*, Ottawa, ON, Canada, Sep. 2010.
- [104] —, “Aggregate interference and capacity-outage analysis in a cognitive radio network using cooperative sensing,” in *Proc. IEEE Canadian Conf. on Electrical and Computer Engineering (CCECE)*, Niagara Falls, ON, Canada, May 2011.
- [105] —, “Aggregate interference and capacity-outage analysis in a cognitive radio network,” *IEEE Trans. Veh. Technol.*, vol. 61, no. 1, pp. 196–207, Jan. 2012.
- [106] L. Bao and E. Hossain, “Resource allocation for spectrum underlay in cognitive radio networks,” *IEEE Trans. Wireless Commun.*, vol. 7, no. 12, pp. 5306–5315, Dec. 2008.
- [107] N. Gatsis, A. G. Marques, and G. B. Giannakis, “Power control for cooperative dynamic spectrum access networks with diverse QoS constraints,” *IEEE Trans. Commun.*, vol. 58, no. 3, pp. 589–600, Mar. 2010.
- [108] G. Buchwald, S. Kuffner, L. Ecklund, M. Brown, and E. Callaway, “The design and operation of the IEEE 802.22. 1 disabling beacon for the protection of TV whitespace incumbents,” in *Proc. IEEE Intl. Symp. New Frontiers in Dynamic Spectrum Access Networks (DySPAN)*, Chicago, IL, USA, Oct. 2008.
- [109] W. Yu-chun, W. Haiguang, and P. Zhang, “Protection of wireless microphones in IEEE 802.22 cognitive radio network,” in *Proc. IEEE Intl. Conf. Commun. (ICC)*, Dresden, Germany, Jun. 2009.
- [110] A. P. Hulbert, “Spectrum sharing through beacons,” in *Proc. IEEE Intl. Symp. on Personal, Indoor and Mobile Radio Commun. (PIMRC)*, Berlin, Germany, Sep. 2005.
- [111] T. Yucek and H. Arslan, “A survey of spectrum sensing algorithms for cognitive radio applications,” *IEEE Commun. Surveys Tuts.*, vol. 11, no. 1, pp. 116–130, Mar. 2009.

- [112] S. Mishra, A. Sahai, and R. Brodersen, “Cooperative sensing among cognitive radios,” in *Proc. IEEE Intl. Conf. Commun. (ICC)*, Istanbul, Turkey, Jun. 2006.
- [113] G. Ganesan and Y. Li, “Cooperative spectrum sensing in cognitive radio, Part I: Two user networks,” *IEEE Trans. Wireless Commun.*, vol. 6, no. 6, pp. 2204–2213, Jun. 2007.
- [114] —, “Cooperative spectrum sensing in cognitive radio, Part II: Multiuser networks,” *IEEE Trans. Wireless Commun.*, vol. 6, no. 6, pp. 2214–2222, Jun. 2007.
- [115] J. Ma, G. Zhao, and Y. Li, “Soft combination and detection for cooperative spectrum sensing in cognitive radio networks,” *IEEE Trans. Wireless Commun.*, vol. 7, no. 11, pp. 4502–4507, Nov. 2008.
- [116] M. Derakhshani, T. Le-Ngoc, and M. Nasiri-Kenari, “Efficient cooperative cyclostationary spectrum sensing in cognitive radios at low SNR regimes,” *IEEE Trans. Wireless Commun.*, vol. 10, no. 11, pp. 3754–3764, Nov. 2011.
- [117] Y. Zeng, Y. Liang, A. Hoang, and R. Zhang, “A review on spectrum sensing for cognitive radio: Challenges and solutions,” *EURASIP J. Applied Signal Process.*, vol. 2010, no. 2, Jan. 2010.
- [118] H. Urkowitz, “Energy detection of unknown deterministic signals,” *Proc. IEEE*, vol. 55, no. 4, pp. 523–531, Apr. 1967.
- [119] F. Wang, J. Huang, and Y. Zhao, “Delay sensitive communications over cognitive radio networks,” *IEEE Trans. Wireless Commun.*, vol. 11, no. 4, pp. 1402–1411, Apr. 2012.
- [120] J. Huang and V. Krishnamurthy, “Transmission control in cognitive radio as a Markovian dynamic game: Structural result on randomized threshold policies,” *IEEE Trans. Commun.*, vol. 58, no. 1, pp. 301–310, Jan. 2010.
- [121] M. V. der Schaar and F. Fu, “Spectrum access games and strategic learning in cognitive radio networks for delay-critical applications,” *Proc. IEEE*, vol. 97, no. 4, pp. 720–740, Apr. 2009.
- [122] J. Filar and K. Vrieze, *Competitive Markov Decision Processes*. New York: Springer-Verlag, 1997.